"SELF-DIFFUSION ON METAL SURFACES"

by

J.M. Blakely

Thesis for the degree of Ph.D.
University of Glasgow
May 1961.

ProQuest LLC.
789 East Eisenhower Parkway
P.O. Box 1346
Ann Arbor, MI 48106 – 1346

Preface

The work described in this thesis is concerned with the measurement of the rate of self-diffusion on metal surfaces. Experiments have been carried out on nickel, gold, iron and platinum. The work was performed under the supervision of Dr.H.Mykura at the University of Glasgow, during the period 1958 to 1961. The technique developed for the diffusion measurements is based on measuring, by interference microscopy, the rate of smoothing of scratches on metal surfaces. Part of the experimental work on single scratch smoothing on nickel and on adsorption effects on nickel, was carried out jointly with Dr. Mykura. The multiple groove nickel experiments and the work on gold, iron, and platinum, were performed independently by the candidate who was also responsible for the interpretation of the results.

Part of this work has already been reported in the form of papers for publication. These are :

(1)" The Measurement of Surface Self-Diffusion Coefficients of Nickel by a Mass Transfer Technique"

(J.M.Blakely & H.Mykura : Acta Met., 9,23,(1961).)

(2)" The Effect of Impurity Adsorption on the Surface Free Energy and Surface Self-Diffusion of Nickel"

(J.M.Blakely & H.Mykura : accepted by Acta Met., submitted Dec. 1960)

(3)" The Effect of Impurity on Surfaces of Heated Gold"

(J.M.Blakely : accepted by Trans. Faraday Soc., submitted Jan.1961)

A reprint of the first is included at the end of this thesis.

Acknowledgments

The author wishes to thank Dr. H.Mykura for valuable advice during the course of this work, Dr.G.A.P.Wyllie for helpful discussions, and Professor P.I.Dee for encouragement; D.S.I.R. for providing a maintenance grant; the Director of the National Engineering Laboratory (East Kilbride) for the use of the Zeiss-Linnick interference microscope; Dr.J.Holden (N.E.L.) for the use of the Hilger microfocus X-ray set; Dr. Holborn of Aberdeen University for helpful advice on the design of the ruling machine; B.I.S.R.A. for the gift of some high purity iron sheet ; Dr.W.W.Mullins (Carnegie Institute of Technology) and Dr.N.A.Gjostein (Ford Motor Company) for sending copies of papers prior to publication. The author is also very much indebted to Mrs. K. Robb for valuable assistance in the photographic work.

CONTENTS

Illustrations

I. General Introduction

Studies of the migration, or diffusion, of atoms in crystalline media are of great interest both from a practical and a theoretical point of view. An understanding of processes such as sintering, crystal growth, recrystallization, for example, requires an appreciation of the basic mechanisms by which atoms of a crystal lattice may migrate. On the other hand, experimental determinations of diffusion rates in crystals, and in particular of the energy required for the fundamental diffusion act, would be expected to shed some light on the nature of those regions of the crystal under observation.

In polycrystalline materials diffusion problems can be divided into three distinct classes. These are (a) diffusion within the lattice of the crystal, referred to as volume or bulk diffusion, (b) diffusion at the bounding surfaces of crystals, and (c) diffusion along line imperfections, dislocations. Class (b) can be subdivided according as the bounding surface is free, or is adjacent in the polycrystalline aggregate to another of different atomic arrangement so producing a discontinuity in the periodic lattice. Such a discontinuity is called a grain boundary.

In general, theories of volume diffusion under thermal activation, are based on three fundamental processes, viz the atom (or ion) interchange mechanism in which an atom alters its position by exchanging lattice sites with a neighbour, the interstitial mechanism where the path of the migrating atom

passes only between normal lattice sites, and the vacancy mechanism. The last of these processes depends on the presence of point defects within the crystal, vacant lattice sites, whose migration through the lattice is equivalent to the motion of the atoms themselves. The mechanism dominant in any particular migration problem will depend both on the nature of the migrating atoms and of the lattice through which they move. Thus for example the diffusion of carbon, whose atoms are relatively small, in gamma iron is adequately explained (1) in terms of the interstitial process. On the other hand, for self-diffusion in face-centred cubic (f.c.c.) metals, theoretical calculations (1, 2, 3, 4) of the thermal energy which must be supplied for each of the three diffusion processes, show that in general the vacancy mechanism is energetically most favourable. The activation energy Q_v can in this case be divided into two contributions, the energy required to create a vacancy Q_f, and that for its motion in the lattice Q_m. Q_v and Q_f can be independently determined by tracer measurements of the temperature variation of volume self-diffusion coefficients D_v related to Q_v by the equation, $D_v = \text{const.}\exp(-\frac{Q_v}{kT})$ and from measurements of the residual resistivity r, in quenched materials expressed in terms of Q_f and the quenching temperature by $r = \text{const.}\exp(-Q_f/kT)$. Such measurements have for example been carried out on Cu (5, 6). The agreement of theory and experiment is reasonable, indicating that to a first approximation $Q_f \approx \frac{1}{2}Q_v \approx Q_m$. ($Q_v \approx 2$eV).

While a considerable amount of experimental data is now

available on volume diffusion, very little quantitative data exists in connection with the problem of diffusion at grain boundaries and free surfaces of metals. As pointed out by Le Claire (7)(1953), this is due largely to the fact that while volume diffusion can be studied separately from boundary diffusion the reverse is not true.

The principal aim of the work described in this thesis is to determine the rates of atomic migration on metal surfaces, to derive activation energies for the process, and to investigate the variation of diffusion rate with surface orientation. It was hoped that such studies might provide information on the nature of the diffusion process on metal surfaces, and perhaps on the structure of surfaces at high temperatures. The technique employed for diffusion measurements is based in principle on observing, by use of the interference microscope, the rate of change of a geometrically simple surface profile, namely the decay of a sine wave. Certain observations have also been made on the closely related topic of the variation of the surface free energy of metals with crystallographic orientation.

The relatively meagre amount of data on surface diffusion, available at the commencement of this work, is discussed below together with some more recent and apparently more reliable results. A brief review is also given of previous surface energy work on metals in so far as it is relevant to the present observations.

II. Review of Experimental Data

IIa Surface Diffusion

It is generally believed that atoms at the free surface of a crystal are more mobile than those either within the region of grain boundaries or in the interior of the crystal. Following Turnbull (8)(1951), this can be expressed by stating that if the rates of diffusion at free surfaces, grain boundaries, and within the lattice of a particular material are expressed in terms of diffusion coefficients, D_s, D_b and D_v respectively, the activation energies for the three processes being Q_s, Q_b and Q_v, then it is expected that at any given temperature, $D_s > D_b > D_v$ and also $Q_s < Q_b < Q_v$. However, sufficient data is not yet available to allow a direct comparison of the constants of the three types of diffusion, except perhaps in the case of self-diffusion in silver and the diffusion of thorium in tungsten (Turnbull (8)) which support the above statements.

Evidence for surface mobility

The high mobility of atoms on crystal surfaces was first demonstrated experimentally in the work of Volmer and Esterman (9)(1921). In their study of the growth of hexagonal crystals of mercury, from the vapour phase, it was found that the linear rate of growth in directions in the plane of the hexagon was about 1000 times greater than could be explained by calculations of the number of atoms impinging on the edges. This led them to postulate that atoms which impinged on the hexagonal planes, might migrate over the surface and become incorporated in the

lattice at the edges before evaporation can occur. Modern theories of crystal growth (Burton, Frank and Cabrera(10)(1951)) also include the role of the surface diffusion process. Observations on the rate of growth of crystal whiskers for example (Nabarro and Jackson(11)(1958)) can only be interpreted satisfactorily by taking account of migration along the whisker shanks. Gomer(12)(1957, 1958) has studied the rate of growth of mercury whiskers in the field emission microscope and derived a value for the surface self-diffusion coefficient of Hg at $-78^{\circ}C$ of $5.4 \times 10^{-5} cm^2/sec$. Using equation (4)p20 he estimates a surface diffusion activation energy Q_s of about 0.05eV. It should be noted that Gomer's result and other evidence of high surface mobility from crystal growth experiments, really applies only to planes of low Miller indices such as occur in growth forms. Further evidence of high rates of diffusion on random surfaces, compared to diffusion within the interior of crystals, came from observations on the spreading and aggregation of thin films.

Detection and Measurement of Surface Diffusion

(i) Thin Film Work

The spreading and aggregation of thin films has provided further though largely qualitative information on surface diffusion. Critical reviews of these early experiments exist in the literature (Barrer(13)(1941), Turnbull(8)(1951)). Since the present work is concerned with surface diffusion in a one-component system, only a very brief account of the techniques and results will be given here.

Several observations have been made, by optical microscopy,

of the break-up of thin metal films on a variety of substrates, at temperatures where volume diffusion would be expected to be negligible. Thin films of Ag and Au on quartz for example, were found to break up forming a series of small globules ($\sim 1\mu$ diameter) separated by relatively large distances up to 10μ, at temperatures below 300 and 400°C respectively (Andrade(14)(1935)). Similar conclusions were drawn from electrical resistivity measurements on thin films of alkali metals on pyrex (Appleyard (15)(1937)).

As pointed out by Turnbull(8) considerable care should be taken in drawing any conclusions from this type of experiment. This caution is based on the uncertainty as to the actual transport process, and on the belief that the thermodynamic properties of material in very thin films may be quite different from those of larger crystals.

The first actual quantitative measurements of surface diffusion were concerned with the migration of certain foreign atoms over the surface of metallic tungsten. These studies were based on the discovery that foreign atoms such as Ba, Cs, K, Th, etc. on surfaces of tungsten produce changes in the photoelectric or thermionic properties of the metal. Thus the work function of pure W is $\approx$ 4.5eV while that of thoriated tungsten is $\approx$ 2.6eV (16). Bosworth(17)(1935) for example made use of this effect to study the migration of sodium over tungsten by observing changes in the photoelectric current emitted when a narrow light beam traversed the surface.

The increase in thermionic emission from tungsten due to the

presence of thorium on the surface, was used to provide the first quantitative data on the relative magnitudes of diffusion within the lattice, along grain boundaries, and at the surface of a metal. The results of these experiments have been collected and analysed by Langmuir(18)(1934). He finds that the three diffusion coefficients can be expressed as

$$D_v = 1.0 \exp\left(-\frac{120{,}000}{RT}\right) \quad cm^2/sec$$

$$D_b = 0.74 \exp\left(-\frac{90{,}000}{RT}\right) \quad "$$

$$D_s = 0.47 \exp\left(-\frac{66{,}400}{RT}\right) \quad "$$

which is in agreement with the postulate $D_s > D_b > D_v$ and $Q_s < Q_b < Q_v$. However, this data cannot by any means be regarded as establishing the relative relationship between the constants of the three types of diffusion. In no case were measurements made both of diffusion coefficients and activation energy. D_v and D_s were determined only at one temperature in each case, 2400°K and 1655°K respectively, Q_b was derived from experimental measurements while the other constants were deduced from the semi-empirical Dushman-Langmuir equation (19)(1922)[$D \approx \frac{d^2 Q}{N_o h} \exp(-\frac{Q}{RT})$, where $\underline{d}$ is the atomic distance, N_o is Avogadro's number, and h is Planck's constant].

The measurements just described although of historical importance, are not sufficiently accurate or complete to contribute significantly toward an understanding of diffusion on metal surfaces. The scope of this technique is very limited and in order to investigate surface diffusion in a wider range of systems other methods have been devised.

(ii) Radioactive Tracer Techniques

The use of radioactive isotopes for the study of volume self-diffusion is now well established and fairly refined experimental techniques are in use (eg see ref.(5),(20)). It would appear at first that the radioactive tracer technique should also be well suited to an investigation of surface self-diffusion. The difficulties involved in its use are however fairly serious and considerable care must be exercised both in the design of experiments and in the analysis of the measurements. These difficulties arise from the fact, stated earlier, that surface diffusion is always accompanied by diffusion within the lattice and in the case of polycrystalline specimens by diffusion along grain boundaries. In addition radioactive atoms may be lost by evaporation. It has been suggested (Le Claire (7)(1953)) that a correction can be made for loss of active material by diffusion into the lattice by applying Fisher's analysis (21)(1951) of the corresponding grain boundary problem. No treatment has yet been given of the correction to be applied for lateral diffusion along grain boundaries. In addition to these inherent difficulties, considerable attention should also be taken to ensure that no sharp changes in curvature exist on the surface along the direction in which diffusion is measured. The existence of large curvature gradients would produce nett transfers of material on the surface (as described in the next section) and so might introduce some error in the final analysis which is based on a purely random walk problem.

Due to these difficulties the radioactive tracer technique

has not yet yielded any extensive or reliable data on the problem of surface self-diffusion. No really well defined experiment has yet been carried out. For such an experiment it would be desirable to use single crystals (Turnbull(8)) apply corrections for lateral diffusion, and to provide some assurance of the validity of these corrections by integrating the initial and final surface activity distributions.

Nickerson and Parker (22)(1950) measured the rate of diffusion of active silver along the surfaces of a bundle of polycrystalline wires. Radioactive silver was deposited from the vapour at one end and the distribution of activity along the wires, after annealing at a fixed temperature in vacuum, was found using a counter with a lead collimator to allow small regions of the surface to be counted. The temperature range used was very small, 225 to 350°C and the actual values of D_s have a fairly large scatter. These authors, assuming that the diffusion coefficient could be written as $D_s = D_o \exp(-Q_s/kT)$, derived values of $D_o = 0.16$ cm^2/sec and $Q_s = 0.45$eV. Such values appear to be reasonable when compared with the results of grain boundary and volume diffusion measurements in silver which were found to follow the equations $D_b = 0.025 \exp(-Q_b/kT)$ with $Q_b = 0.9$eV (Hoffman and Turnbull(23)(1951)) and $D_v = 0.89 \exp(-Q_v/kT)$ with $Q_v = 2$eV (Johnson(24)(1941)). Nickerson and Parker's results are however liable to the errors arising from loss of material into the lattice, along grain boundaries and by evaporation. These errors would be expected to increase with temperature so that the activation energy found is probably less than the true value.

Winegard and Chalmers (25)(1952) carried out further studies on silver surfaces. In this work both polycrystalline and single crystal specimens were used in the temperature range 250 to 400°C. The annealing atmosphere is not stated explicitly but this was presumably nitrogen as used in preparing the single crystal specimens. The spreading of a vapour deposited film of Ag^{110} was detected by the autoradiographic technique. Certain assumptions were made in interpreting film blackening in terms of the concentration of active silver, but the authors claim that even with such assumptions the values of D_s obtained are correct to within an order of magnitude. These are shown in table I. The chief conclusion drawn from this experiment was that the measured diffusion coefficient decreased with annealing time, attributed to changes in surface shape, such as the smoothing of single crystal surfaces and grain boundary grooving, which were presumed to occur during the initial stages of annealing. This effect together with the sources of error already mentioned suggest that the results should be treated with reserve. The inconsistency of radioactive tracer results on silver is apparent from table I; the two sets of results differ by a factor of $\approx 10^4$ in the value of D_s at the same temperature.

The rates of migration on surfaces of copper single crystals was investigated by Hackerman and Simpson (26)(1956). These workers measured D_s only at one temperature, 750°C, the annealing being carried out in a hydrogen atmosphere. The aim of this experiment was to measure the relative rates of diffusion on the three principal planes of Cu, i.e.(111), (100) and (110) and to see how these rates varied along different crystallographic

Table 1

Results of Surface Diffusion Experiments on Ag, Cu.

		Temperature(°C)	D_s (cm^2/sec)	
Nickerson & Parker(22)		225	0.56×10^{-6}	
		250	0.83×10^{-5}	
		350	0.41×10^{-4}	
Winegard & Chalmers (25)	single crystals	250	No diffusion detected	
		325	2×10^{-9}	
		400	3×10^{-9}	(mean values)
	poly-crystalline	250	2×10^{-9}	
		325	5×10^{-9}	
		400	2×10^{-9}	
Hackerman & Simpson(26)		750	(100) plane: 6.6×10^{-5}	[110] axis
			(100) plane: 2.8×10^{-5}	[100] axis
			(111) plane: 2.6×10^{-5}	
			(110) plane: 5.4×10^{-5}	

directions on these planes. Their results are summarised in table I. In this case a sharp point of a fine Cu wire was placed in contact with the surface to provide an effective point source. Lateral diffusion was again neglected. According to Mullins and Shewmon(27)(1959) if loss of Cu^{64} atoms into the bulk is included, the true values of D_s are at least 100 times greater than those reported. The actual orientations of the surfaces used did not coincide exactly with the low index planes under investigation, and may have been several degrees from these planes - the authors do not state this clearly and express the deviations as percentages, the meaning of which is not at all obvious. The values given in table I should be regarded as applying to surfaces near these low index planes* although the angle between the actual surface and the plane may not be the same in all three cases.

Hackerman and Simpson put forward an explanation of the apparent anisotropy of diffusion on the (100) plane (i.e. D_s along $[110] \approx 2\frac{1}{2}$ times D_s along $[100]$, fig(1)) in terms of 2nd nearest neighbour interactions. The difference is however more likely to be due to the deviation of their surface from a (100) plane; the measured D_s might for example be expected to depend on the direction relative to the general direction of surface steps.

The only other investigation of surface diffusion on metals using the tracer technique, described in the literature, is that of Fraunfelder (28)(1950). He studied the diffusion of Cu^{64} over surfaces of polycrystalline silver and obtained the result that at 750°C, $D_s = 8.3 \times 10^{-7}$ cm^2/sec.

*-See Over /-

x The surface referred to as (100) actually deviated from this plane by about 10^{0} and was close to (510)
(Private communication with Professor Hackerman).

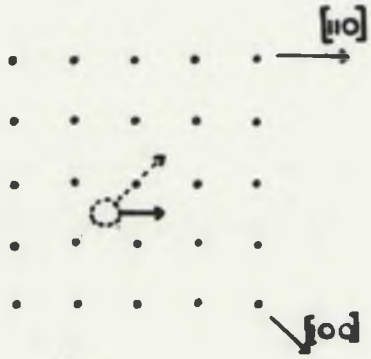

fig. 1

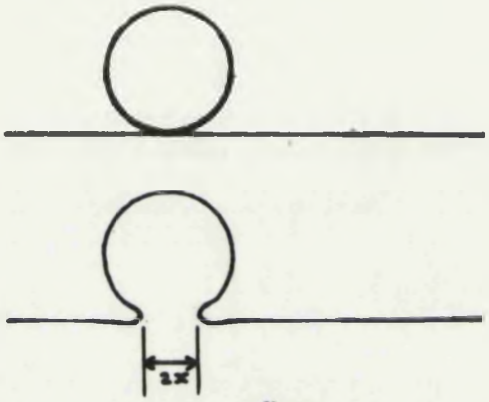

fig. 2

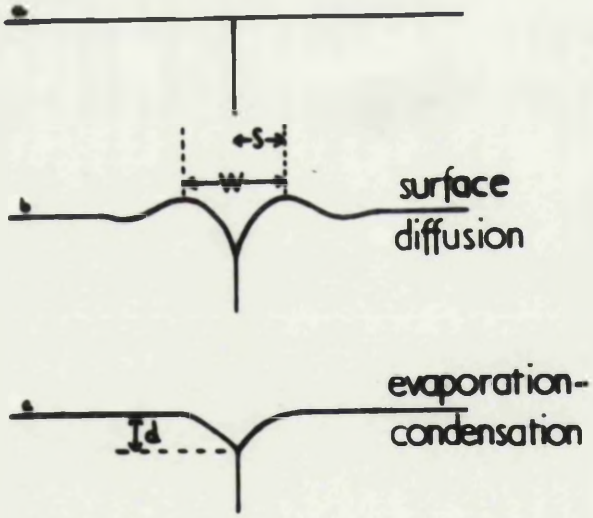

fig. 3

Grain boundary groove profiles.

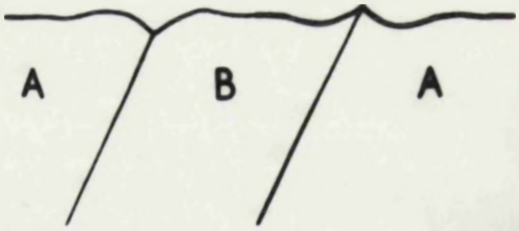

fig. 4

Profile at the intersection of a pair of twin boundaries with the surface. (after Mykura (60))

(iii) Mass Transfer Techniques

The measurements of surface self-diffusion described above depend on the use of distinguishable atoms. Other techniques have been developed in which diffusion data is found by measurement of a nett transport of material. This transport generally occurs under the action of surface tension forces and is in such a direction as to effect a decrease in the overall surface free energy of the system. Since curvature gradients must exist in the surface profile in order to produce a nett transfer of material the method necessarily involves a range of surface orientations. In certain techniques, this range can be very large with the result that their use for an investigation of the dependence of surface self-diffusion rates on orientation is virtually impossible. With the method used in the present work greater control of the orientation range involved can be achieved than in any other technique.

Herring, in his paper "Surface Tension as a Motivation for Sintering" (29)(1951), has given an excellent discussion of the transport of material in and on crystals under the influence of surface tension forces. This work has provided a mathematically sound foundation on which the apparently most successful techniques for the measurement of surface self-diffusion are based. Herring has shown that the transport of matter can be described in terms of gradients of chemical potential. Under the assumption of surface-volume equilibrium, i.e. free interchange of vacant lattice sites and interstitial atoms between the surface and the region immediately beneath it, he calculates the difference in the chemical potential μ of an atom and μ_h of a lattice vacancy immediately beneath a smoothly curved surface of principal radii

of curvature R_1 and R_2 :

$$(\mu - \mu_h) - \mu_c = \Omega\left[\gamma_s\left(\frac{1}{R_1}+\frac{1}{R_2}\right)+\frac{\partial^2\gamma_s}{\partial n_x^2}\frac{1}{R_1}+\frac{\partial^2\gamma_s}{\partial n_y^2}\frac{1}{R_2}\right] \quad \ldots\ldots\ldots (1)$$

where μ_c is the value of $(\mu - \mu_h)$ corresponding to a planar surface $(R_1, R_2 = \infty)$, Ω is the atomic volume, γ_s the surface free energy per unit area and n_x and n_y correspond to directions on the surface associated with R_1 and R_2. The importance of equation (1) will be discussed in some detail in section III.

The actual mechanisms for material transport have also been considered by Herring (29,30,31). These are plastic flow, volume diffusion, surface diffusion, and evaporation-condensation. The mechanism dominant in any particular transport problem depends on the linear dimensions involved (30) and on the relative rates of the three processes for the material under consideration. In general when the linear dimensions are very small the dominant transport mechanism will be surface diffusion, while volume diffusion and vapour transfer become more important with increasing dimensions. Thus for example the rate of growth of the neck in the sintering of a particle to a plane (fig(2)) will, in the initial stages, be due to surface diffusion and this will become relatively less important as the neck diameter increases.

Sintering

Prior to Herrings' theoretical work (29), Kuczynski (32) (1949)(33)(1950) carried out a set of experiments on the sintering of small spheres of Cu and Ag to plane surfaces of these materials. The annealing atmosphere used was hydrogen in the case of Cu, and hydrogen or air in the silver experiments. In the latter case no dependence on the atmosphere was detected. Kuczynski's theory predicted that the diameter of the neck between particle and

plane (fig. 2) should vary as $t^{\frac{1}{2}}$, $t^{\frac{1}{3}}$, $t^{\frac{1}{5}}$ or $t^{\frac{1}{7}}$ according as the dominant transport mechanism was plastic flow, evaporation-condensation, volume diffusion or surface diffusion. In the majority of the measurements the neck diameter was found to vary as $t^{1/5}$ so that the mechanism was identified as volume diffusion. For very small spheres of Cu, however ($< 10\mu$ diameter) the measurements indicated a $t^{1/7}$ dependence at temperatures of 400, 500 and 600°C. Results were in this case calculated on the basis of surface diffusion. The resulting values of D_s were fitted to the usual Arrhenius equation, $D_s = D_0 \exp(-Q_s/kT)$, to give $D_0 = 10^7 cm^2/sec$ and $Q_s = 2.4eV$.

Some idea of the accuracy of an experiment of this type may be obtained by comparing the volume diffusion results found for Cu with the most recent tracer values (Kuper et al,(5),(1954)). The constants D_0 and Q_v found from the two methods were:

Kuczynski $D_0 = 70\ cm^2/sec$: $Q_v = 2.4eV$

Kuper et al $D_0 = 0.49\ cm^2/sec$: $Q_v = 2eV$

These correspond to values of D_v differing by a factor of 10 at 1000°C. Due to the different activation energies this factor will be more or less at different temperatures.

The assumption of surface diffusion dominance at small particle sizes and low temperatures has been criticised by Cabrera (34)(1950), who suggests that $x \propto t^{1/5}$ both for surface and volume diffusion. Herring (31), on the other hand, supports Kuczynski's treatment of surface diffusion but states that further experimental data is required before accepting his results. No further results on surface diffusion have however appeared from this source although several investigators (see eg. Meechan(35)(1960)) (Kingery and Berg(35)(1955)).

have found a $t^{1/5}$ relation which they attribute to volume diffusion.

Field Emission Microscopy

Müller(36)(1949) used the field emission microscope to study the rate of blunting of very fine tungsten points of radius of curvature, $r < 1\mu$. The change in curvature at the tip was followed by measuring the voltage necessary to maintain a fixed electron emission current, and using the relationship between r and the voltage required. Muller assumed surface diffusion to be the dominant transport mechanism at the lower temperatures used, and derived an activation energy, $Q_s \approx 4.6$eV for self-diffusion on tungsten. The validity of Muller's assumption that surface diffusion accounts for the observed changes has been questioned by Herring(31). Boling and Dolan(37)(1958) have however provided experimental evidence to support Muller. More recently Barbour et al(28)(1960) have used a refined technique to study self-diffusion on tungsten. These workers used a pulsed electric field, micro-second pulses applied 30 times per second, so that the time during which the field acted was very small. The effect of the electric field on the surface migration was thus considered negligible. By assuming that surface diffusion rates and surface free energy (γ_s) are independent of orientation a simplified version of Herring's equation (1) was used to find a theoretical expression for the rate of shortening of a tungsten needle. Comparison with measured rates led to the following values for self-diffusion on tungsten.

$$Q_s = 3.14 \pm 0.08\text{eV}$$

$$D_o = 4 \text{ cm}^2/\text{sec.}$$

These experiments were carried out in a vacuum ($\sim 10^{-12}$ mm Hg) at

temperatures between 1500 and 2600°C. The above values of Q_s and D_o are average values over a large number of surface orientations. The wide range of orientations which is necessarily involved in experiments of this type makes the technique impractical for an investigation of the orientation dependence of surface diffusion.

Grain boundary grooving.

The appearance of grooves at grain boundary-free surface intersections on annealed metal specimens has been observed by many workers (see eg. Chalmers, King and Shuttleworth(39)(1948)). The kinetics of groove formation have been treated in detail by Mullins (40)(1957) who considers the role of the two transport processes surface diffusion and evaporation-condensation. The theory developed is essentially that used for the present work and will be considered later. Mullins has shown that when surface diffusion is the dominant transport mechanism, the rate of change in surface profile is described by a 4th order partial differential equation

$$\frac{\partial z}{\partial t} = -B\frac{\partial^4 z}{\partial x^4} \quad \ldots\ldots (2) \quad \text{(see fig 5)}$$

where $B = \frac{D_s \gamma_s \Omega^2 \nu}{kT}$, Ω = the atomic volume, ν = number of atoms/unit area of surface. The 4th order dependence is implicit in Herring's scaling laws (30) and an equation similar to (2) was derived by Mykura(41)(1954). Mullins has found a solution of (2) for the case of grain boundary grooving. If $\underline{w}$ is the distance between the maxima of the profile on either side of a grain boundary intersecting the surface normally, fig(3), then

$$w = (4.6)(Bt)^{1/4} \quad \ldots\ldots\ldots (3)$$

From equation (3) it will be seen that w varies as $t^{1/4}$ if surface diffusion only need be considered. In the case of

grooving by evaporation the profile is of the form fig(3c), i.e. no maxima but the depth d varies as $t^{1/2}$. Mullins has not considered the case of grooving by volume self-diffusion in the solid metal, but from the scaling laws, w should vary as $t^{1/3}$.

This theory has been applied to measure surface self-diffusion constants for Cu. Mullins and Shewmon(27)(1959) have tested the theory by observing, by interference microscopy, the development of grain boundary profiles on bicrystals of Cu annealed in hydrogen at 930°C and 1035°C. Within the accuracy of their results w was found to increase as $t^{1/4}$ at both temperatures even up to widths of about 26 microns at 1035°C. Recently Gjostein (42)(1961) has used the same technique to obtain more extensive data on the variation of the self-diffusion coefficient of Cu with temperature. The initial surfaces of the bicrystals used by Gjostein were $8\frac{1}{2}$ to 11° from a (100) plane. At temperatures above 825°C, he found deviations from the $t^{1/4}$ relationship which he attributes to a contribution to grooving from volume diffusion. At a temperature of 1020° C the average slope of the log w versus log t curve was found to be 0.31, the error probably being $\pm$ 0.02. Gjostein's curves do not show any consistent increase in slope with increasing w, at a particular temperature, as would be expected since surface diffusion will always be dominant at very small groove widths. Corrections were made for the effect of volume diffusion using a method suggested by Mullins and Shewmon(27). The temperature range used in these experiments was 720 to 1070°C, all anneals being carried out in hydrogen. The resulting diffusion coefficients agree reasonably well with the values found by Mullins and Shewmon and give

$Q_s = 1.7$ eV/atom

$D_o = 6.5 \times 10^2$ cm^2/sec.

At 720°C and below, surface roughening and pitting were observed.

The grain boundary grooving technique for diffusion measurements was developed during the course of the work described in this thesis, by Mullins and Shewmon, and Gjostein. It has been used here principally to provide values for comparison with those found by the technique described later.

The results of surface self-diffusion experiments available in the literature are summarised in table II.

II(b) Dependence of D_s on surface orientation

It appears to be generally agreed that the rate of surface diffusion, defined by the coefficient D_s, should be dependent on the crystallographic orientation of the surface. The experimental evidence to support this is however largely qualitative. The only quantitative data available in the literature is that from the experiments of Hackerman and Simpson(26) on tracer diffusion on Cu (table I). Their results show a dependence of D_s on orientation but due to the uncertainty in orientation and the fact that only three different surfaces were used, no generalizations on the variation of D_s as a function of orientation, for the f.c.c. lattice of Cu, are possible. The variation of D_s with direction on a surface near the (100) plane of Cu is perhaps more strongly supported by Hackerman and Simpson's results.

As stated earlier (p.12) Herring(29) has shown that mass transfer can be described in terms of chemical potential gradients or curvature gradients. The fact that material is transported across extensive regions whose curvature is below the limit of observation, has been taken to imply high surface diffusion

Table 11

Reference	Method	Metal	Atmosphere	Temp.Range
Winegard & Chalmers (25)	Tracer	Ag	Nitrogen	250-400°C
Nickerson & Parker(22)	Tracer	Ag	Vacuum (10^{-4} mm Hg)	225-350°C
Li & Parker(43)	Tracer	Au		
Hackerman & Simpson(26)	Tracer	Cu	Hydrogen	750°C
Kuczynski (32)	Sintering	Cu	Hydrogen	400-600°C
Gjostein (42) & Mullins & Shewmon(27)	Grain boundaries	Cu	Hydrogen	720-1070°C
Barbour et al (38)	Field emission points	W	Vacuum (10^{-12} mm Hg)	1500-2600°C

Table II (contd.)

Orientation	D_o (cm^2/sec)	Q_s (eV)	Q_b (eV)	Q_v (eV)	Q_s/Q_v
Single & Polycrystal	-	-	0.9 (23)	2.0 (24)	-
Polycrystalline wires	0.16	0.45	"	"	0.23
Polycrystalline	7.6	0.68	-	1.81 (20)	0.37
Near (100),(111) & (110)	-	-	-	2.0 (5)	-
	10^7	2.4	-	"	1.2
Near (100)	6.5×10^2	1.7	-	"	0.9
Large range of orientations	4.0	3.14	-	6.1*	0.51

*Estimated by Van Liempt (44) by assuming Q_v, the activation energy for self-diffusion in tungsten is the same as that for the diffusion of iron in tungsten.

coefficients for these regions. Thus Moore(45)(1958) has suggested that D_s is very large on the (100) and (111) facets observed in his study of striations on silver. Similar conclusions were reached by Gomer (46)(1953) in his emission microscope studies of Nickel filaments.

II(c) Surface Diffusion Models

The problem of surface self-diffusion has received very little attention from the theoretical point of view. In the majority of surface diffusion experiments which have been carried out to date, it is extremely doubtful if any serious claim could be made that pure surfaces were involved. It would however be of importance to consider the possible mechanisms for atomic migration on a pure surface before attempting to take account of the presence of foreign atoms.

In this section previous models of surface diffusion are discussed together with some further suggestions. Two types of surface can be distinguished according as they coincide with atomically smooth or low index planes or with atomically rough planes of high index.

(i) Atomically smooth surfaces

It has been shown theoretically by Burton, Frank and Cabrera (10)(1951) that surfaces consisting of the most closely packed planes of a crystal will remain ordered, with respect to the height of the surface all the way up to the melting point. This view has been supported by Mullins(47)(1960) whose calculations apply to the (100) plane of a simple cubic crystal. The only imperfections existing on such a surface will be single self-adsorbed atoms and vacant surface sites. In this case surface migration may be

pictured as the motion of atoms between identical equilibrium sites above the completely filled layer. Interactions between diffusing atoms may be neglected provided that the number of such atoms is $\ll$ the number of adsorption sites available on the surface. This type of surface migration has been considered by Lennard-Jones(48)(1937) and is the diffusion model generally assumed in treatments of evaporation (Knacke and Stranski (49) (1956)) and crystal growth (10). Lennard-Jones has shown that for atoms migrating on an atomically smooth surface, the diffusion coefficient, D_s, may be written as

$$D_s = \alpha a^2 f \exp(-Q_s/kT) = D_0 \exp(-Q_s/kT) \quad \ldots\ldots (4)$$

where α is a geometric constant ($\frac{1}{4}$ for (100) surface, $\frac{1}{3}$ for (111) surface), $f \approx$ atomic vibration frequency, a = average distance moved per jump, and Q_s is the energy of activation, equal to the height of the P.E. barrier between neighbouring equilibrium sites. The height of this P.E. barrier has been calculated (see ref (10) p.302) to be about $\frac{1}{20} L_s$ where L_s is the energy of sublimation. Gomer's value of Q_s for migration along the atomically smooth surfaces of Hg whiskers is in fair agreement with this estimate; here $Q_s \approx \frac{1}{13} L_s$ where L_s the heat of sublimation of Hg $\approx$ 0.65eV(50). In the case of Ni, where $L_s \approx$ 4.3eV, Q_s for migration on a smooth surface might be expected to be about 0.3eV.

a the distance moved per jump is usually put equal to the interatomic spacing. It appears plausible however that an activated atom may next be adsorbed several spacings distant. An increase in jump distance to 10 interatomic spacings would increase D_s by a factor of 100.

Thus for close-packed surfaces self-diffusion may be pictured as the motion of atoms between equilibrium adsorption sites with a very small activation energy the actual distance moved per jump being perhaps many times the distance between neighbouring sites.

(ii) Atomically Rough Surfaces

For surface orientations corresponding to planes of high Miller indices, the theory of Burton Frank and Cabrera (10) shows that at temperatures considerably below the melting point of the metal, 'surface melting' occurs. Thus at high temperatures one may picture the surface as a partly disordered layer in which there is a more or less random concentration of vacant sites. For such a model the most probable mechanism for surface diffusion is the vacancy mechanism. The activation energy should be considerably smaller than the corresponding process in the bulk, as the vacancies are inherent on the surface and each is surrounded by a smaller number of metal ions. Thus Q_s in this case would be expected to be $< Q_m$, the energy for vacancy motion in the bulk. $Q_m \approx \frac{1}{2}Q_v$ (3)(5), so that Q_s should be $< \frac{1}{2}Q_v$. For Ni where Q_v = 2.75eV (Reynolds et al(51)(1957), Hoffman et al (52) (1956)) a value of $Q_s < 1.3$eV would be expected. Similarly for Cu, Q_s should be $<$ 1eV. According to equation (4) the diffusion coefficients for atomically rough surfaces should be smaller than for low index planes. This difference is liable to be greater than that due to the different activation energies as in the case of high index surfaces the jump distance is likely to be only of the order of the interatomic distance. The frequency factor D_o ($= \frac{1}{4}a^2 f$) would be expected to be $\approx 10^{-3}$ to 10^{-4} cm^2/sec taking

$a = 3\text{Å}$, $f = 10^{12}$/sec which are typical values for metals.

(iii) Comparison of the tracer and Mass transfer techniques:

The fundamental difference between the tracer and mass transfer techniques is that the first involves a fixed surface orientation, while the latter requires a range of orientations, and this range changes with time.

For surfaces whose orientations do not lie very close to low index planes, the two methods should yield the same values for diffusion coefficients. This will be the case for general surfaces. When surfaces very close to atomically smooth planes are considered the situation is liable to be quite different. Since the surface free energy of crystals is expected to vary with crystal orientation (discussed below) the driving force for mass transfer is not known unless both the surface orientation and surface free energy variation is known. For any plausible variation of surface free energy (γ_s) with orientation, the range of orientations to which the mass transfer technique is inapplicable will be very small. Only when the surface profile under observation contains an orientation within about 5° of the (111) or (100) poles in the case of f.c.c. metals should any error be incurred.

In his work on grain boundary grooving in copper, Gjostein (42)(1961) used bicrystals with surfaces near (100). In this case the curved surfaces of the grooves would generally include orientations very close to (100), so that the assumption that the surface free energy does not vary over the range of orientations involved may not be valid. On the basis of Herring's predictions (31)(1953) regarding the effect of temperature on the variation

of γ_s with orientation, the error should be greatest at low temperatures. Gjostein does in fact report that at 720°C and below pitting and roughening of the surface did take place. This he attributes to a surface reaction or thermal faceting. If the latter is true the assumption of constant γ_s would certainly not be valid. Gjostein's activation energy of 1.7eV for surface migration on Cu seems very large in relation to the value of $Q_v \approx$ 2eV(5). The explanation may lie in false assumptions in the theory. Since the calculated value of D_o is very sensitive to changes in Q_s the large value, 6.5×10^2 $cm^2/sec.$, may be due to the apparent high activation energy.

(iv) Effect of impurity on surface diffusion

It has been suggested by Gomer (53)(1959), in his study of the diffusion of adsorbed gases on surfaces, that adsorbed atoms may be arranged on an atomically rough surface in such a way that it resembles a close packed plane. The effect of adsorption in this case is to cause an enhancement of diffusion across the surface. The experiments of Mair et al (54)(1959) have shown that impurity on surfaces of gold causes a suppression of evaporation. The latter result indicates that surface atoms are bound more tightly in the presence of impurity. Since changing surface orientations are involved in mass transfer experiments Mair's conclusions are more relevant than those of Gomer. It would be expected therefore, that impurity on surfaces would lead to a suppression of surface diffusion which produces a nett transfer of material.

II(d) Surface Energy

The changes in surface shape measured during the present work, and in other mass transfer methods, are motivated by changes in the total surface free energy of the system. Values of the specific surface free energy γ_s are required to evaluate surface diffusion coefficients from measured shape changes. The methods that have been used to measure the mean surface energies ($\bar{\gamma}_s$) of metals have been critically reviewed by Udin (55)(1952), Fisher and Dunn (56)(1952), and Mykura (41)(1954). It appears that the 'wire pulling' technique is the most successful and the values of γ_s used in the present thesis were obtained by workers using this method. The values for the metals used (Ni, Au, Fe, Pt) are listed in table III, together with the atmosphere in contact with the various surfaces during measurement.

The work of Buttner Funk and Udin (55) has shown that adsorption of oxygen on silver surfaces causes a decrease in the average surface free energy. The experimental value of $\bar{\gamma}_s$ for silver in contact with air was 450 ergs/cm^2 as compared to 1140 ergs/cm^2, when a helium atmosphere was used. Herring (31) has discussed the variation of the surface free energy of crystals with orientation (the γ_s-plot) and the possible effects of adsorption on this variation. He predicts that the adsorption of impurity atoms on crystal surfaces, in amounts sufficient to change the average surface free energy significantly, will probably also produce appreciable changes in the shape of the γ_s-plot.

Information on the dependence of γ_s on orientation has been obtained from observations on faceting, the break-up of flat

Table III

Metal	Atmosphere	γ_s (ergs/cm^2)	Reference
Nickel	Argon	2,000*	(67)
Gold	Helium	1,450	(55)
Iron	Argon	2,000	(77)
Platinum		2,000**	

* see also Table V.

** No reference to a measurement of γ_s for solid Pt has been found in the literature. A value of 2,000 ergs/cm^2 has been assumed.

surfaces into striations, grain boundary migration, and from a study of twin boundary-free surface intersections. The formation of low index flats on wires of tungsten, tantalum and molybdenum, directly heated in an inert atmosphere (Smith(57)(1954), Nichols (58)(1954)) has been taken to indicate the presence of γ_s-plot cusps at these orientations. Similar faceting has been observed on the sharp points used in the field emission microscope (Müller (36)(1949).

Striations have been observed on the surfaces of a large number of metals. The appearance of striations on silver has been studied most extensively (see eg. Moore (45)(1958), Chalmers, King and Shuttleworth(39),(1948)). These investigations indicate that in the presence of oxygen the surface energies of the (111) and (100) planes are respectively about 0.8 and 0.9 of the value for a random surface. The disappearance of striations on heating in nitrogen or hydrogen is taken as evidence that γ_s does not vary appreciably with orientation unless oxygen is present. In this case the effect of adsorption is to accentuate the cusps in the γ_s-plot at those orientations where they would normally be expected to occur for a clean f.c.c. metal, and in addition the close-packed (111) plane still has the lowest free energy. The work of Walter and Dunn (59)(1960) on silicon-iron (b.c.c.) has shown, however that impurity adsorption can make the surface energy of the (100) plane less than that of the (110) plane; the latter is the most closely packed plane of the b.c.c. lattice and in clean conditions should have the lowest free energy. Walter and Dunn observed the migration of grain boundaries motivated by a decrease in surface free energy, between crystals whose surfaces were close

to (110) and (100) planes. In vacuum ($\approx 10^{-4}$ mm Hg), the (110) oriented grains grew at the expense of the others while in impure argon, those with surfaces near (100) extended, and developed marked striations. Evidence will be presented later in this thesis to show that impurity adsorption has an appreciable effect on the γ_s-plot of Ni.

Mykura (60)(1957, 1961) has shown how the γ_s-plot of f.c.c. metals can be derived from a study of twin-boundary-free surface intersections. Herring's equations (29) for the intersection of three interfaces, were applied to the case of a pair of twin boundaries meeting a flat surface. When $\frac{\partial \gamma_s}{\partial \theta}$ is appreciable at the orientations of the twin surfaces, there are effectively forces acting at right angles to the surfaces. At one of the twin boundary-surface intersections these forces act in the same direction as γ_T the twin boundary tension, while at the other they act in the opposite direction. As shown by Mykura the effect of the orientation derivatives of γ_s is to produce a profile as shown in figure (4) where one 'groove' is inverted. Such profiles were first observed by him on specimens of Ni and Cu. Inverted grooves need not necessarily be confined to the intersection of twin boundaries with the surface, but may also occur for low angle boundaries provided the boundary energy is sufficiently small. The occurrence of the latter has not yet been reported in the literature.

III Theory

(i) The Sine Wave Technique

On the basis of Herring's work (29), the theory of mass transfer along a curved surface of a crystal has been given by Mullins (40)(1957), (61)(1959). Mullins has considered contributions from each of the three transport processes, surface diffusion volume diffusion, and evaporation-condensation. Since the assumptions of Mullins' theory are important in the present work the derivation of the equation governing mass transfer by surface diffusion will be outlined briefly.

Consider a surface which lies near the x-y plane and is everywhere parallel to the y-axis, so that the shape of the surface is specified by its intercept on the x-z plane (fig 5). Let K be the curvature at any point on the profile. Then from equation (1) p. 13 , the increase in chemical potential of an atom transferred from a point of zero curvature to one of curvature K is

$$\mu(K) = \Omega \gamma_s K \qquad \ldots\ldots\ldots (5)$$

assuming γ_s is independent of orientation. If it is also assumed that the surface diffusion coefficient D_s, is independent of orientation, Herring's equation for the flux of atoms across the surface becomes

$$J = -\frac{\nu D_s}{kT}\frac{\partial \mu}{\partial s} = -\frac{\nu D_s \gamma_s \Omega}{kT}\frac{\partial K}{\partial s} \qquad \ldots\ldots\ldots (6)$$

where s is the arc length measured along the profile, ν = no. of atoms/unit area. When γ_s is independent of orientation, Herring's statement that mass transport is motivated by gradients in chemical potential is equivalent to saying that material is transported due to curvature gradients. The increase in the number of atoms per unit area per unit time = $\frac{\partial J}{\partial s}$ and the rate at which any element of the profile moves normal to itself = $\Omega \frac{\partial J}{\partial s} \approx \frac{\partial z}{\partial t}$

fig.5

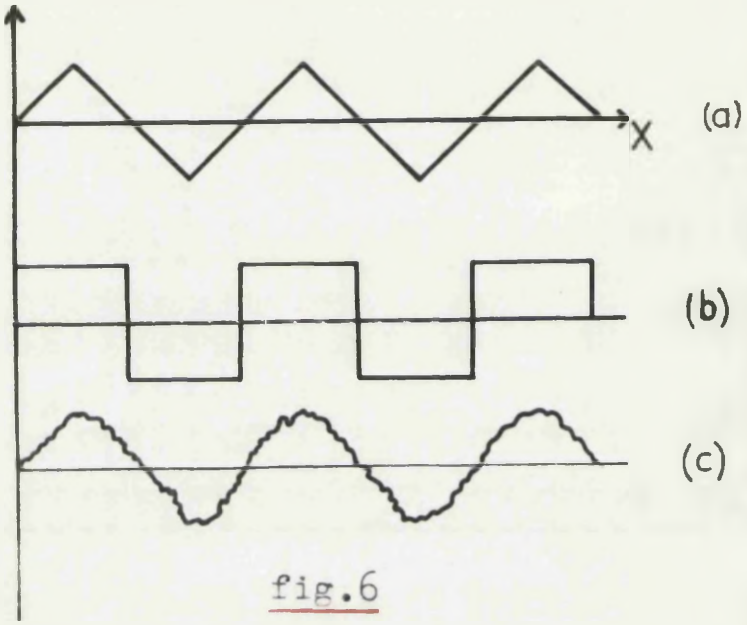

fig.6

Possible initial surface profiles which after sufficient annealing would become sinusoidal.

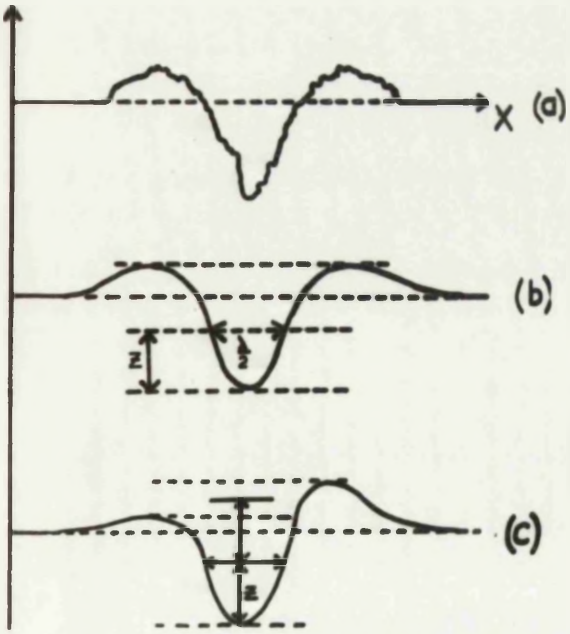

fig.7

Scratch profiles (a)initial form,(b)after a short anneal (c)an asymmetric profile. (b) and (c) show the dimensions z and $\lambda/2$.

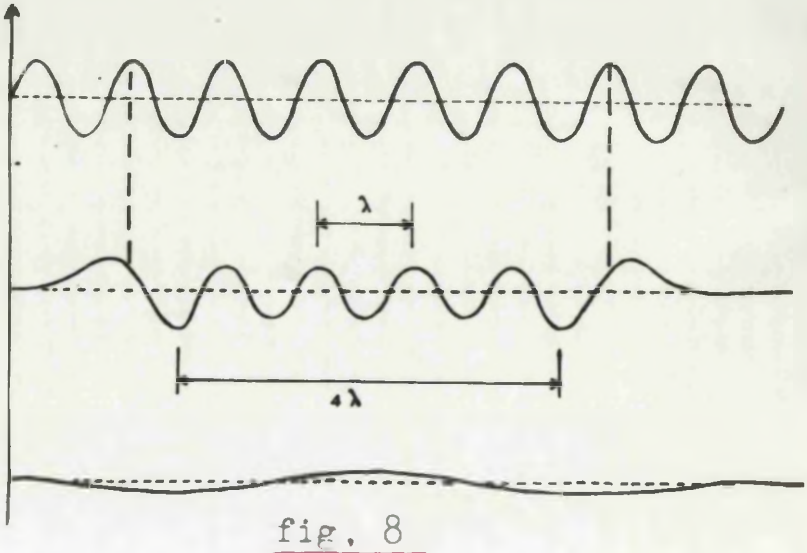

fig. 8

(a) Perfect sinusoidal profile,(b) typical profile used in experiments (c)profile after a very long annealing period.

for small slopes.

Also for small slopes $\frac{\partial^2 K}{\partial s^2} \approx \frac{\partial^4 Z}{\partial x^4}$, so that we get

$$\frac{\partial Z}{\partial t} = -B\frac{\partial^4 Z}{\partial x^4} \qquad \ldots\ldots\ldots\ldots (7)$$

where $B = \frac{D_s \gamma_s \Omega^2 \nu}{kT}$.

Equation (7) is the differential equation governing the transport of material on crystals by surface diffusion, and is the equation derived by Mullins.

If Mullins' assumption, that the surface diffusion coefficient is independent of orientation, is not made, the equation becomes considerably more complicated. That is if $\frac{\partial D_s}{\partial \theta}$ terms are not neglected the equation is of the form

$$\frac{\partial Z}{\partial t} = -D_s \frac{\Omega^2 \nu \gamma_s}{kT} \frac{\partial^4 Z}{\partial x^4} - \frac{\Omega^2 \nu \gamma_s}{kT} \left(\frac{\partial D_s}{\partial \theta}\right)\left(\frac{\partial^2 Z}{\partial x^2} \cdot \frac{\partial^3 Z}{\partial x^3}\right) \qquad \ldots\ldots (8)$$

where γ_s is still assumed to be constant.

Equation (7) has been solved by Mullins for the case of a grain boundary groove as mentioned earlier, and also for an initial sinusoidal profile.

For an initial sinusoidal profile Z_o - a sin wx where $w = \frac{2\pi}{\lambda}$, λ = wavelength, the form after time $\underline{t}$ is

$$Z(x,t) = Z_o \exp(-Bw^4 t) \qquad \ldots\ldots\ldots (9)$$

and

$$\frac{\partial Z}{\partial t} = -Bw^4 Z \qquad \ldots\ldots\ldots (10)$$

The theory thus predicts that an initial sinusoidal profile will decay exponentially due to surface diffusion, with a decay constant proportional to $1/\lambda^4$.

The corresponding solution when all three transport processes are taken into account is

$$Z(x,t) = Z_o \exp\left[-(Bw^4 + Cw^3 + Aw^2)t\right] \qquad \ldots\ldots (11) \text{(Mullins(61))}$$

where Cw^3 and Aw^2 are the decay constants due to volume diffusion and evaporation-condensation. $C = \frac{D_v \gamma_s \Omega}{kT}$, and $A = \frac{p_o \gamma_s \Omega^2}{(2\pi m)^{1/2}(kT)^{3/2}}$

where p_o is the equilibrium vapour pressure (dynes/cm^2) over a flat surface, and m is the mass of a molecule of the vapour from the solid.

It should be noted that the contributions to surface smoothing of the three transport processes, surface diffusion, volume diffusion and evaporation-condensation depend respectively on $\frac{1}{\lambda^4}$ $\frac{1}{\lambda^3}$ and $\frac{1}{\lambda^2}$.

Application for the measurement of surface diffusion coefficients

Mullins' theory of surface smoothing has been applied in the present work for the measurement of surface self-diffusion coefficients. It will be assumed for the moment that surface diffusion is effectively the only transport mechanism contributing significantly to smoothing. The validity of this assumption will be discussed later.

It will also be assumed that γ_s and D_s are constant over the range of orientations involved in the measurements. In certain cases however, this latter assumption is shown to be invalid, and the observed mass transfer would probably be described better by an equation of the form (8).

Consider a general surface corrugation parallel to the y-axis with a profile in the x-z plane of the form shown in fig(6) These profiles may for example have been produced by chemically etching, or by ruling a set of parallel grooves with a sharp instrument.

Such profiles could be represented by Fourier series,

$$Z_o = A_1 \sin\omega x + A_2 \sin 2\omega x + \cdots + A_n \sin n\omega x + \cdots \quad \ldots\ldots\ldots (12)$$

Applying equation (9) to each sinusoidal component, shows that after time t the profile will be

$$Z(x,t) = (A_1 \sin\omega x)\exp[-B\omega^4 t] + \cdots + (A_n \sin n\omega x)\exp[-Bn^4\omega^4 t] + \cdots \quad \ldots\ldots (13)$$

Due to the factor n^4 in the exponential, all terms after the first decay very rapidly and the surface soon approaches a pure sinusoidal form. For instance after a time of one fifth of the characteristic time, $\tau = 1/B\omega^4$, the fundamental has decreased to 82% of its initial amplitude, the second harmonic to 4% and all higher harmonics have effectively disappeared. For $B \approx 10^{-20}$ cm^4/sec, and $\lambda \approx 10^{-3}$cm, (which are typical values shown later) 0.2τ is $\approx$ 3hr.

Use has been made of this principle in the present work, where sets of parallel grooves were produced by a simplified ruling machine, on the surfaces of cold-rolled metal specimens. On annealing for a short time at a high temperature, recrystallization occurs and the surface smooths by surface diffusion to assume an almost sinusoidal profile. Measurement of the rate of smoothing of such profiles will then yield values of B (and hence D_s) using equation (9).

Single Scratches.

In the initial experiments, facilities for producing sets of closely spaced parallel grooves were not available. In view of this, single scratches were used. A single scratch on a metal surface, made with a rough instrument will have an initial profile as in fig(7a), assuming that no material is removed. If such a specimen is now annealed for a short time at a high temperature, surface diffusion causes the profile to become smooth, of the form fig(7b).

From equation (10) the constant B can be written as

$$B = \frac{\Delta Z\, \lambda^4}{\bar{Z}\, 16\pi^4 \Delta t} \qquad \ldots\ldots (14)$$

where $\Delta Z = (Z_1 - Z_2)$, Z_1, and Z_2 are the amplitudes before and after an annealing time Δt, and $\bar{Z}$ is the mean amplitude during this interval ($\approx \frac{Z_1 + Z_2}{2}$).

If we now assume, that for a single scratch, the surface between the two maxima on either side of the groove smooths like a pure sine wave, then measurement of the rate of smoothing will yield a value of B using equation (14) and hence D_s. This assumption obviously involves considerable approximation. The net mass transfer depends on the curvature gradient and beyond the maxima of the scratch profile, this is clearly less than that which would result from a sinusoidal profile. This causes the maxima to move apart as the scratch smooths so that λ increases with time and also leads to a smaller value of ΔZ. In the measurements on single scratches $\lambda/2$ was measured at a level midway between the crests and the base of the scratch as shown in figure (7b). In some cases slightly assymmetrical scratches were also used. The values of z and $\lambda/2$ used for these are indicated in fig(7c). Due to the increase in λ during experiments, the value used in equation (14) was that given by

$$\lambda^4 = \frac{1}{2}\left(\lambda_1^4 + \lambda_2^4\right) \qquad \ldots\ldots\ldots (15)$$

where λ_1 and λ_2 are the effective wavelengths before and after annealing.

Due to these approximations, the absolute values of B and D_s obtained from measurements on single scratches, are liable to a systematic error. The magnitude of this error is difficult to estimate. The value of λ used, (given by (15)) is probably too small, so the resulting values of B and D_s are likely to be smaller than the true values. The systematic error may be of the order of 50%.

The relative values of D_s at different temperatures, or for different surface orientations are not affected by this, so that no error in activation energies for example can be attributed to

this source.

Multiple Scratches.

In this case the systematic errors discussed above are not present, and the main errors arise from inaccuracies in experimental measurements. These will be discussed later. It is however difficult experimentally to produce on a metal surface a set of parallel grooves of spacing $\approx$ 10 microns, which, after an initial smoothing anneal, gives a perfect sinusoidal profile of constant wavelength and amplitude (fig 8a) as required by the theory. Fig (8b) shows a more typical profile used in these experiments. For convenience of measurement, sets of 4 or 5 parallel grooves of spacing about 10 microns were normally used. After an initial smoothing anneal, profiles of the form in fig (8b) were observed, where the reduction in depth of the extreme grooves was less than average, due to a lateral shift of the extreme maxima as described above for single scratches. In such cases, measurements were made on the central portion of the profile as indicated, and the value of B found from a plot of log (amplitude) against time. Some error is involved in this as after a sufficiently long annealing time the profile would be of the form in fig(8c), i.e. of wavelength 4λ. However since the decease in amplitude in a given time is proportional to $\frac{1}{\lambda^4}$(equation(14)), the error in the measured decrease is only of the order of 1 part in 200, i.e. $\approx$ 0.5%. Even for a set of 3 parallel grooves the error from this source would be $<$ 10%.

Contributions of the Transport Processes

The discussion so far has assumed that only surface diffusion is operative in causing smoothing. Also it will be noted that no

contribution from the mechanism of plastic flow has been included in Mullins' equation (11). The transport of matter by plastic flow has been considered by Herring (31), who suggests that for crystals the mechanism is inoperative in cases of material transport motivated by changes in surface free energy. There is no experimental evidence that plastic flow can occur under the action of surface tension forces.

The most convenient range of wavelengths for sinusoidal surface profiles, from the experimental point of view, is from 5 to 20 microns. For a large number of metals, surface diffusion will be the dominant process causing amplitude decay at temperatures which can readily be obtained (up to about 1300°C). The dominance of surface diffusion can however be readily checked in the following ways.

1. The decay constant in equation (11) is measured experimentally. It is then assumed that $Bw^4 \gg Cw^3 + Aw^2$ or $B \gg \frac{C}{\omega} + \frac{A}{\omega^2}$ .... (a) so that the measured decay constant = Bw^4, and values of B calculated accordingly. The validity of this assumption can then be tested by comparing the resulting values of B with those found by computing the quantities $\frac{C}{\omega}, \frac{A}{\omega^2}$, from published data on volume diffusion and vapour pressure for the metal considered. Suitable corrections may then be applied. Generally assumption (a) need only be justified at the highest temperature used since the activation energy for surface diffusion is expected to be less than that for volume diffusion or evaporation.

11. If several sets of grooves of different spacing are measured at the highest temperature used, then a plot of log (decay const) against log (λ) will serve to decide the dominant transport

process. The slope of such a curve would be -4 for surface diffusion alone, -3 for volume diffusion, or -2 for evaporation-condensation. The measured slope will then indicate the relative importance of the three processes.

The latter method is more direct and does not depend on the accuracy of volume diffusion or vapour pressure data. However, its application is much more tedious but is necessary in cases where insufficient data on volume diffusion or evaporation is available, and would be preferred in cases where the contribution of the other processes is comparable to that of surface diffusion.

It should be noted, that only that part of the bulk diffusion coefficient which is due to the vacancy or interstitial mechanism should be used in assessing the importance of volume diffusion in the observed profile changes. Only these mechanisms are capable of producing a nett transfer of material. In cases where diffusion occurs by direct interchange or a ring mechanism, the value of D_v to be used in the above calculations will be less than that determined by the radioactive tracer technique.

If volume diffusion is dominant at large wavelengths then the technique could be applied to the measurement of volume self-diffusion coefficients.

(ii) Grain boundary Groove technique:

The use of Mullins' solution (40) of equation (7) for the case of grain boundary grooving has been described earlier. From equation (3) p.16 it is easily seen that if s_1, and s_2 are the semi-widths of a grain boundary groove (fig 3) before and after an annealing time Δt at a fixed temperature, then B at that temperature is given by

$$B = \frac{S_2^4 - S_1^4}{(2.3)^4 \Delta t} \qquad \ldots\ldots\ldots\ldots (16)$$

Equation (16) has been used to determine values of B from grain boundary groove measurements, during the present work.

IV. General Experimental Technique

Experiments have been carried out on the metals nickel, iron, gold and platinum. The general experimental procedure will be described here and details applying to particular cases will be mentioned later.

(i) Specimen preparation

Specimen materials used were normally obtained as flat cold-rolled sheet of thickness 0.1 to 0.5 mm.. Specimens of area ~ 1 square cm. were used. These were used in some cases in the as-rolled condition while others were mechanically polished. On annealing such specimens for a short period at a high temperature (eg. 3 hr at 1000°C for Ni) complete recrystallization occurs generally producing stable grains extending through the thickness of the sheet. With specimens used for scratch smoothing measurements, the scratches were made while the specimens were in the cold-worked condition. The initial anneal then served to produce smooth scratch profiles on the individual crystal surfaces of the polycrystalline specimens.

(ii) Scratching and Ruling

Single scratches were made on specimen surfaces with a clean razor blade to form a cross grid pattern. Approximately symmetrical profiles (fig 7a) were selected for measurement the 'wavelength' generally being about 10 microns.

Sets of closely spaced parallel grooves were produced by means of a simplified diffraction grating ruling machine.*

* Dr. Holborn of Aberdeen University provided much useful advice in the design of this instrument.

This is shown in fig(9). The soft iron head D, to which the ruling diamond is attached, is held against the smooth face of the brass block due to a flat pole magnet housed in a cavity within the block. The diamond, with a tip radius of curvature of about 3μ, rules a groove on the specimen surface on moving the carriage I parallel to the smooth face of the brass block. Further grooves are produced after displacing the platform J and specimen by rotating the graduated circle. A rotation of about 10^{0} produced a groove spacing of 7.2 microns. The load on the ruling head was adjusted by adding lead weights and was normally 10-20 gm wt. For a set of parallel grooves of average spacing 10μ deviations in spacings were normally $< 1\mu$.

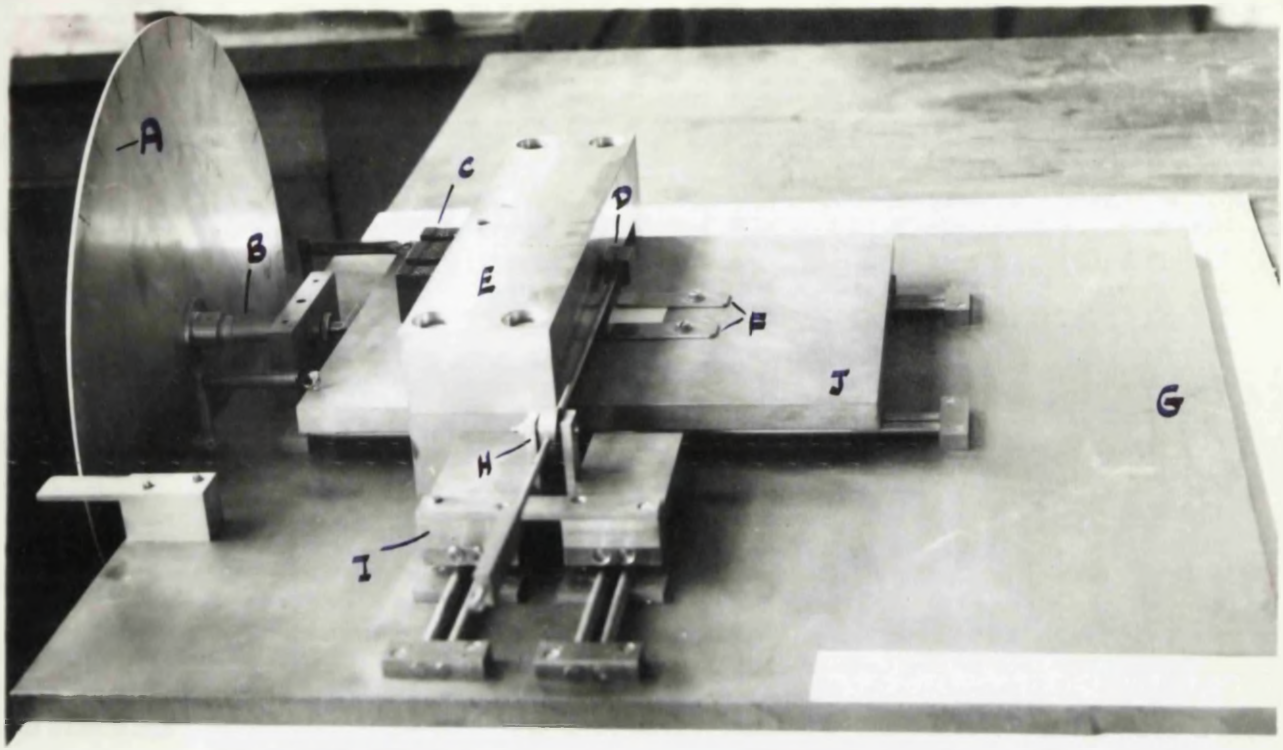

fig. 9

A: Graduated Aluminium disc.
B: Micrometer screw
C: Flat pole Magnet
D: Adjustable soft iron head supporting the ruling diamond and with soft solder contacts on brass block E.
F: Specimen clamps
G: Ground flat steel base
H: Loose pivot
I: Carriage which moves the diamond in a direction perpendicular to the direction of motion of the platform J.
J: Movable platform to which specimen is clamped.

(iii) Specimen annealing

Heat treatment of specimens was generally carried out in two vacuum furnaces. The basic design of the type of furnace used has been described by Mykura (41) and the arrangement used in the present experiments is shown diagrammatically in fig(10). The specimen is contained in the crucible C and placed with its plane near the vertical to minimize the effect of grain boundary sliding along grain boundaries at right angles to the surface. The crucible lid and radiation shields S_1 and S_2 were generally of the specimen material while the outer radiation shields S surrounding the winding were of commercial Ni sheet. It was hoped that with this arrangement, any impurity present in the residual furnace atmosphere would be deposited preferentially on the cooler outer shields. In one furnace the crucible, crucible and winding supports, and thermocouple insulation were of alumina, while in the other they were of fused silica. Molybdenum windings were used in the alumina furnace, in which the highest temperature heat treatments were carried out, and platinum or nichrome windings in the silica furnace. Power was supplied as shown in the circuit in fig(10), the current through the winding being controlled by a variac transformer. The outer vacuum-tight case was water-cooled, the flow rate being kept constant at about 4 litres per min., as measured by a 'Flowtrol' meter. A pressure of $< 10^{-5}$ mm Hg, indicated by a Penning gauge, was maintained within the furnace during annealing by an apiezon oil diffusion pump backed by a rotary pump. It was believed that the residual atmosphere was mainly hydrocarbon oil vapour. The heating and cooling times were normally short ($\sim$ 15 minutes) compared to the annealing

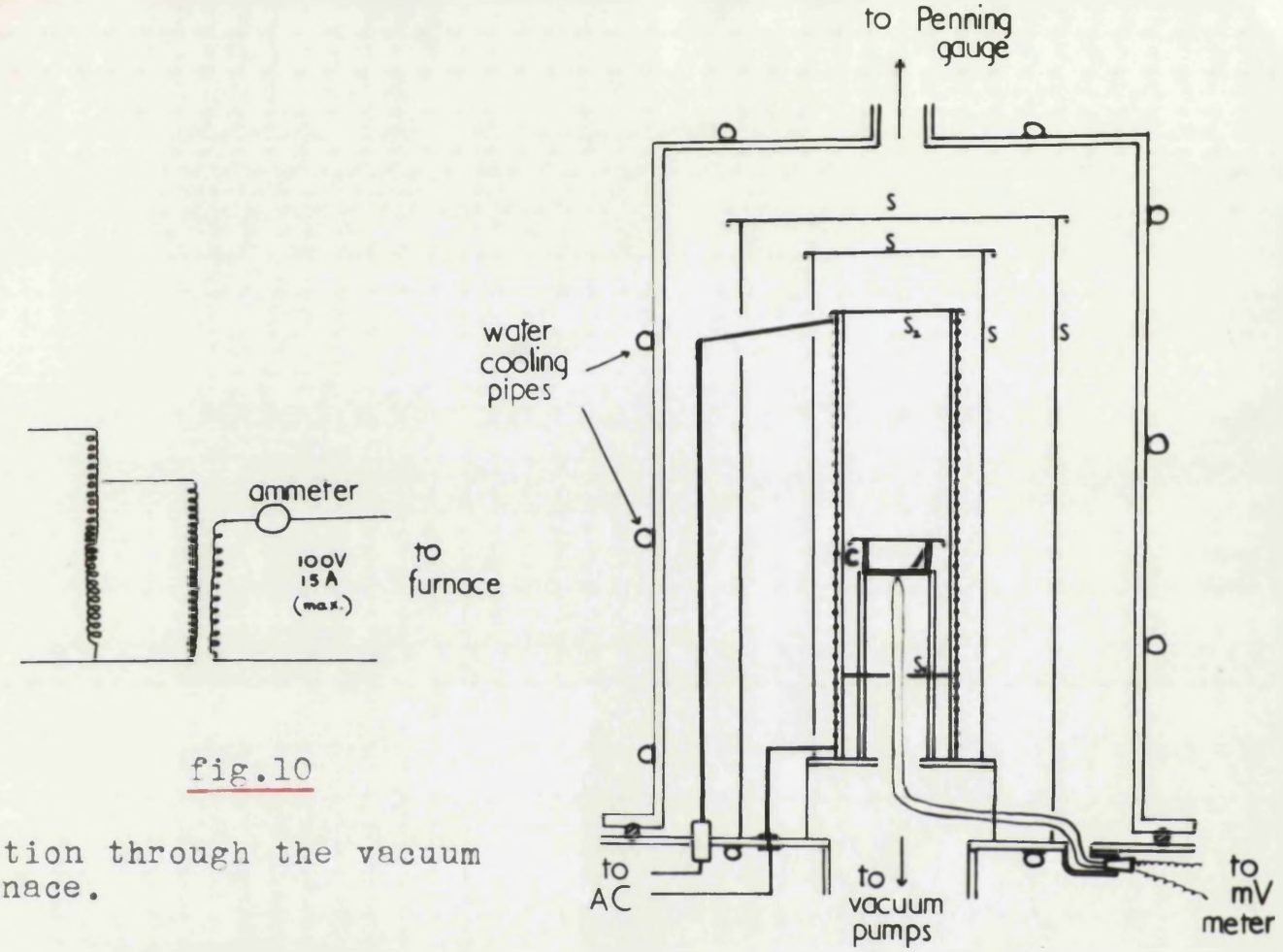

fig.10

Section through the vacuum furnace.

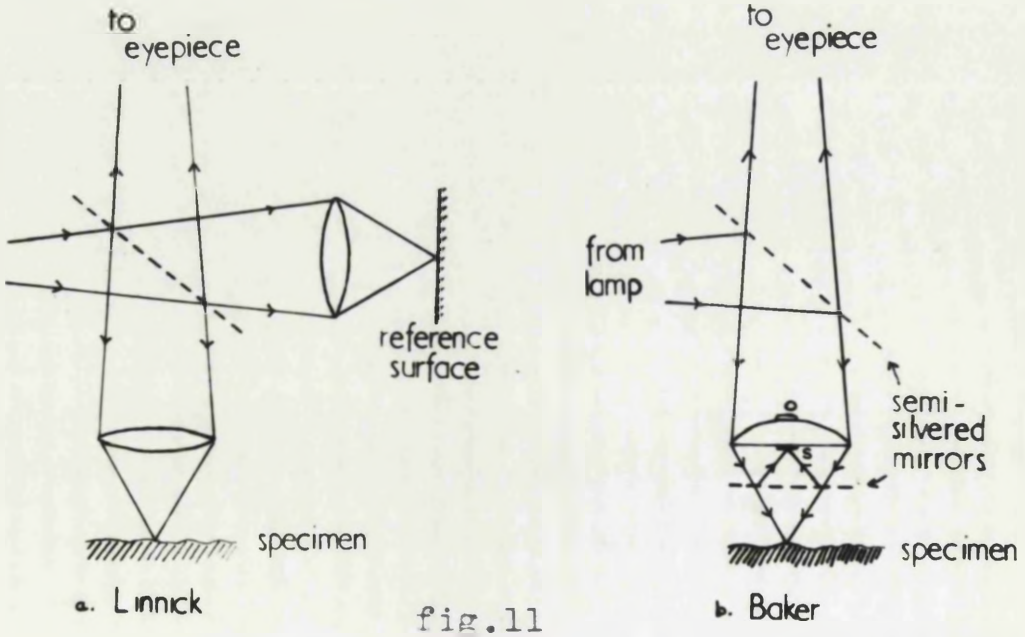

fig.11

Diagrams showing the optical equivalence of (a) the Linnick and (b) the Baker interference microscope systems.

intervals used (3 to 200 hours), and should cause negligible error. A safety switch ensured that the power supply to the furnace and diffusion pump were cut whenever there was a break in the water supply.

Temperatures were measured with chromel-alumel thermocouples except for heat treatments in the alumina furnace at temperatures above 1200°C when a Pt-13% Rh thermocouple was used. These were calibrated using data from Smithell's 'Metals Reference Book' (16) (1949) and the calibrations checked against the melting point of gold. During anneals temperatures were maintained constant to better than ± 10°C.

During periods when the furnaces were not in use they were held under vacuum, to reduce adsorption on the various components, and consequent degassing on further heating.

(iv) Specimen Observation

Specimens were examined in air by ordinary and interference microscopy. The mass transfer technique developed in this work, in conjunction with interference microscopy provides a fairly accurate method for the measurement of surface self-diffusion coefficients. The results reported later are mainly derived from measurements on micro-interferograms.

Measurement of surface topography with the interference microscope

The aim of the micro-interferometric technique is to provide an accurate contour map of the surface under observation from which the size, shape etc. of small topographical detail may be found. Although accurate data can be derived from interferograms considerable care must be used in their interpretation. Several authors (Mykura (41)(62)(1954), Ingelstam(63)(1960), Tolman and Wood (64)(1956) Gates (64) (1956)) have discussed the sources of error in interference

microscopes. Those which are important in the present work are discussed briefly.

A Baker interference microscope was used. Optically, this is almost identical to the Linnick system in which interference fringes are formed by light reflected from the specimen surface and a flat reference surface. These systems are shown in fig(11). In the Baker microscope the reference surface is contained within the objective lens (silvered spot S) in which there is also an opaque disc (O) to prevent light being reflected directly into the eyepiece. Variation of the wedge angle between reference and specimen surface is achieved by means of a tilting stage. The chief disadvantage of having the reference surface fixed within the objective arises from the fact that it is generally not exactly parallel to the focal plane of the lens. Thus only in a small region, on either side of the line of interception of the focal plane and the virtual image of the reference surface, are sharp fringes produced. Outside this area the path difference is too great. In addition the area over which sharp fringes are obtained depends on the direction of tilt of the stage, the area being greatest when the stage is tilted about a horizontal axis parallel to the tilt axis of the reference surface. The area of specimen illuminated cannot be easily controlled with the result that light, scattered into the objective from regions outside the field of view, causes a reduction in fringe contrast.

The simple relation between the fringe system and the depth of the wedge between reference and specimen surface, (i.e. 1 fringe $\equiv \frac{\lambda}{2}$), holds only for normal incidence, Tolman and Wood, and Gates (64). When strongly convergent illumination is used, as in the Linnick or

Baker systems with objectives of high numerical apertures (N.A.), the above relation does not hold exactly and leads to errors of the order of 10%.

To eliminate this source of error the Baker instrument was calibrated for a 4 mm interference objective as follows.

The height of a cleavage step on a silvered mica surface was measured at objective aperture settings of 1.0 to 5.0 scale divisions, (i.e. N.A.'s from 0.15 to 0.7 approximately), assuming the fringe interval to correspond to $\frac{\lambda}{2}$. Due to the central opaque disc in the objective, the aperture cannot be reduced sufficiently to produce almost parallel illumination and allow a close estimate of the true step height. For this purpose a Linnick instrument was used, employing a X25 objective and aperture 0.5 scale divisions, N.A.$\approx$ 0.05. The results are summarised in table IV which shows the percentage error at different aperture settings and the effective values of $\frac{\lambda}{2}$ to be used. At the setting generally used in photographing surface profiles (3.0 scale divisions) the fringe interval was taken as 0.3 microns for calculation purposes.

Although the effect of oblique illumination must be taken into account when absolute values for the height of surface irregularities are required, or in angle measurements, it does not introduce an error in measuring the rate of decay of sinusoidal profiles. Provided that approximately the same fringe spacing is used for successive interferograms (see eg. fig(24)) the error can be eliminated by taking one fringe as the unit of depth in plotting the rate of smoothing. All measurements were made on prints enlarged to a magnification of x1000 so that 1 mm$\equiv$ 1 micron.

The experimental error in diffusion coefficients from scratch smoothing measurements (eg. fig(24)), arises from inaccuracies in

Table IV

Calibration of the Baker Interference Microscope

	Baker (Hg green light λ = 5461Å)					Linnick (Tl green$_o$ λ = 5351Å)
Aperture (scale divisions)	1.0	1.5	2.0	3.0	5.0	N.A.≈ 0.05
Fringe displacement (No. of fringes)	5.05	5.03	5.00	4.89	4.81	5.38
Apparent step height (microns)	1.379	1.375	1.366	1.337	1.315	1.46
True step height (microns)						1.46
Error	5.5%	5.8%	6.4%	8.4%	9.9%	-
Effective $\lambda/2$ (microns)	0.2894	0.2900	0.2920	0.2986	0.3035	

the wavelength λ, and slope of the decay curve. λ can be measured to within about 0.25μ. For a wavelength of 10μ, this introduces an error of about 10%; the final error is of the order of $\pm$ 20%.

Orientation Measurements:

Surface orientations were determined, in the case of f.c.c. crystals, from measurements of the angles between the traces of annealing twins. The problem is essentially the determination of the direction cosines of an arbitrary plane, from a knowledge of the angles between its intercepts on the surfaces of a regular tetrahedron. The solution can be obtained graphically (Barrett (65)(1952), Mykura(66)(1958)) and this method has been used in the present work. An analytical solution has recently been derived* but this has not yet been tested. The orientations determined by the twin trace technique are generally accurate to about 2°.

For b.c.c. specimens of α-iron, the x-ray back reflection technique was used, employing a Hilger microfocus X-ray tube (see fig(46)). The orientations found by this method are also believed to be accurate to within 2°.

* Mainly by Dr. J. Cumming of the Physics Dept. of Glasgow University.

V. Surface Self-Diffusion Experiments

The experiments performed on nickel, gold, iron, and platinum will be considered separately and a general discussion of the results given later.

Va. Experiments on Nickel

Introduction

Measurements were made on the rate of smoothing of single and multiple scratches on individual crystals of polycrystalline nickel specimens. The results show a marked variation of self-diffusion coefficient with crystal orientation. It was also found that "flats" of exact (100) and (111) orientation develop when a curved surface includes such a low index plane, and this is taken to indicate that the surface diffusion coefficient for such a plane is much greater than for one of random orientation. At the lower temperatures used impurity adsorption was found to have a large effect on the variation of both surface diffusion and surface energy with crystal orientation.

Experimental

The experiments were carried out on Ni sheet. In one set of runs 'specpure' Ni (from Johnson, Matthey & Co.) was used, the main impurities being: Fe 0.002, Cu 0.0002, Ag 0.0001 per cent., non-metallic impurities not given. Another set of runs was made on commercial Ni sheet whose main impurities were: Fe 0.2, Cu 0.2, Mg 0.1, C 0.05, S 0.005 per cent.

Both grades were used in the "as-rolled" condition, except for pure Ni specimens used at 900°C and 1200°C, which were mechanically polished. Single and multiple scratch experiments were carried out at different times so that the same specimens were

not used for both sets of experiments. Single scratch experiments were performed on both 'specpure' and commercial Ni sheet, while in multiple scratch experiments only the latter was used. Annealing was carried out in a continuously pumped vacuum ($\approx 10^{-5}$mm Hg) at temperatures between 800 and 1220°C. In the case of single scratch specimens, the cumulative heating times were 2, 6, 12, and 22 hr at 1200°C, 3, 23, 70 and 170 hr at 800°C and proportionate times at intermediate temperatures. For multiple groove specimens the corresponding times were 3, 8 and 18 hrs at 900°C, and 1, 3 and 5 hrs at 1220°C. All specimens were subjected to a short initial anneal at a temperature of 1000°C or higher when recrystallization produced stable grains of about 150μ diameter, many grains extending through the thickness of the sheet.

The specimens were examined and photographed after each heat treatment by ordinary and interference microscopy. The scratch profiles were obtained from measurements of the interferograms. Measurements were only made on single scratches which were approximately symmetrical and multiple scratches of nearly uniform depth. At each temperature the rate of scratch smoothing was measured on at least 25 different crystal surfaces. Data on the variation of D_s with orientation was obtained by determining the orientations of a large number of crystals on the 1000°C and 900°C single scratch specimens, by the twin boundary trace method.

(i) Results on single scratches

The smoothing of a typical single scratch profile is shown in fig(12). The values of B and D_s calculated are given in table Va. These are averages of the measured values and are thus averages over all orientations. The values of γ_s required to calculate D_s

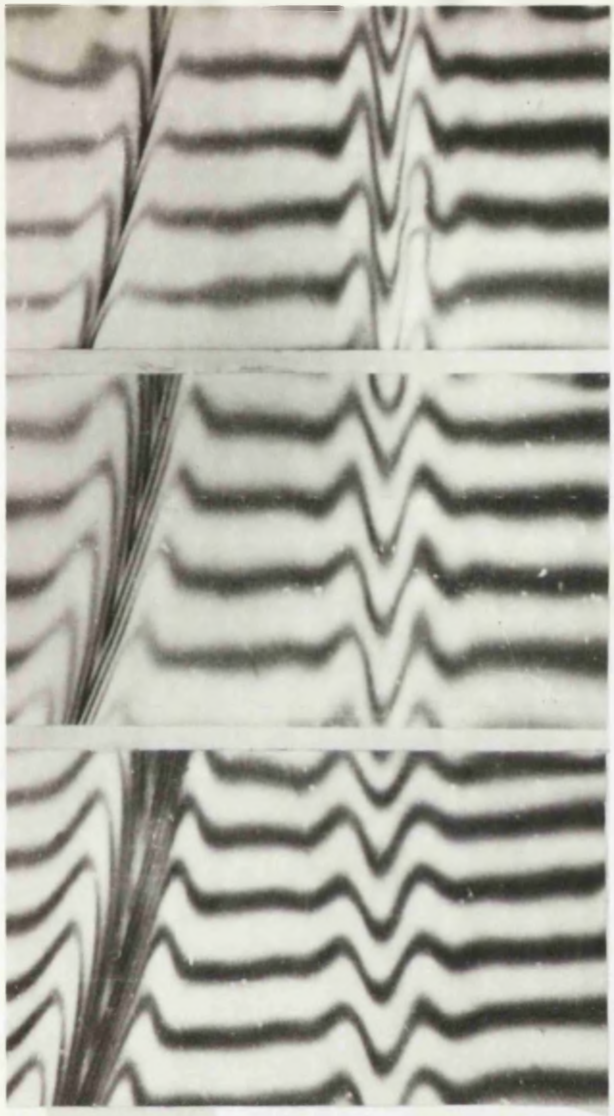

fig.12

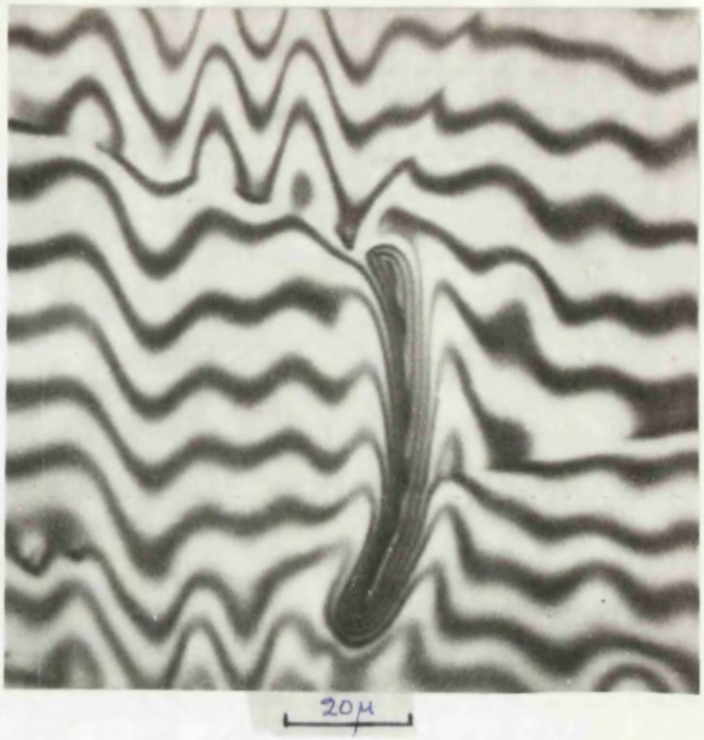

fig.13a

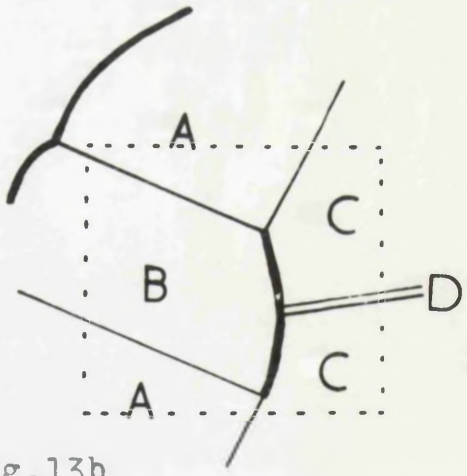

fig.13b

fig.12: Smoothing of an approximately symmetrical scratch and development of a grain boundary groove (a)after 2 hr at 1000°C, (b) after 21½hr at 900°C,(c) after 47 hr at 800°C. The value of D_s calculated from this scratch is 0.1 x 10^{-6} cm^2/sec and from the grain boundary 0.8 x 10^{-6} cm^2/sec.

fig.13: Abrupt change in the smoothing rate of a multiple scratch (heated at 1000°C) where the orientation changes due to twinning. The arrangement of twin and grain boundaries is shown in fig.13b. For grain A, D_s = 0.6 x 10^{-7} cm^2/sec; for B, 7 x 10^{-7}, and from the grain boundary BC, 6 x 10^{-7} cm^2/sec.

Table V

Surface Diffusion Results on Ni

	Temperature (°C)	γ_s (ergs/cm^2)	Pure Nickel B (cm^4/sec) (x 10^{-20})	Pure Nickel D_s (cm^2/sec) (x 10^{-6})	Impure Nickel B (cm^4/sec) (x 10^{-20})	Impure Nickel D_s (cm^2/sec) (x 10^{-6})
Va	1200	1800	2.1	6.07	1.9	5.5
Single Scratch Results	1100	1850	1.4	3.67	1.0	2.6
	1000	1900	1.2	2.84	0.7	1.6
	900	1950	0.5	1.06	-	-
	800	2000	0.29	0.55	0.16	0.3
Vb	1220	1790			3.25	9.73
Multiple Scratch Results	1100	1850			1.69	4.5
	1000	1900			0.83	2.01
	900	1950			0.31	0.66

from B ($= \frac{D_s \gamma_s \Omega^2 \nu}{kT}$) are extrapolated from Hayward and Greenough(67) (1960); $\Omega^2\nu$ was put equal to d^4 where d is the interatomic distance ≈ 2.5Å. In addition to the systematic errors discussed in section III p.31, these values may be in error by $\pm$ 50 per cent. due to measuring inaccuracies and possible bias in the orientation of the crystals measured.

Values of B and D_s were also calculated from measurements on 20 approximately symmetrical grain boundaries at 1000°C using equation (16), to give a mean value of D_s of 5.5×10^{-6} cm^2/sec for pure Ni. The development of a grain boundary groove can also be seen in fig(12). It will be noted that the value of D_s at 1000°C from grain boundaries is almost twice as large as the value in table Va. The agreement is however tolerable, as some boundaries with one slow diffusing grain were rejected due to assymmetry, so that the result may be biased toward orientations with higher values of D_s.

Dependence of D_s on surface orientation

The effect of surface orientation is shown by the marked change in scratch smoothing rate observed at some twin and grain boundaries. Fig(13) shows an example of this. Here the differential smoothing of parallel grooves can be seen. These were produced during the rolling of the material. The relation between surface orientation and diffusion rate was studied at 1000°C and 900°C for pure Ni. The rate of smoothing of similar scratches on the surfaces of crystals of different orientations was assigned a relative value: fast, medium, slow or very slow. The results are shown in fig(14ab). In fig(14a) the directions of diffusion are also shown. It will be noticed that in fig(14b) (900°C

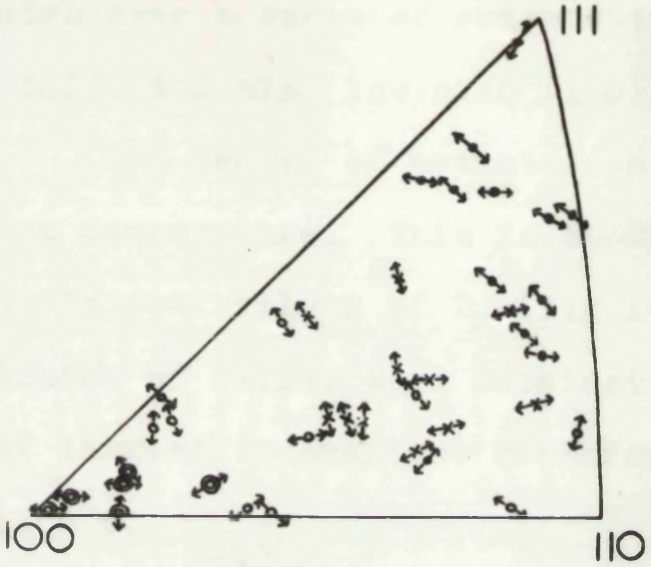

fig.14a

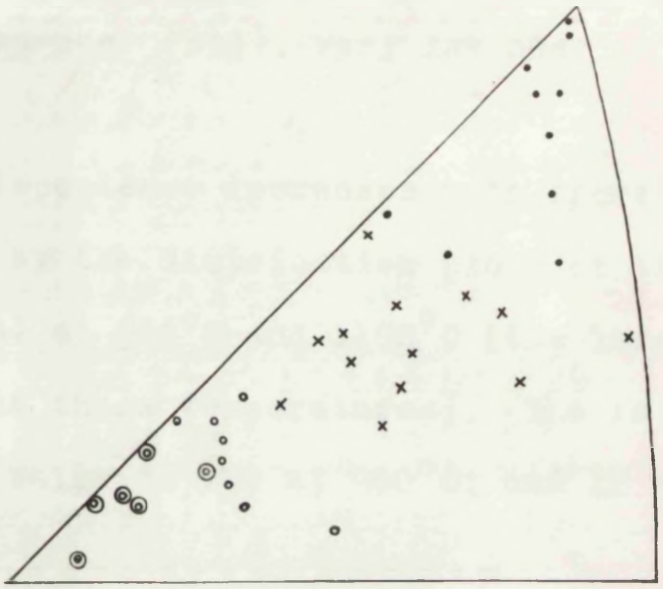

fig14b

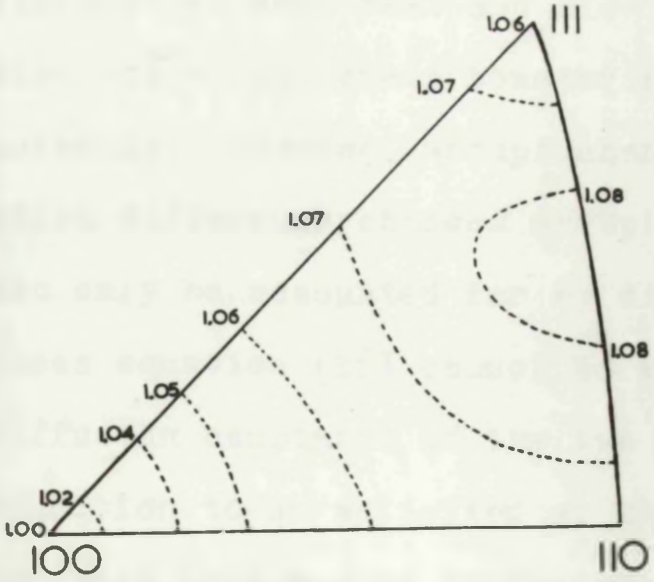

fig.14c

Variation of diffusion rate (a) at 1000°C and (b) at 900°C, with surface orientation for pure nickel. • fast, × intermediate, ° slow, ◎ very slow.
(c) Variation of the surface energy (γ_s) with orientation for nickel (Mykura(60)). Values of γ_s are normalised to give a value of unity for the (100) plane.

result) no points have been included near (110); this will be explained later. The results show that the diffusion rate is high over a range of orientations near (111), very low near (100), and also low near (110).

The degree of orientation dependence decreases with increasing temperature. This is shown by the distribution plots of the individual values of D_s (fig 15a) at 900°C and 1100°C (the largest number of values were obtained at these temperatures). The ratio of largest to smallest measured value is 250 at 900°C, and 12 at 1100°C.

The large variation of D_s with orientation also causes the formation of assymmetrical grain boundary grooves, as indicated in fig(16c), between fast and slow diffusing grains. Assymmetry could also arise when grain boundaries do not intercept the surface normally. However, abrupt changes in assymmetry when the orientation difference changes abruptly at twin boundaries (fig 18a,b), can only be accounted for by different diffusion rates. In such cases equation (16) cannot be applied separately to give the diffusion constants of the two grains, since there is a continuity condition to be satisfied at the groove root. Thus it might be expected that a slow diffusing grain would appear to have a larger diffusion constant by being adjacent to a fast diffusing one, and vice versa.

In addition to the variation of D_s in cases of general orientation there is an even more striking change at exact (111) and (100) orientation. When the orientation range covered by the curved surface of a smoothing scratch or of a grain boundary, includes these low index planes, the normal profile is distorted

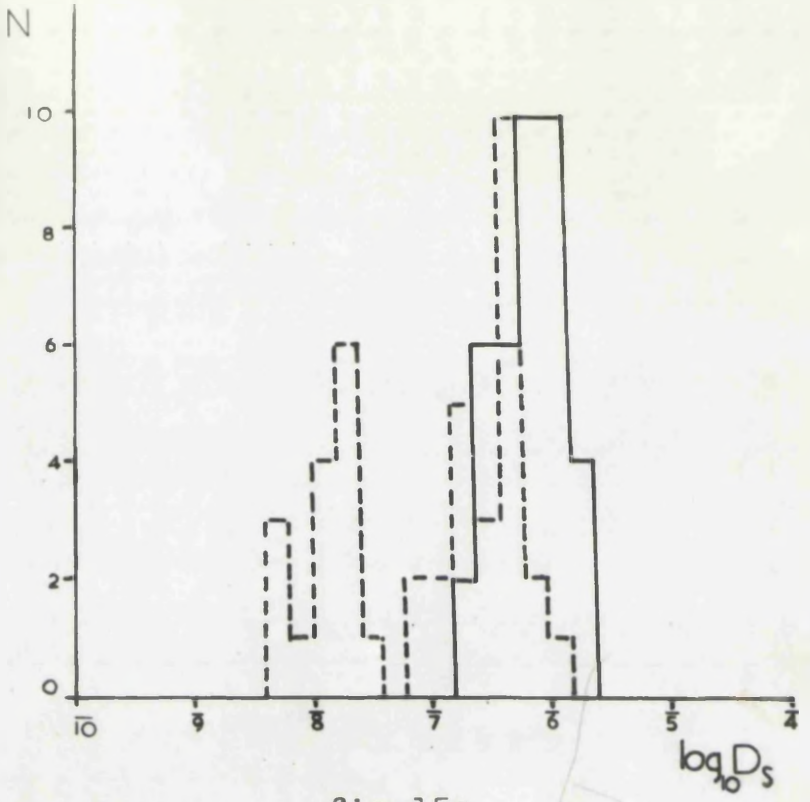

fig.15a

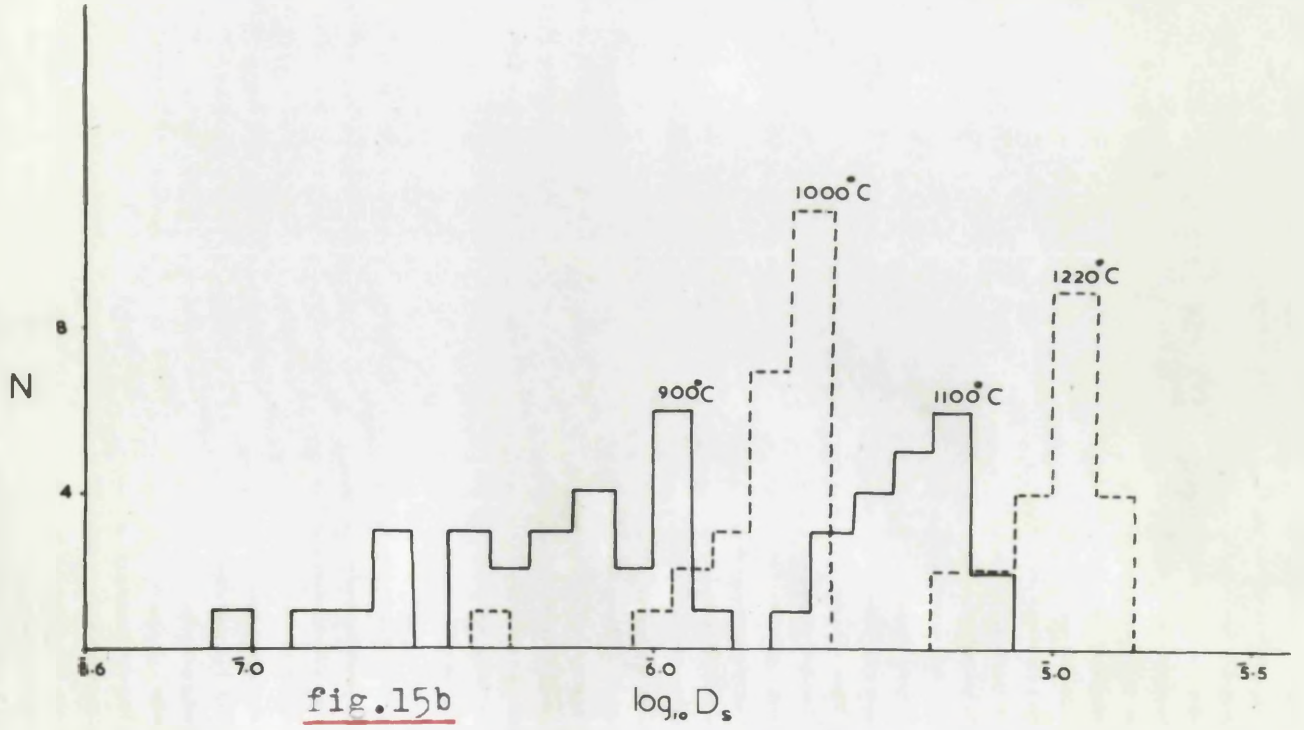

fig.15b

(a) Distribution plots of values of D_s at 900°C (----) and 1100°C (——) from single scratch measurements.

(b) corresponding plots for multiple groove results.

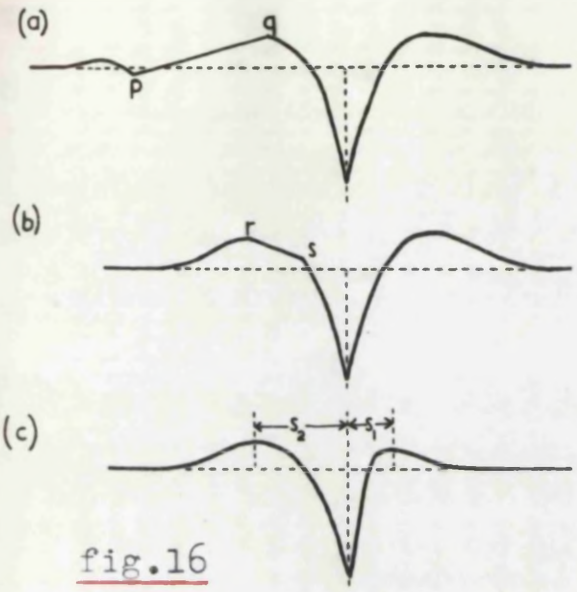

fig.16

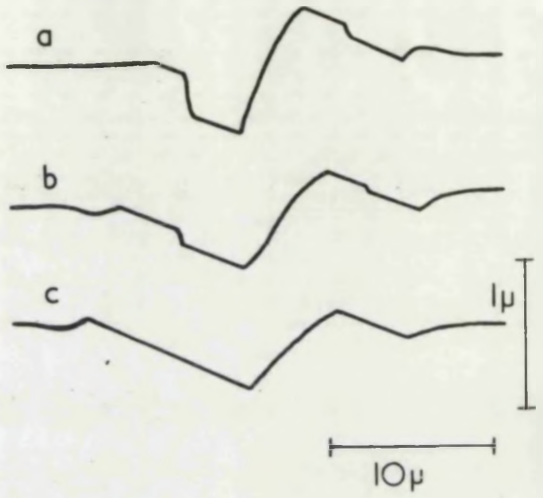

fig.17

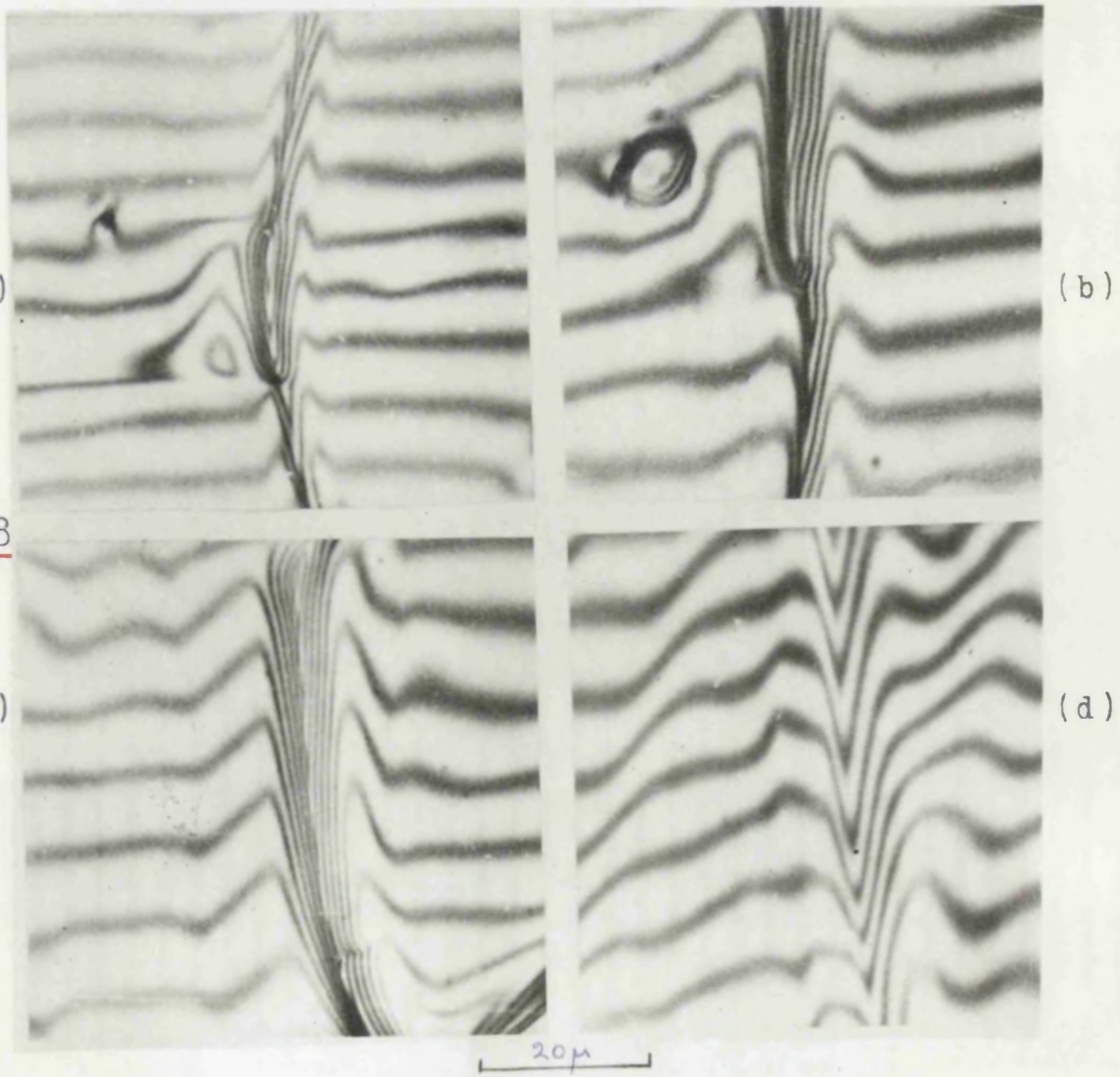

fig.18

fig.16 (a)(b): Distortion of grain boundary groove profiles due to the formation of flats pq and rs. (c) asymmetrical groove between grains of different surface diffusion coefficients.

fig.17: (111) flats observed on a scratch profile on annealing at 1000°C, after (a)30 hr, (b) 60 hr, (c)100 hr.

/over

fig.18: Interferograms (a) and (b) show marked change in grain boundary asymmetry where the misorientation changes abruptly due to twinning. (c) and (d) show examples of exact (111) and (100) flats respectively.

and flat regions of the low index plane appear (figs 16, 17, 18). The formation of low index flats is thought to be due to a lower surface free energy at these orientations. That they persist on reheating shows that there is active diffusion across them. Any curvature of the facets is too small to be measurable; assuming that in this case also the rate of mass transfer is proportional to curvature gradient, the diffusion constant for the low index plane must be much greater than for the adjacent general surface. Similar conclusions have been reached by Moore (45)(1958) from his study of striations on silver and by Gomer(46)(1953) in work with the field emission microscope.

No evidence was obtained on the variation of D_s with direction for a given orientation. The techniques used are, however, more sensitive to variations with orientation than to variation with direction for a fixed orientation.

Each individual value of D_s must be interpreted as applying to the small range in orientation covered by the curved profile of the scratch. The value of D_s obtained will be biased toward the smallest value for the orientations included as this portion of the profile will determine the net flux of atoms. This is also true for D_s calculated from grain boundary grooves, and the range of orientation is usually much larger in this case. In fig(19a) the poles of crystals A and B (fig 13a,b) are shown, together with the range of orientation and direction of diffusion of the scratches. Fig(19b) is the corresponding stereogram for crystals B and C and the grain boundary groove between them. As can be seen the surfaces at the grain boundary range over about 12° in each crystal while at a scratch it may range over $\pm$ 4° and this

decreases on further annealing and is still measurable at $\pm$ 2°.

Discussion of single scratch results

That volume diffusion and evaporation-condensation can be neglected is shown by the graphs in fig(20). Here the variation of the decay constants Bw^4, Cw^3, and Aw^2 (equation (11)) with temperature has been plotted for values of the wavelength λ ($= \frac{2\pi}{\omega}$) of 2, 10 and 50 microns. The values for the vapour pressure required to calculate A were taken from Dushman (68)(1949), volume diffusion constants used in the calculation of C from Reynolds et al (51) and Hoffman et al (52) and the measured values were used for B. The graphs show that at low temperatures and short wavelengths, surface diffusion is highly predominant and even at the melting point the other processes may be neglected for wavelengths up to 10 microns. The assumption that surface diffusion is effectively the only process operative is therefore justified.

The small difference in results obtained with the pure and the commercial nickel indicates that any contamination is more likely to have come from the furnace atmosphere than from impurities present within the specimen. At the higher temperatures, the furnace should be self-cleaning and no difficulty was experienced. At lower temperatures the surfaces of some grains broke up into striations and in a few cases visible deposits appeared. Fig(21) shows a typical region of a contaminated Ni specimen. Such specimens were rejected and measurements made only on specimens which appeared clean and on unstriated crystal surfaces. It is quite possible that, even though such specimens were clean to microscopic examination, they had adsorbed impurity on the surface during annealing.

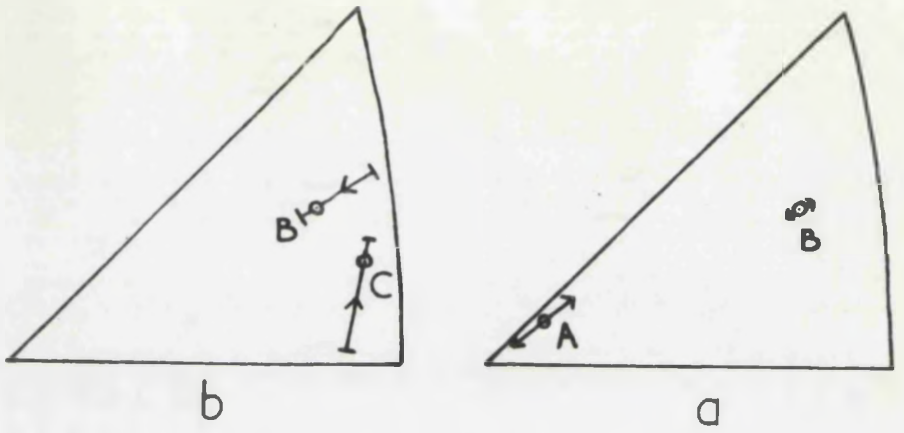

fig. 19

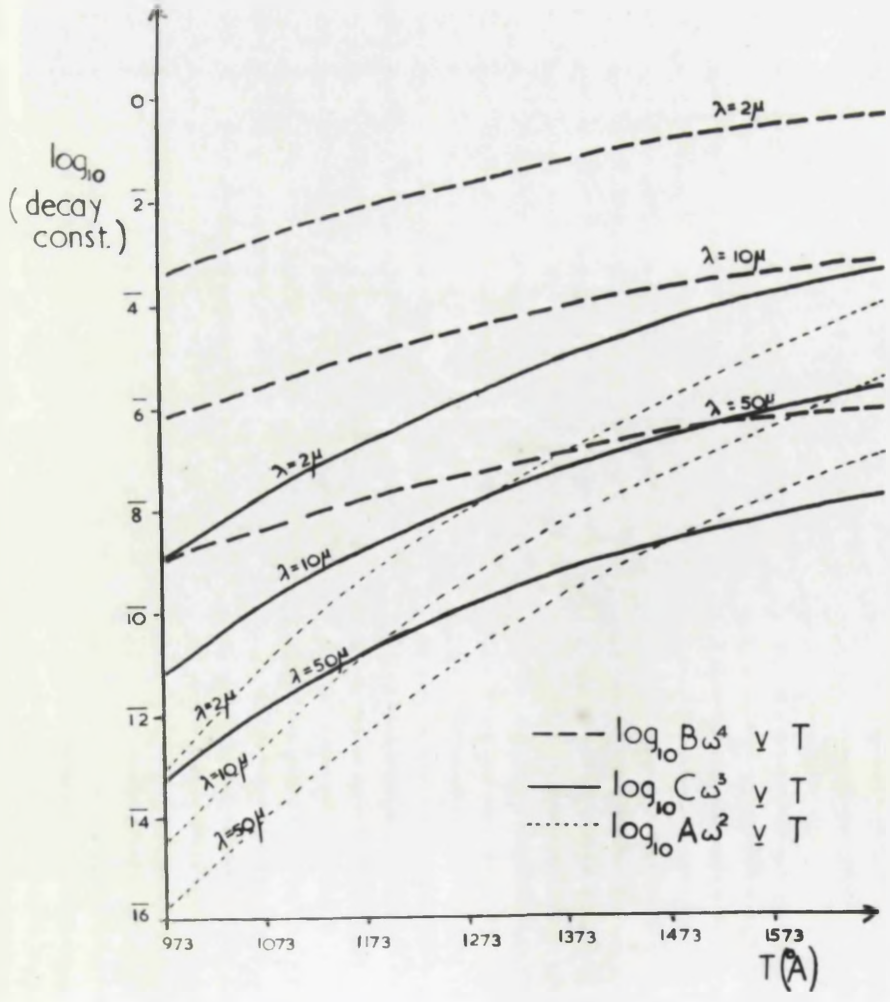

fig.20

fig.20 :Variation with temperature of the relative importance of the three transport mechanisms in causing surface smoothing. At the melting point the surface diffusion contribution exceeds the others by factors of 10^3, 10^2, and 3 ,for wavelengths of 2, 10, and 50μ , respectively. For $\lambda > 150\mu$, evaporation - condensation predominates.

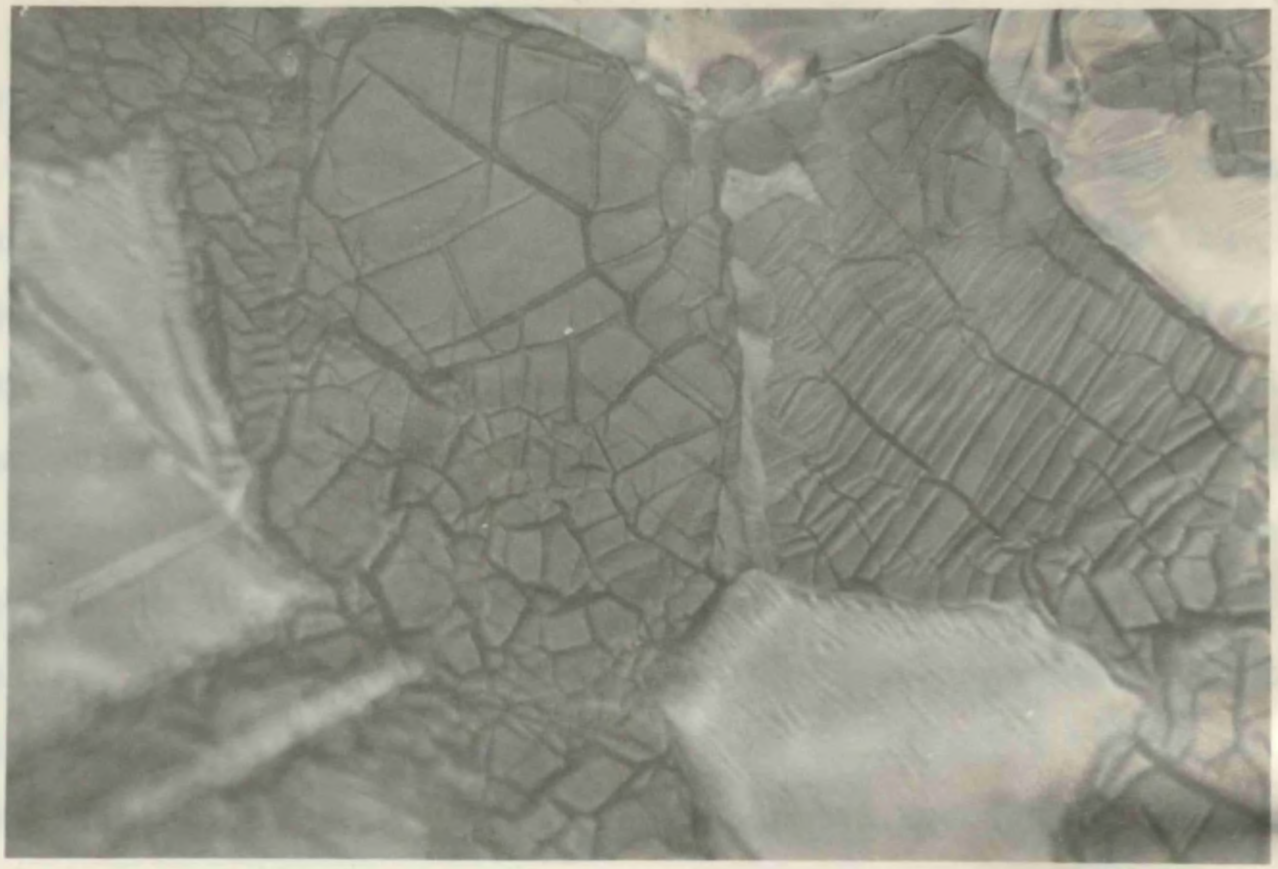

fig.21

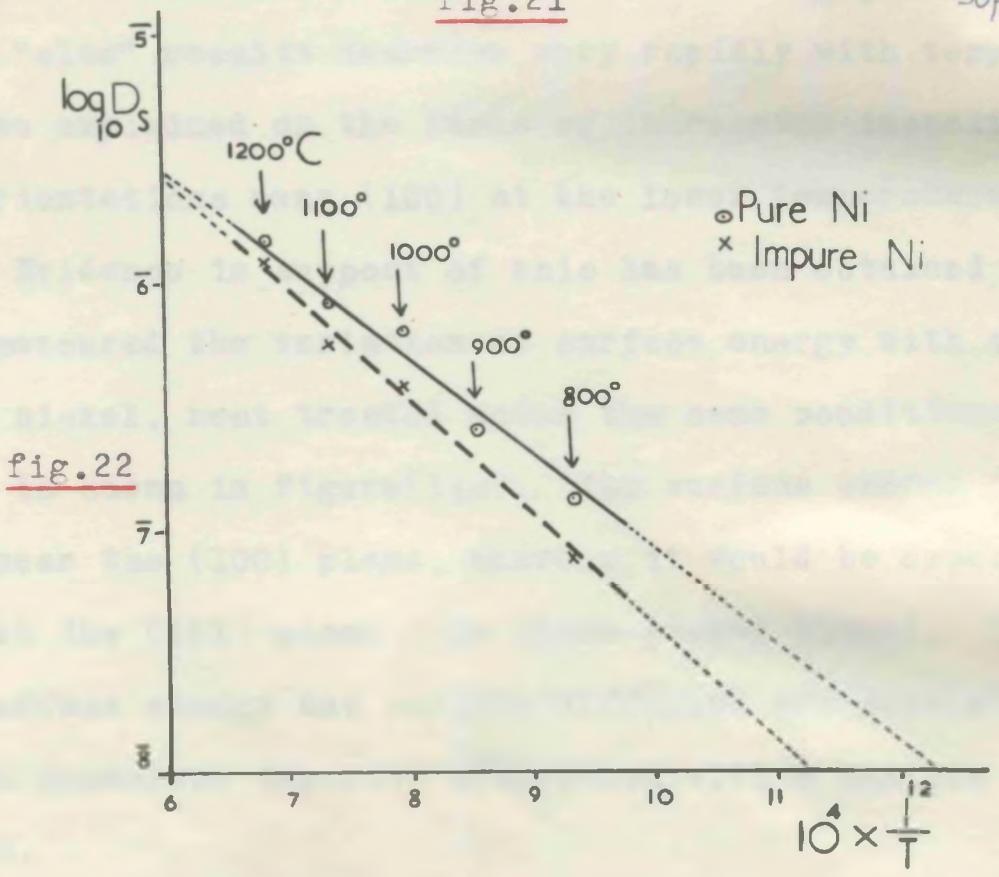

fig.22

fig.21: Orientation dependent contamination on the surface of a pure nickel specimen annealed in a poor vacuum.

fig.22: Plots of $\log_{10} D_s$ against 1/T for pure and impure nickel.

The average values of D_s from table Va can be fitted to the usual equation $D_s = D_o \exp(-Q_s/kT)$ as in fig(22) and give $Q_s = 0.78 \pm 0.1$eV and $D_o = 3.0(\pm 1) \times 10^{-3}$ cm^2/sec for pure nickel and $Q_s = 0.92 \pm 0.1$eV and $D_o = 6.8(\pm 2) \times 10^{-3}$ cm^2/sec for the impure nickel. As the spread in measured values of D_s increases with decreasing temperature, the activation energies for particular orientations will be larger and smaller than these. If it is assumed that D_s varies with orientation at all temperatures in the same way as measured at 1000°C and 900°C (fig 14ab), the measured values at each temperature can be divided into a "fast" half corresponding to orientations near (111), and a "slow" half for orientations near (100). The separated average values for the pure nickel results are plotted as $\log_{10} D_s$ against $1/T$ in fig(23). The "slow" results decrease very rapidly with temperature and can be explained on the basis of increasing impurity adsorption on orientations near (100) at the lower temperatures.

Evidence in support of this has been obtained by Mykura(60) who measured the variation of surface energy with orientation for pure nickel, heat treated under the same conditions at 1000°C. This is shown in figure(14c). The surface energy is lowest at and near the (100) plane, whereas it would be expected to be lowest at the (111) plane (the close-packed plane). The variation of surface energy and surface diffusion are consistent with orientation dependent impurity adsorption with a maximum near the (100) plane.

From fig(23), $Q_s = 0.62(\pm 0.08)$eV and $D_o = 1.9(\pm 0.6) \times 10^{-3}$ cm^2/sec for orientations near (111), while near (100) $Q_s = 1.7$ (± 0.2)eV and $D_o = 0.66$ cm^2/sec. From equation (4) section IIc,

D_o can be written as $\alpha a^2 f$ where $\alpha = 1/3$ or $\frac{1}{4}$. Taking the jump distance $a \approx 2.5 \times 10^{-8}$ cm. for nickel and $f \approx 9 \times 10^{12}$ sec^{-1} from the Debye theory (69), gives $D_o \approx 1.5 \times 10^{-3}$ cm^2/sec which is in fairly good agreement with the measured value of D_o near (111). The activation energy, 0.62eV, also is reasonable in relation to the known activation energies for volume self-diffusion of nickel 2.75eV(51,52) and grain boundary diffusion 1.1eV (Upthegrove and Sinnot(70)(1958)). The apparent activation energy of 1.7eV obtained for surface self-diffusion on orientations near (100) can then be interpreted as the combination of a true activation energy plus the suppression of diffusion at lower temperatures by increasing impurity adsorption. The very large D_o obtained for these orientations is due to the fact that the value of D_o calculated is very sensitive to changes in Q_s.

It is interesting to note that the experiments of Gjostein (42) on grain boundary grooving in Cu, surfaces near (100) were used and there also a large activation energy (1.7eV) was found. It is possible that this is partly due to impurity adsorption on the Cu surfaces, although Gjostein claims that this did not occur.

More will be said later about the effect of impurity on Ni surfaces at the lower temperatures used.

(ii) Results on Multiple scratches

Sets of parallel scratches of spacing less than 10μ were made on the surfaces of specimens of commercial Ni as described earlier (section IV). The smoothing of a typical multiple scratch profile of wavelength about 6.5μ is shown in fig(24). Measurements were made on symmetrical portions of the profiles and values of B calculated from graphs of the type shown, the

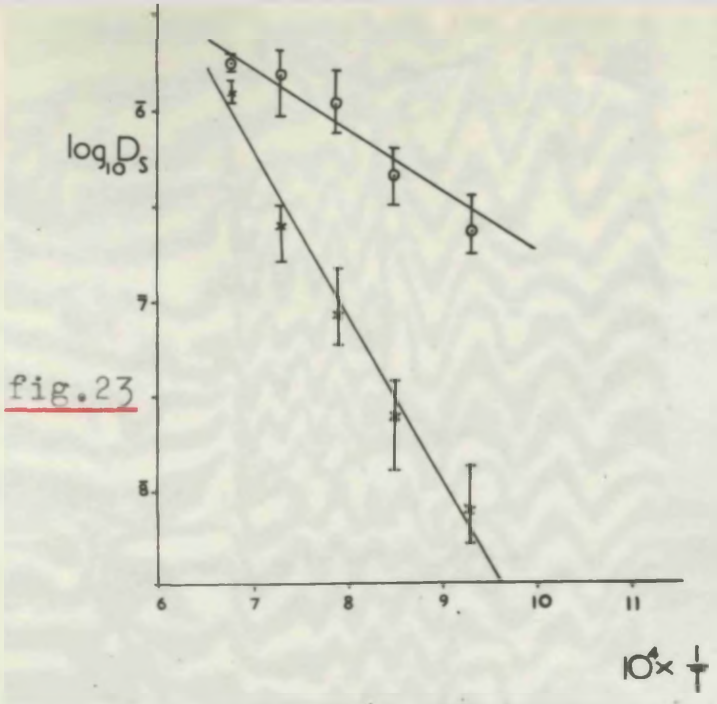

fig.23

fig.23: Plots of $\log_{10} D_s$ against $1/T$ for nickel surface orientations near (111) (circles) and near (100), (crosses).

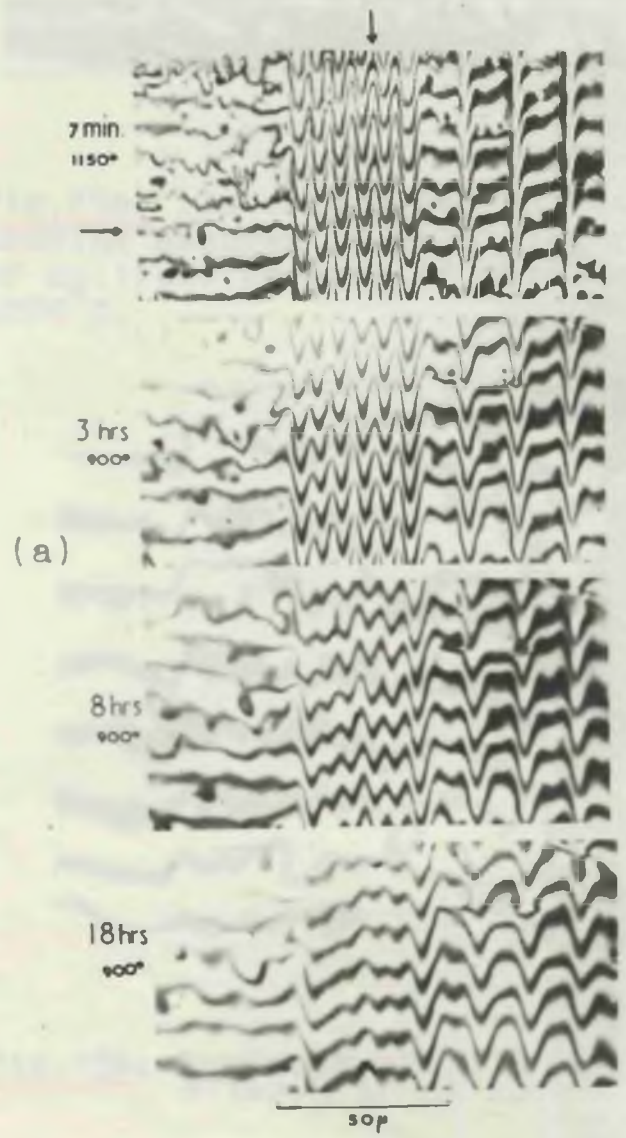

(a)

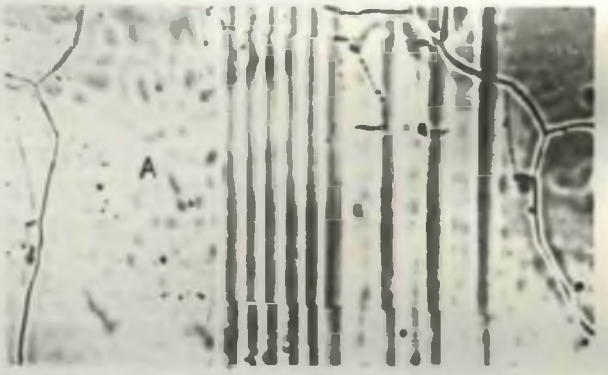

(b)

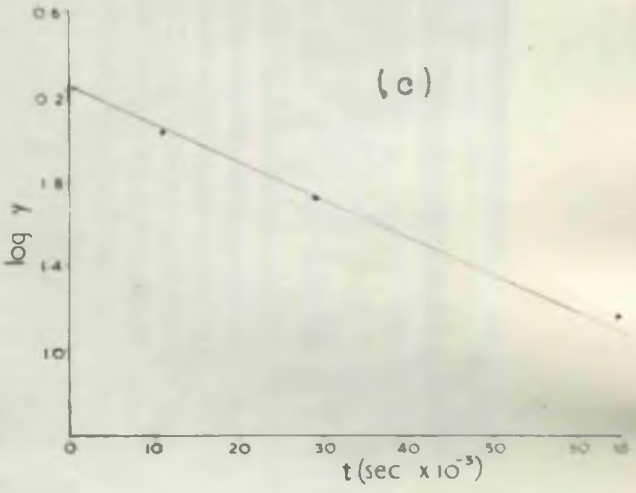

(c)

fig.24

fig.24 : (a) Smoothing of a multiple scratch on a Ni crystal surface. (b) Ordinary photograph showing the twin A to which the interferograms refer. (c) Corresponding plot of log(amplitude) against time. (λ = 6.5 microns).
Note that the extreme grooves have smoothed more slowly as described earlier. (fig.8)

fig.25a: Interferogram and corresponding ordinary photograph showing changes in smoothing rate at twin and grain boundaries of multiple grooves of wavelength 8 microns after annealing at 1000°C.

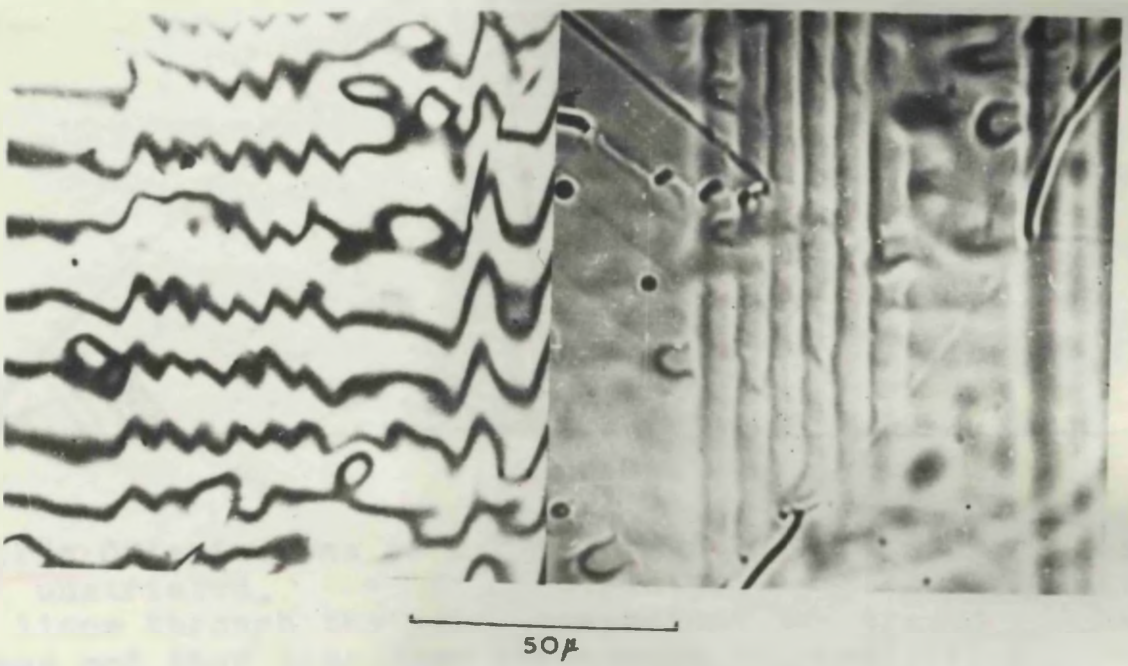

fig.25b: Sawtooth profile due to (100) facets on multiple grooves after 5 hr at 1100°C.

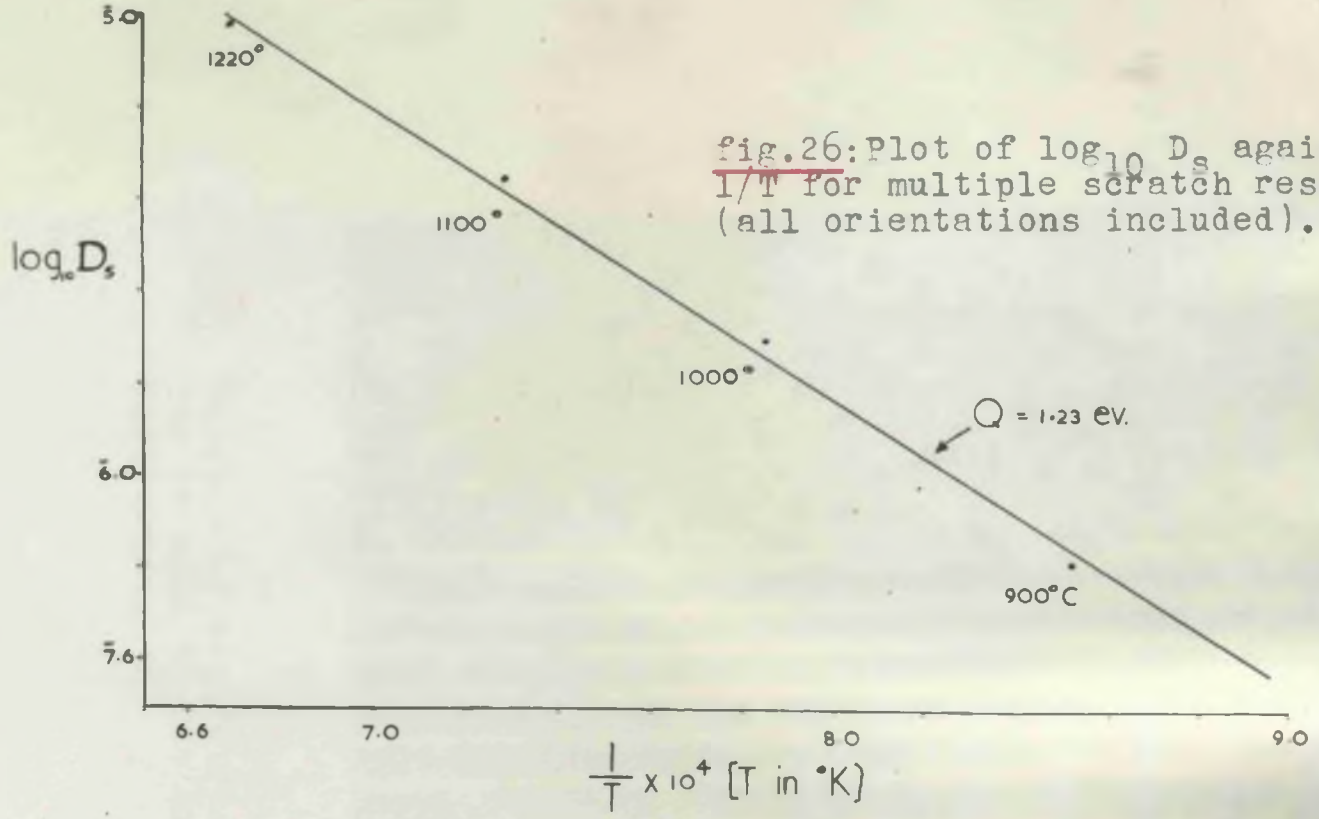

fig.26: Plot of $\log_{10} D_s$ against 1/T for multiple scratch results (all orientations included).

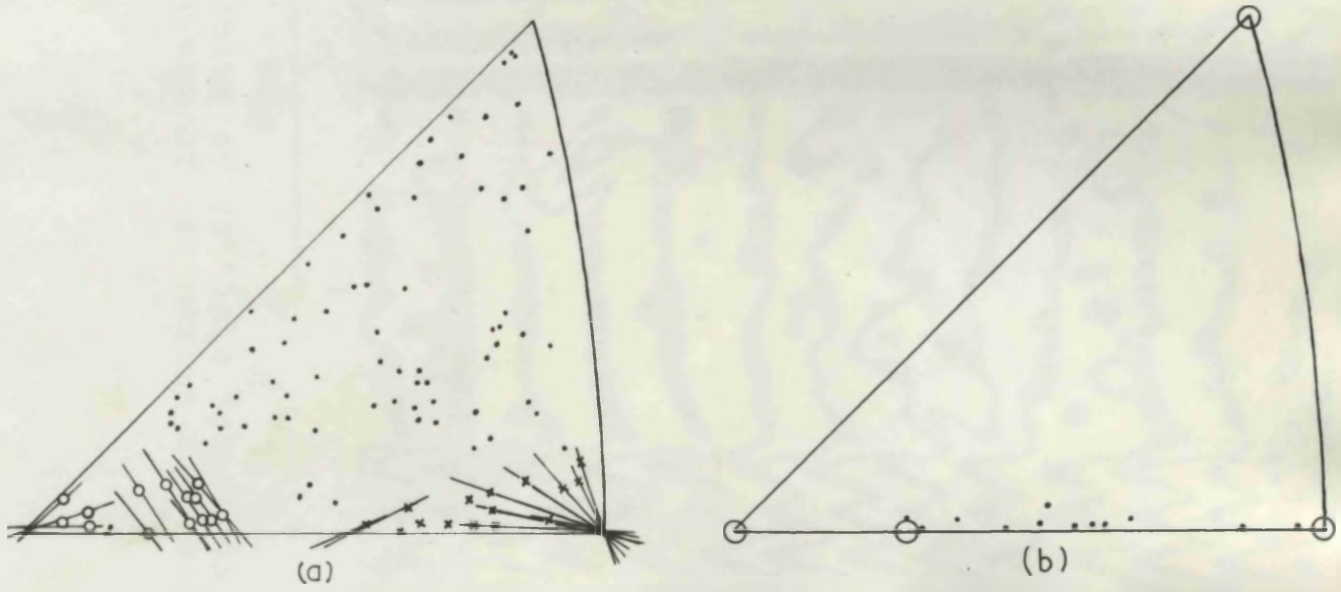

fig.28a: Orientations of striated and unstriated surfaces at 900°C
• unstriated, ○ faint striated, × strong striations.
The lines through the points represent the traces of the exposed planes and show that they correspond to (100), (110), (210), and to a range of orientations near (410) along the base of the unit triangle.

fig.28b: Orientations at which exact flats were observed. The open circles indicate the most common orientations. At (111), 8 flats were observed, 4 at (100), 9 at (110), and 7 near (410). Accuracy of orientation of the flats was better than 3°.

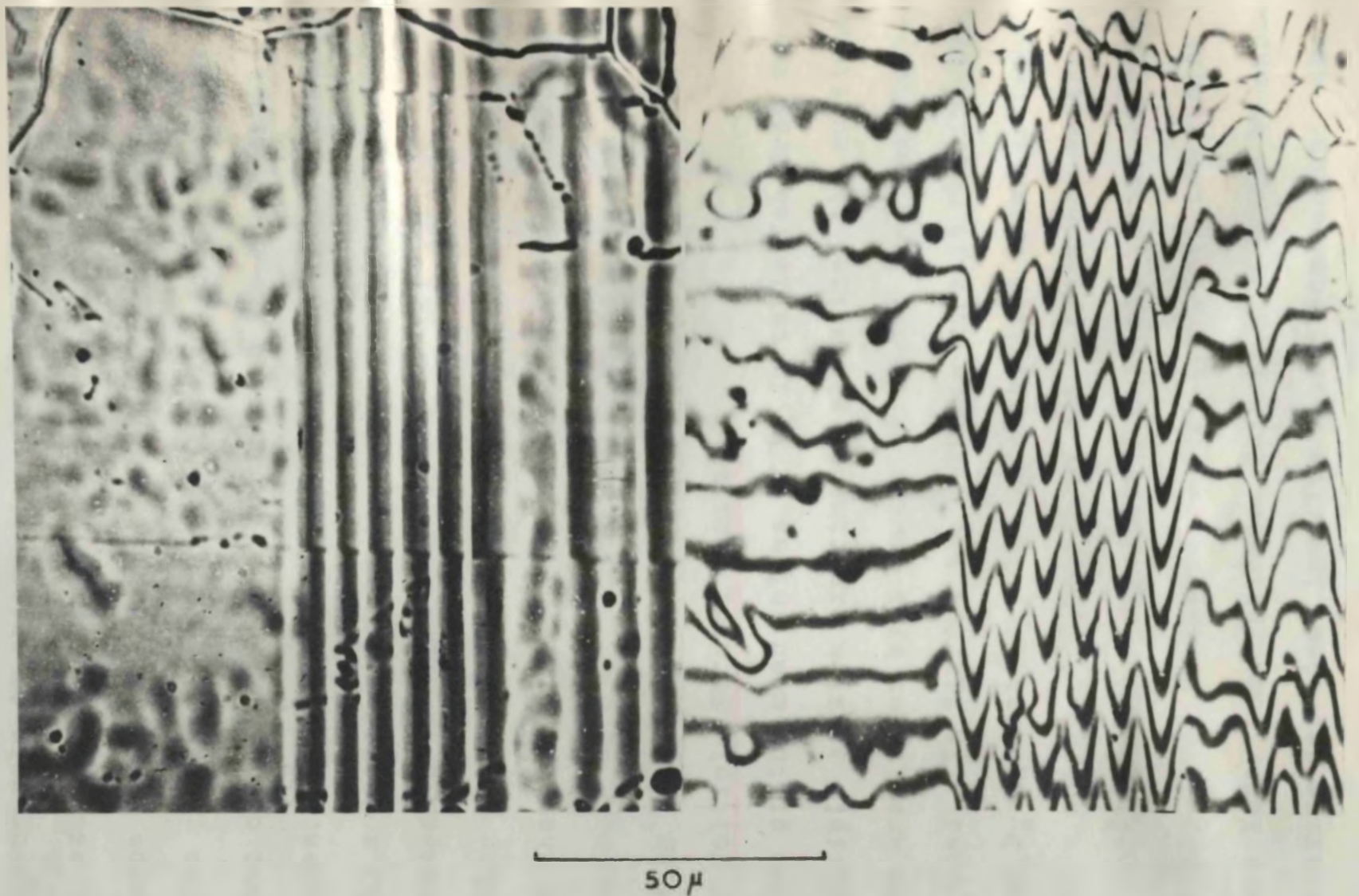

fig.27: Example of asymmetric smoothing of multiple scratches on Ni. This can be seen by the displacement of the maxima across the twin boundaries.

experimental error in individual values of B, being about ± 20%. Experiments were carried out at 900, 1000, 1100 and 1220°C. The average values of D_s obtained are shown in table Vb. The dependence of smoothing rate on orientation was again found to be very marked and an example is shown in fig(25a). Fig(25b) shows a 'sawtooth' shape due to the formation of (100) flats on the groove profiles. The range in the individual values of D_s found at each temperature was considerably smaller than in the measurements on single scratches. At 900°C the smallest and largest values of D_s differed by a factor of about 15 and at 1100°C by a factor of about $3\frac{1}{2}$, as compared to 250 and 12 in the single scratch case. The distribution plots of the individual D_s values from multiple scratches are shown in fig(15b) which provide further evidence that the dependence of diffusion constant on orientation increases with decreasing temperature.

Discussion of Multiple Scratch Results

Comparison of the mean values of D_s in table Vab from the single and multiple scratch experiments shows that the multiple scratch values are larger by a factor of almost 2 at the highest temperatures used. In fig(26) the multiple scratch results are plotted as $\log_{10} D_s$ against $1/T$; the straight line drawn corresponds to an activation energy of 1.2(± 0.1)eV and a frequency factor D_0 of about 2×10^{-2} cm^2/sec. The positions of the points (fig(26)) suggest that they could be fitted better to a curve increasing in gradient toward lower temperatures. This is what would be expected when temperature dependent impurity adsorption occurs; the gradient of the curve should tend to the value for a clean surface at high temperatures. However a larger number of points would be

required before it could definitely be established that this in fact occurs in the present case.

The difference in the values of Q_s and D_o, and in the range of the individual values of D_s from the single and multiple scratch experiments, can be explained on the basis of the different orientation ranges covered by the profiles in the two cases. For the multiple scratches used (see fig(24)) the curved profiles included orientations up to about 12^o on either side of the general surface, i.e. a range of about 24^o; for single scratches the range was generally less than 10^o. D_s obtained in each measurement in the multiple case refers to a range of orientations of about 24^o and will probably be biassed toward the slowest value for this range. Thus the very large values of D_s and also the smallest are not included in the results.

In some cases, the range of orientations is such that D_s varies appreciably over the curved profile even when this does not include a low index plane. In this case the profile decay would be better described by equation (8); an approximate solution shows that this predicts an asymmetric decay. This effect can just be detected across the twin boundaries in fig(27), where a lateral shift of the maxima has occurred.

(iii) Impurity adsorption effects at 900^oC

In the surface diffusion measurements described above, only unstriated crystal surfaces were used. However it was noticed that striations were visible on the 800^oC and 900^oC specimens.

Fig(28a) shows the distribution in the unit triangle of a number of striated and unstriated surfaces oriented on the 900^oC specimen. The traces of the exposed facet planes have been drawn.

In fig(28b) orientations are plotted at which exact flats formed at surface irregularities such as grain boundary grooves, scratches, and humps caused by embedded particles of polishing material. Fig(29) shows examples of the facets observed.

The photomicrographs (a)(b)(c) and (d) of fig(30) are typical examples of the types of striations observed. In (a) faint striations can be seen on a surface near (100): in (b)(210) striations are shown; (c) and (d) are examples of (110) striations. In (d) the striations can be seen to persist across a twin boundary as the two twins have this common (110) plane. The effect shown in fig(30c) where regions near twin and grain boundaries are clear of striations, due to the change in surface orientation, was fairly common. The formation of striations only near grain boundaries was also observed. By counting about 600 twins, it was estimated that the fraction of the total specimen surface broken up into striations was about 16%.

Discussion: Surface energy.

The previous results of Mykura(60) showed that impurity adsorption could cause the surface energy of the (100) plane to be less than that for the close packed (111). A similar relation was found by Walter and Dunn (59) between the (100) and (110) planes in iron-3% silicon alloys (b.c.c.). All these orientations correspond to atomically smooth planes which in clean systems would be expected to have the most prominent surface free energy minima. It is conceivable however that the positions of foreign atoms on other surface orientations may be such as to produce an approach to planarity and indeed to leave a smaller number of bonds unsatisfied than on the simple plane. In such a situation

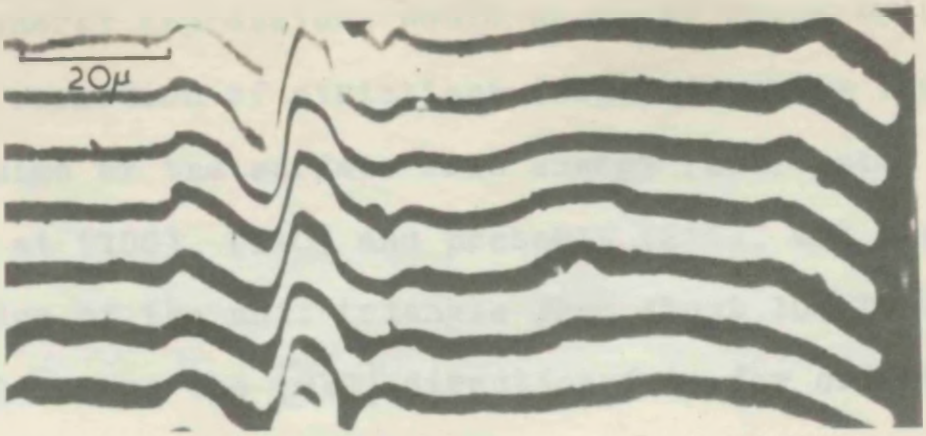

(a)

fig.29

(b)

(c)

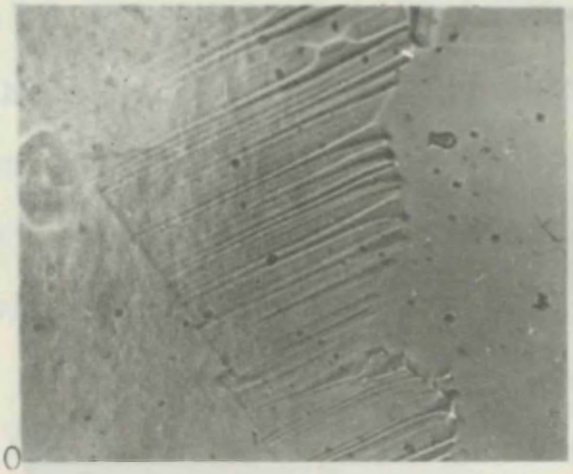

(b)

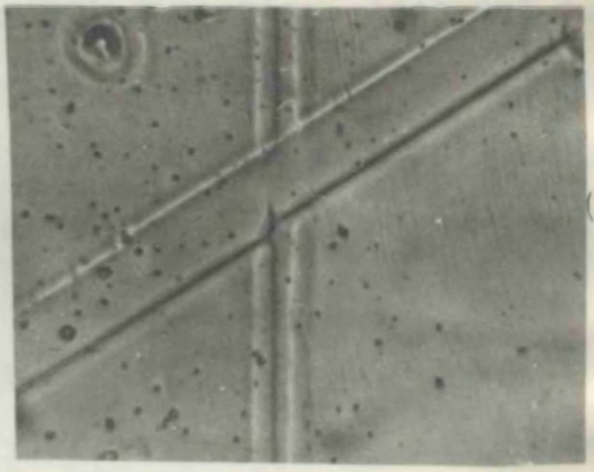

(a)

fig.30

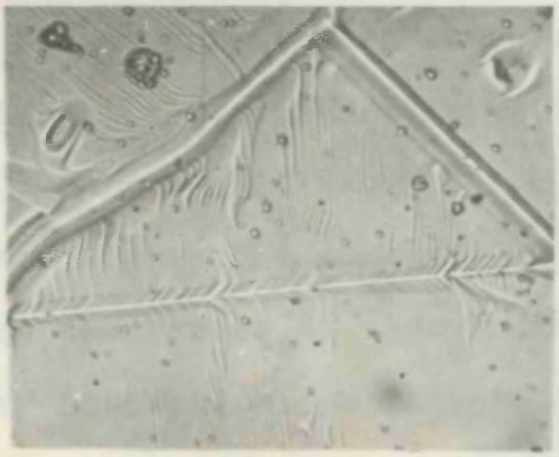

(d)

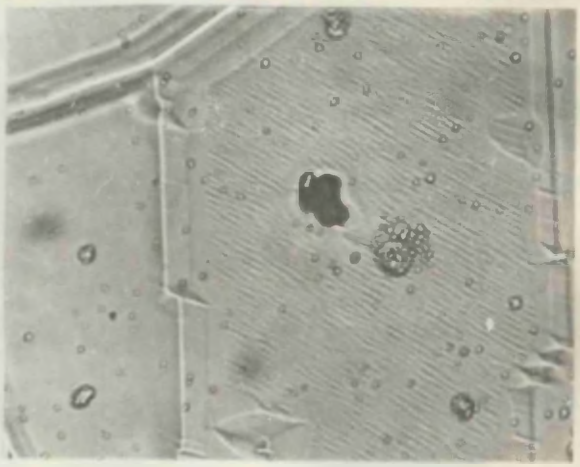

(c)

fig.29: (a) Example of extensive (111) flats on a scratch and grain boundary profiles ; in (b) and (c) faceting is seen at small surface irregularities, in (b) (410) facets, in (c) (110) facets.

fig.30: Striations on Ni surfaces at 900°C . (Described in the text).

greater energy depressions would occur at these orientations.

The formation of striations (fig(30)) shows that there are sharp minima of the surface free energy (i.e. point cusps in the γ_s-plot) at (100), (110) and probably (210), and also a line cusp on the edge of the unit triangle from about 10^o to 15^o from the (100) pole along the [010] direction i.e. for orientations near to (410).

The absence of striations near (111) does not mean that there is no cusp there; for the orientation derivatives of γ_s at orientations near a cusp can prevent striation formation. Similarly the much greater extent of striation formation for the (110) cusp in the $[1\bar{1}0]$ direction than in the [001] direction, does not imply that the surface free energy increases more rapidly or rises to a greater value in the $[1\bar{1}0]$ direction. It is much more likely to be the effect of the orientation derivatives in the equation for striation stability (Mykura(60),

$$\gamma_o < \gamma_\theta \cos\theta - \frac{\partial \gamma_\theta}{\partial \theta} \sin\theta \qquad \ldots\ldots\ldots (17)$$

where γ_o is the surface free energy of the exposed facet plane and γ_θ that for an orientation at an angle θ to it.

Fig(31) shows plausible variations of γ_s and graphs of equation (17) for the [001] and $[1\bar{1}0]$ directions from the (110) pole, which would give the observed limits of striation formation.

The occurrence of the point cusps observed is ascribed to impurity adsorption. Consideration of simple surface models (fig(32)) shows that the (210) and (110) are particularly suited for trapping adsorbed atoms. If it is assumed that the adsorbed impurity consists mainly of oxygen, then a comparison of the radius of the oxygen ion (71) with the spacing of atoms on different

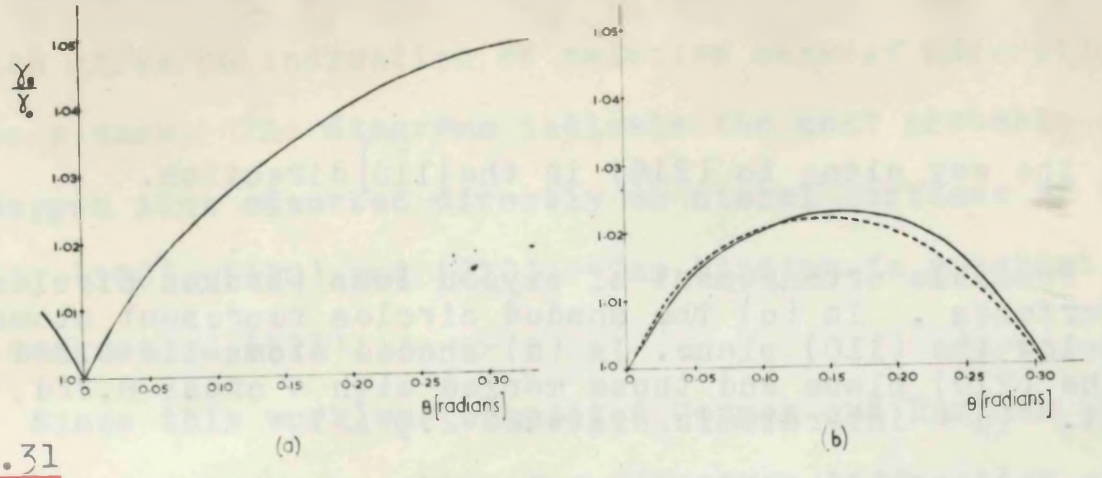

fig.31

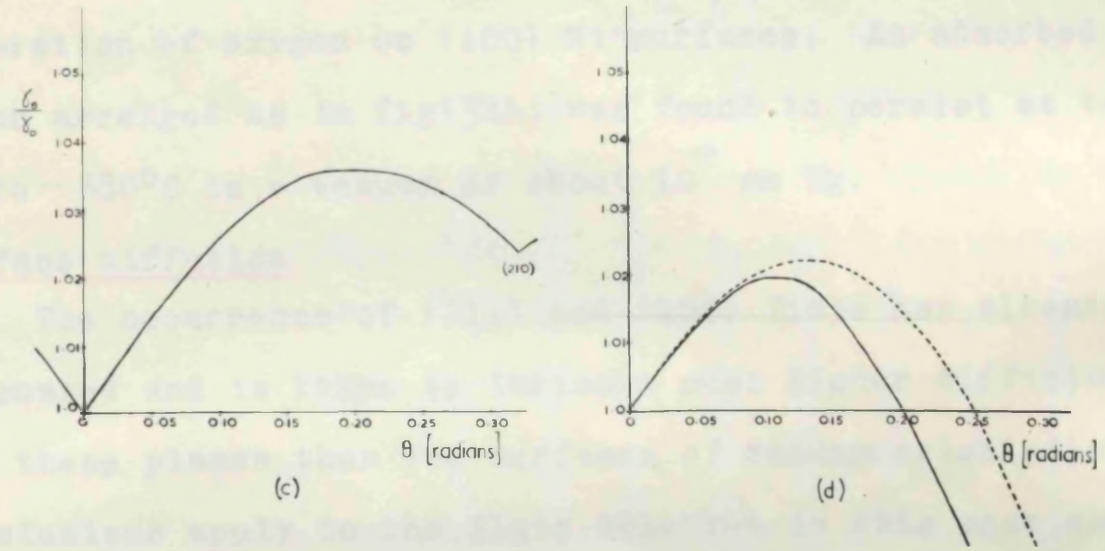

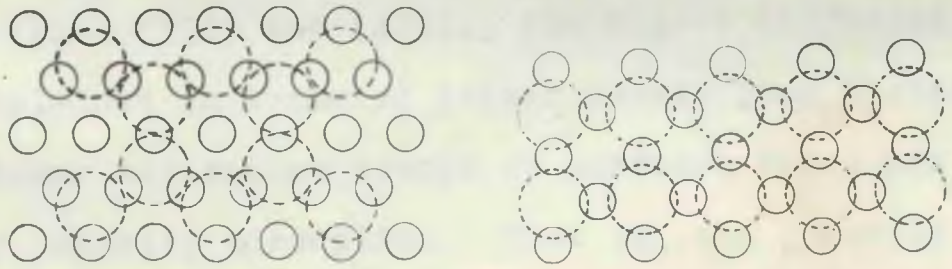

fig.32

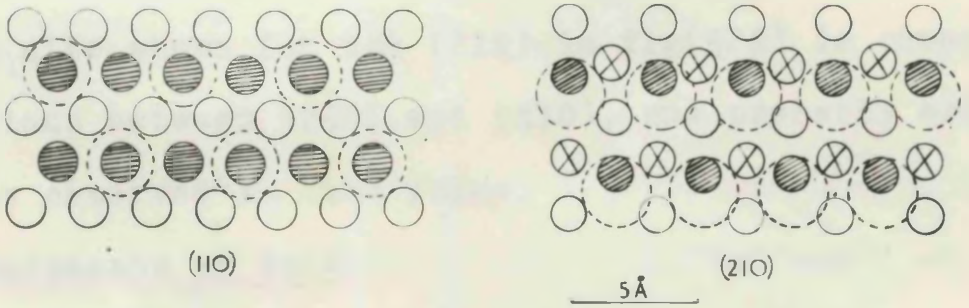

fig. 31: (a) and (c) are plausible variations of the surface free energy near the (110) pole along the [001] and [1$\bar{1}$0] directions respectively. In (b) and (d) the corresponding plots of $(\gamma_\theta/\gamma_0)\cos\theta$ (broken curves) and $1+\gamma/\gamma_0\left(\partial\gamma_\theta/\partial\theta\right)\sin\theta$ (solid curves) show that striations would occur up to about 6° along the [001] direction

over/

and all the way along to (210) in the $[1\bar{1}0]$ direction.

fig.32: Possible arrangement of oxygen ions (broken circles) on Ni surfaces . In (c) the shaded circles represent atoms 0.5 d below the (110) plane. In (d) shaded atoms lie 0.22d below the (210) plane and those marked with a cross 0.22d above it. (d = interatomic distance 2.5 Å)

planes gives an indication of relative ease of adsorption on those planes. The diagrams indicate the most probable arrangement of oxygen ions adsorbed directly on nickel surfaces of orientation (111), (100), (110) and (210). The binding is greatest on (210) and weakest on (111).

Since this work was completed, Germer and Hartman (72)(1960) have published the results of an electron diffraction study of the adsorption of oxygen on (100) Ni surfaces. An adsorbed oxygen layer arranged as in fig(32b) was found to persist at temperatures up to ~ 880°C in a vacuum of about 10^{-10} mm Hg.

Surface diffusion

The occurrence of (111) and (100) flats has already been discussed and is taken to indicate much higher diffusion constants for these planes than for surfaces of random orientation. Similar conclusions apply to the flats observed in this case also at (110) and near (210) (310) and (410). The higher diffusion constants can be explained in terms of larger atomic jump distances and perhaps lower activation energy on surfaces which are rendered smooth by impurity adsorption. That is, the impurity causes atomically rough planes to become effectively smooth and allow other nickel atoms to move across them more easily. The type of trapping site shown for the (210) in fig(32d) is common to all orientations between (210) and (410), and probably accounts for the flats observed in that range.

Vb. Experiments on Gold

Introduction

The effect of different atmospheres on the surface properties of solid gold at high temperatures, has been studied by several workers. The surface tension measurements of Udin et al (55)

(1952), (73)(1953), showed no significant difference when the annealing atmosphere was air or purified helium. Similar experiments on silver did however show a large decrease in surface tension in the presence of oxygen, ascribed to adsorption of oxygen atoms on the silver surface. The work of Mair et al(54)(1959) showed, on the other hand, that the rate of evaporation from heated gold surfaces was enhanced by the presence of oxygen at low pressure. It was concluded in the latter experiments that the observations could be satisfactorily explained as an impurity effect. This impurity was believed to be derived from the apparatus, and the increase in evaporation rate in the presence of oxygen was ascribed to the removal of the impurity as volatile oxides. It was also found that impurities initially present in the gold, diffuse to the surface and produce a larger impurity concentration there.

In the present experiments an attempt was made to measure surface self-diffusion constants for gold. Strong evidence was found to support Mair's conclusions regarding surface contamination. It was also found that the impurity produces an appreciable variation of surface free energy with orientation and probably causes a suppression of surface mobility. The changes in surface topography observed here are attributed mainly to bulk diffusion.

Experimental

Gold of two purity grades (supplied by Johnson, Matthey and Co.) were used: (a) 'specpure' gold, main impurities quoted being Si 3 p.p.m., Ag 1 p.p.m., others less than 1 p.p.m., and (b) assay gold, used only in initial test experiments. Preliminary annealing runs were made both in air and in vacuum ($\approx 10^{-5}$ mm Hg).

Microscopic examination showed that the surfaces were becoming increasingly rough and contaminated as the heating time increased. The amount of contamination was not noticeably dependent on the atmosphere although the degree of roughness was generally less for specimens heated in air. This is consistent with the assumption that the roughness is produced by evaporation from a surface over which there is a non-uniform distribution of impurity, obtained by diffusion from the bulk.

The rate of evaporation was found to be markedly dependent on surface orientation. Fig(33) shows, on a vacuum annealed specimen, a marked change in surface level across twin boundaries, the smoother surface being higher. To reduce the effect of evaporation roughening, and since there appeared to be no direct interaction between the gold surfaces and the atmosphere, specimens used for calculating surface diffusion coefficients were annealed in air in fused silica crucibles within a silica furnace tube.

An attempt was made to remove the impurity by successively melting in air in dense graphite crucibles, dissolving away the surface layers in aqua regia and flattening between 'mirror steel' plates to a form suitable for microscopic examination (i.e. flat sheet about 0.5 mm thick). This was repeated until little or no impurity was visible on the flattened surfaces. This process produced smooth initial surfaces which are difficult to produce on gold by mechanical polishing. Single and multiple scratches were then made on the surfaces in preparation for diffusion measurements

Results

Scratch Smoothing Measurements.

Surfaces initially free from contamination, in general showed

fig.33

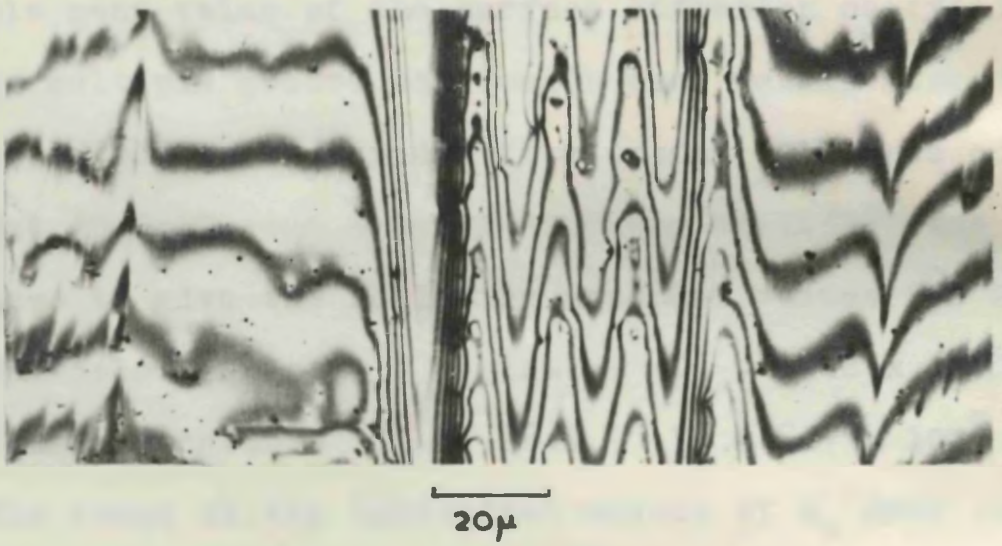

fig.34

fig.33: Interferogram of a gold surface showing how the evaporation rate depends on orientation. The level of the smoother central twin, as measured from the fringe shift, is about 0.6 microns above the other. After 12 hr at 1040°C in vacuum.

fig.34: Distortion of a multiple groove profile on gold due to particles of impurity on the surface.

some residual impurity appearing as experiments proceeded, the amount decreasing with increasing temperature. The amount of this impurity was however small compared to that found in the preliminary anneals. Only scratches of relatively large widths were suitable for smoothing measurements. Smaller ones consistently had a higher concentration of impurity along their lengths producing distorted profiles and inhibiting smoothing. Fig(34) shows a multiple groove profile on a gold surface on which there are particles of impurity. In addition only at the highest temperature used, 1035±5°C, did sufficient crystals remain reasonably smooth and sufficiently free from contamination to provide a sensible mean value of the surface diffusion coefficient. The average multiple groove wavelength used was 14 microns and the average single scratch width 26 microns. The rate of smoothing on about 20 different crystal surfaces at 1035°C was measured in each case to give the following apparent values for D_s

Multiple scratches ($\lambda = 14\mu$) : $D_s = 10 \pm 2 \times 10^{-5}$ cm^2/sec

Single scratches ($\lambda = 26\mu$) : $D_s = 8.7 \times 10^{-5}$ cm^2/sec.

The range in the individual values of D_s from single scratches was 5.5×10^{-5} to 10.7×10^{-5} cm^2/sec i.e. less than a factor of 2 between largest and smallest.

In the calculation of D_s from measured values of $B(= \frac{D_s \gamma_s \Omega^2 \nu}{kT})$, γ_s was taken as 1450 ergs/cm^2 (73), and $\Omega^2\nu$ put equal to d^4, where d is the interatomic distance 2.88Å.

Grain boundary groove measurements

The thermal etching of grain boundary grooves appeared to be less affected by surface impurity. Even at temperatures down to 900°C the majority of groove profiles were apparently of the

normal shape due to surface diffusion. Examples of grain boundaries used in the measurements are shown in fig(35). At each temperature a number of markedly assymmetrical profiles were observed due to grain boundary sliding and migration (fig 36ab), but such boundaries were rejected.

The results (assuming the grooving mechanism to be surface diffusion) obtained from measurements on at least 20 boundaries at each temperature are summarised in Table VI. This variation of D_s with temperature corresponds to an apparent activation energy for surface diffusion of about 3 eV per atom.

At 1035°C dihedral angles were measured on 20 symmetrical grooves to give a mean value of 164° 7', the range in the measured values being 161° 12' to 168° 44'. This corresponds to a boundary free energy γ_b of 0.28 γ_s i.e. 406 ergs/cm^2 taking γ_s = 1450 ergs/cm^2.

Surface Energy Observations

The surfaces of a large number of crystals broke up into striations. Examples of striated gold surfaces are shown in figs (37) and (38). 15 crystals on the 1035°C specimen were oriented from measurements of the angles between the traces of annealing twins. The result is shown in fig(39). The striated surfaces correspond mainly to orientations near (111), only two near (100) and none near the (110) pole. The distribution of striating orientations is assymmetrical with respect to the (111) pole, extending further along the $[01\bar{1}]$ zone than along the $[1\bar{1}0]$ zone.

A large number of twin boundaries were obse along the $[1\bar{1}0]$ inverted grooves of the type described by Mykura (60). An example is shown in fig(40).

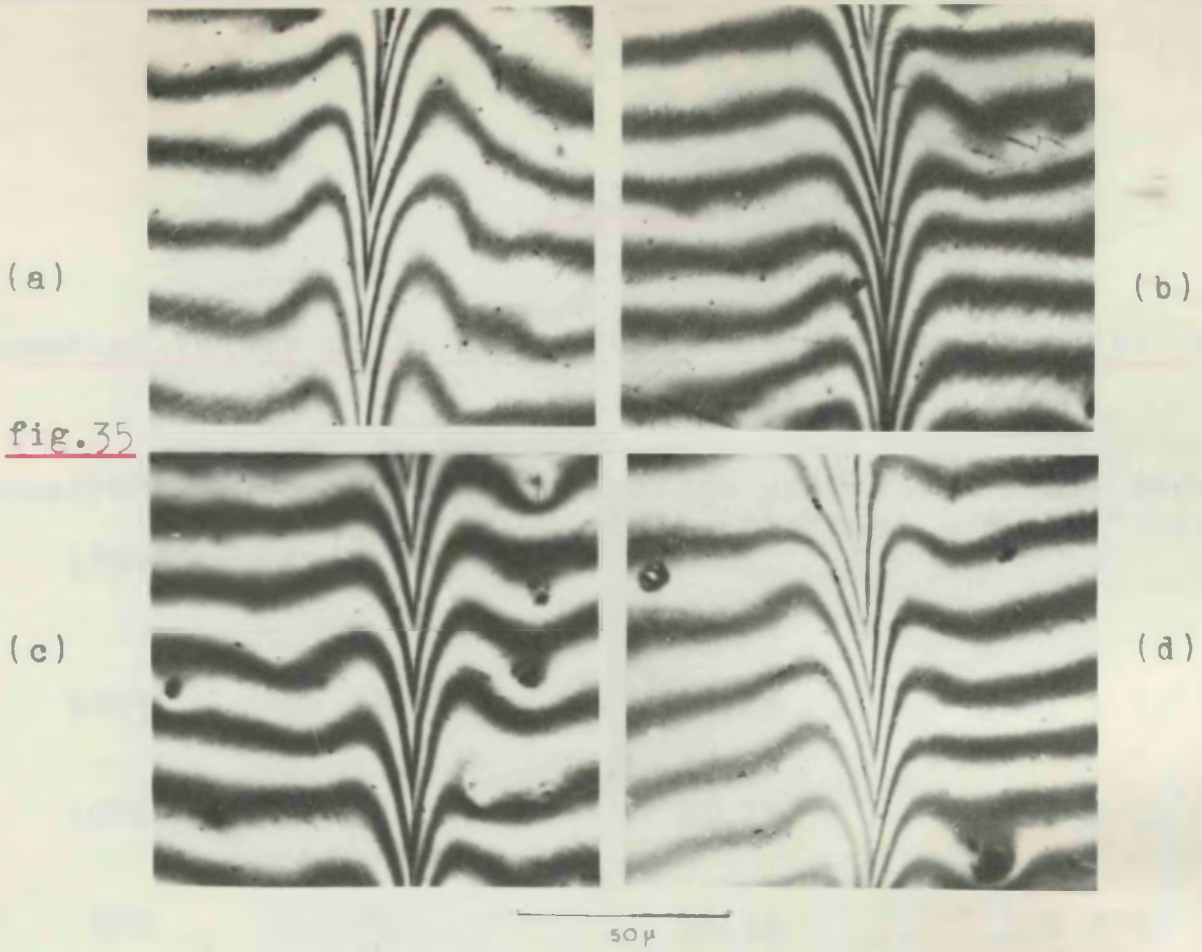

fig.35

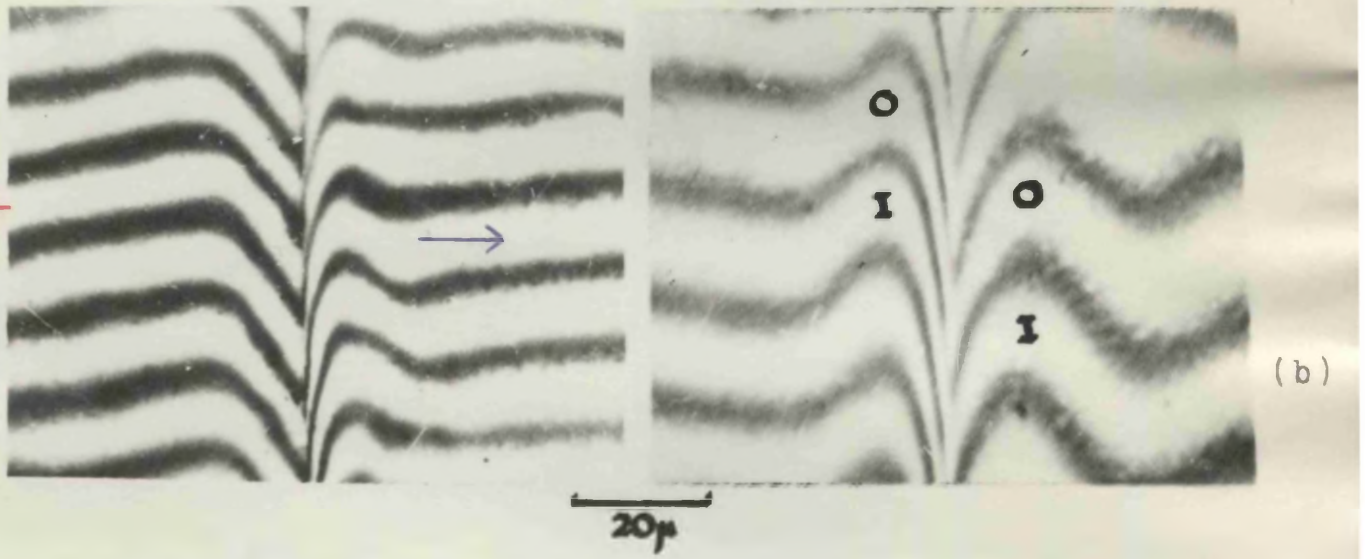

fig. 36

fig.35: Examples of grain boundary groove profiles used for diffusion measurements at 1035°C. (after 18 hr in air)

fig.36: Asymmetrical grain boundaries (a) due to boundary migration in the direction indicated, and (b) due to sliding along the boundary in a direction normal to the surface. In (b) one grain is displaced vertically ~ 0.3μ relative to the other.

Table VI

Apparent Values of D_s from Grain Boundary Measurements on Gold

Temperature (°C)	Annealing Time (hr)	Average Groove width (microns)	Average Apparent D_s (cm^2/sec)
1035	18	24.28	2.1×10^{-4}
1020	23	23.19	1.4×10^{-4}
920	45	16.44	1.6×10^{-5}
900	50	14.73	9.5×10^{-6}

(a)

fig.37

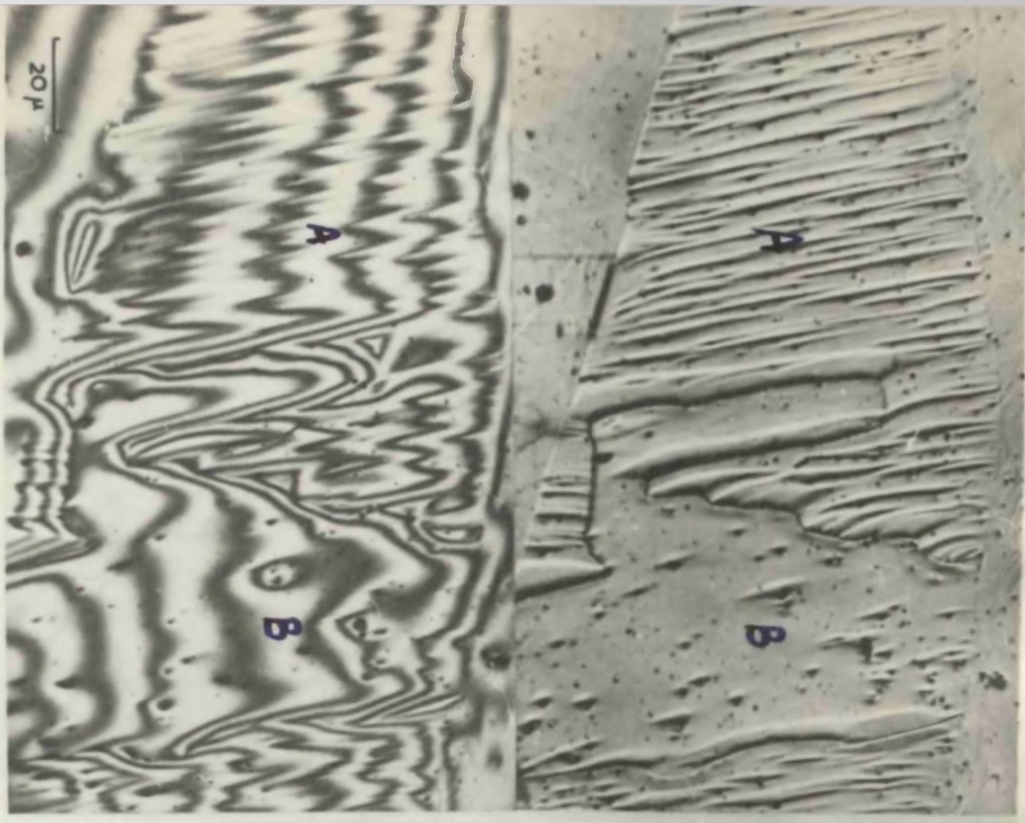

(b)

(a)

fig.38

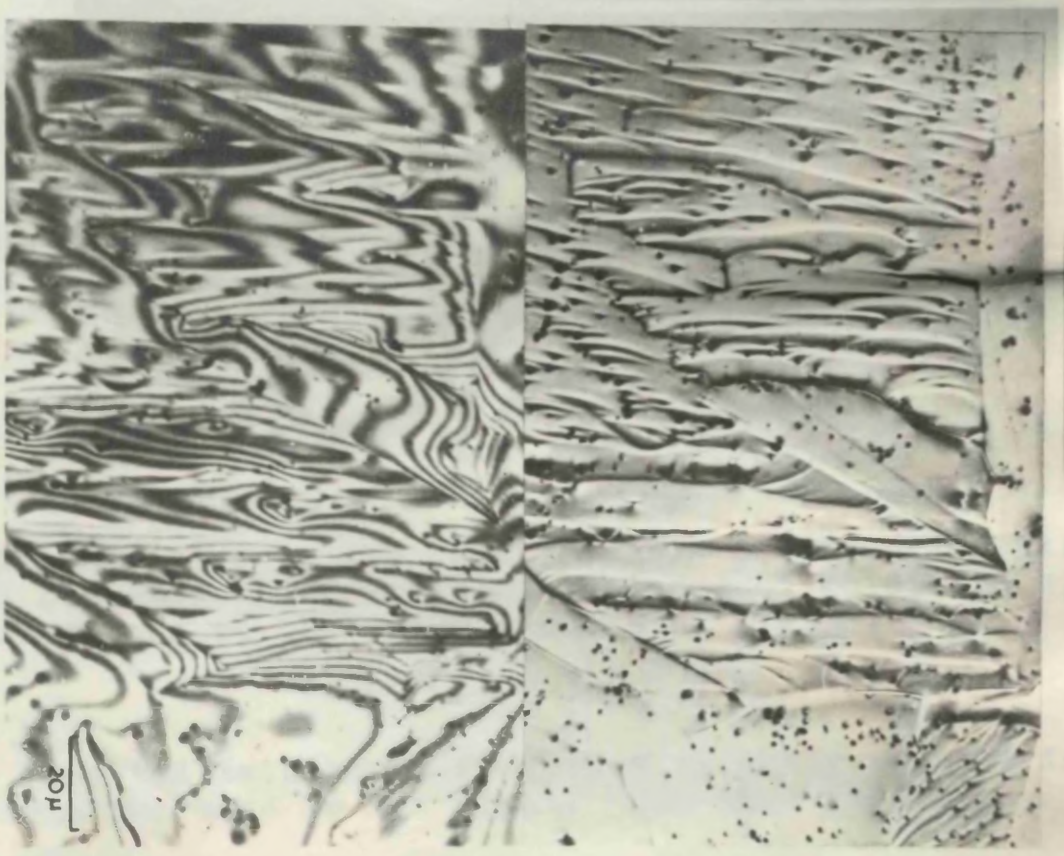

(b)

fig.37: Ordinary photograph and corresponding interferogram showing striations on a gold surface (twin A) oriented about 10° from the (111) pole. Portions of the twinning plane are exposed on both twins A and B although B is un-striated except for facets at surface irregularities. The orientations of A and B are shown circled in fig.39.

fig.38: (111) facets on a set of parallel grooves passing across a striated surface, 6° from the (111) pole.

fig.39

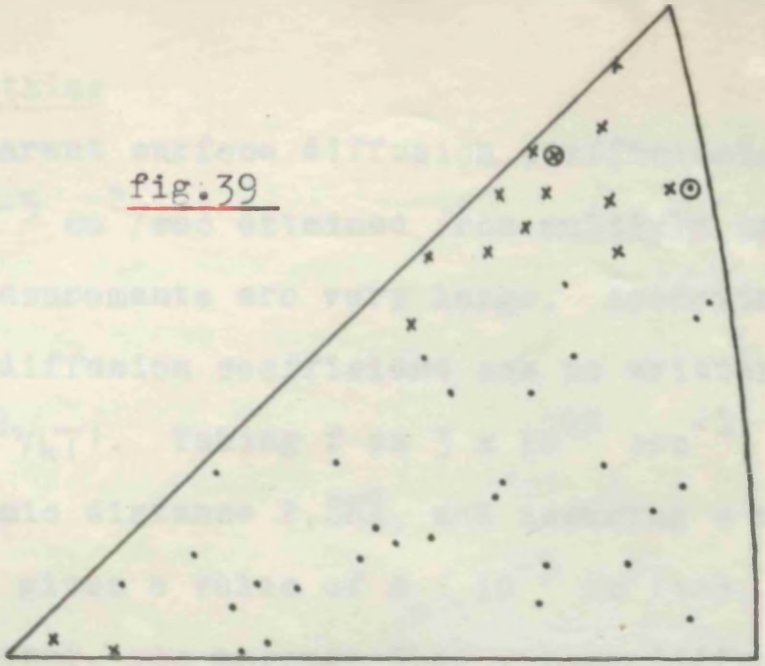

fig.40

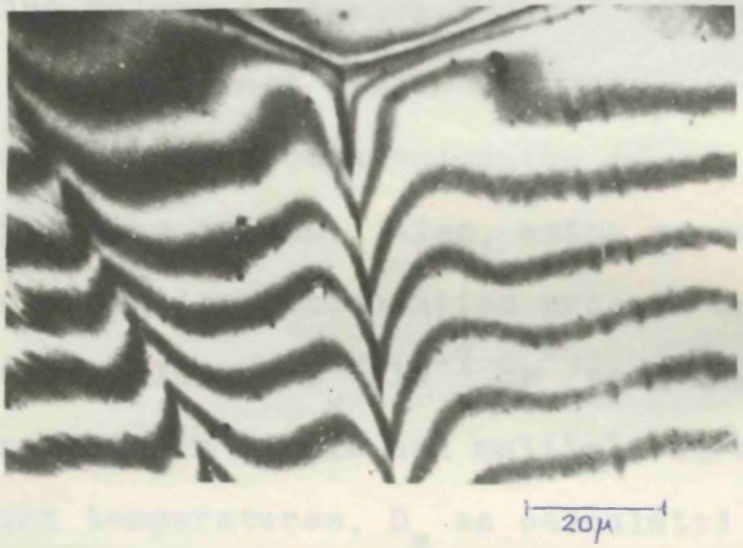

fig.39: Distribution in the unit triangle of the orientations found for striated and unstriated surfaces of gold. The circled points correspond to the twins A and B of fig.37.

fig.40: Inverted twin boundary with a slightly asymmetrical grain boundary groove to the right. See also fig.34.

Discussion

Scratch Smoothing

The apparent surface diffusion coefficients D_s of 10×10^{-5} and 8.7×10^{-5} cm^2/sec obtained from multiple and single scratch smoothing measurements are very large. According to equation (4) the surface diffusion coefficient can be written as $D_s = \frac{1}{4} a^2 f \exp(-Q_s/kT)$. Taking f as 3×10^{12} sec^{-1}, putting a equal to the interatomic distance 2.88Å, and assuming a value as low as 0.4eV for Q_s gives a value of $D_s < 10^{-5}$ cm^2/sec.

If, however, one assumes that volume diffusion is the dominant process causing smoothing then it can be shown (see section III, p.33), using volume diffusion data on Au (20) that at 1035°C one should obtain an apparent surface diffusion coefficient of 6.9×10^{-5} cm^2/sec for scratch wavelengths of 14μ, and 12.8×10^{-5} cm^2/sec for wavelengths of 26μ. Also, using vapour pressure data on Au(50), the evaporation condensation process can be shown to produce an apparent value of $D_s < 10^{-7}$ cm^2/sec. Furthermore, smoothing measurements on single and multiple scratches on Ni have shown that at high temperatures, D_s as calculated from single scratches should be increased by a factor of about 2. It therefore appears reasonable to conclude that the observed rate of scratch smoothing is due mainly to bulk diffusion. The differences between measured and apparent theoretical values of D_s due to volume diffusion may be attributed to a true surface diffusion contribution, but this is rather uncertain as these differences are of the order of the experimental errors.

That volume diffusion accounts for the observed mass transfer is supported further by the fact that no significant dependence

of smoothing rate on surface orientation was detected. For cubic metals volume diffusion should be isotropic whereas surface diffusion would be expected to depend on the arrangement of atoms on the surface, i.e. the surface orientation, as was found in the case of nickel. Abrupt changes in smoothing rate were observed here only at striated grains (fig(38)) for which no measurements were made. This is, however, believed to be a surface energy effect, low index facets being formed in such a way as to produce an energetically stable surface configuration.

Grain boundary grooves

The large apparent activation energy for surface diffusion ($\approx$3eV) found from grain boundary groove measurements, suggests that the mechanism for material transport is not surface diffusion but may again be volume diffusion. The solution for the profile of a grain boundary groove, due to volume self-diffusion in the solid has not yet been obtained. However from Herring's scaling laws (30)(1950), and by comparison with equation (3)p.16 , the width of a grain boundary groove produced by volume diffusion will be $w = \text{const } (Ct)^{1/3}$....(18), where $C(=\frac{D_v \gamma_s \Omega^3}{kT})$ is defined on p.28 i.e. $= \text{const } (D_v t)^{1/3}$..... (19)

From the measured values of w, D_v can be calculated to within a constant factor*, and so the activation energy for volume self-diffusion evaluated.

* Assuming volume diffusion accounts for the average groove width, 24.28μ measured after 18 hrs at 1035°C, the constant in equation (18) can be evaluated using the tracer volume diffusion coefficient (20) at this temperature of 1.02×10^{-8} cm^2/sec. Substituting gives, constant = 4.8, i.e. an empirical formula for grain boundary grooving by volume self-diffusion alone is

$$w = 4.8\ (Ct)^{1/3} \text{ .....(18)a.}$$

Carrying out this process for the present results leads to a value of Q_v of about 2.2eV(±0.3). This is somewhat larger than the value 1.8leV found by a tracer technique on Au(20). In the initiation of a grain boundary groove, surface diffusion will be the dominant process. This will be the case even when surface mobility is low, since the linear dimensions involved are very small. If the true activation energy for surface diffusion is in fact very large, as may well be the case here due to impurity near the surface, then the contribution to the groove width will be greater at high temperatures. This may explain the large apparent value 2.2eV for volume diffusion.

The dihedral angles leading to the value of γ_b are independent of the grooving mechanism. The average value of 164° 7' should be compared with previous experimental values of 164° 30' (Buttner, Udin and Wulff(73)(1953)) and 165° 48' (Hilliard Averbach and Cohen(74)(1960). The agreement is reasonable in view of the possible bias toward selecting either high or low angle boundaries, and helps to justify the assumption that the same value for the mean surface tension reported by Udin applies also in this case.

Surface Energy

The appearance of striations can be taken as evidence of the presence of foreign atoms on the surface. The particles of impurity visible on the surfaces in figs(37, 38) may be oxides of impurities initially present in the bulk. The distribution of contamination was not noticeably dependent upon orientation, as for example was found for the case of adsorbed impurity on Ni surfaces. The effect of the impurity appears to be a lowering

of surface free energy (γ_s) at those orientations where cusps in the γ_s-plot would normally be expected to occur, i.e. (111) and (100). In addition, the greater extent of striations along the $[01\bar{1}]$ zone than along $[1\bar{1}0]$ zone from the (111) pole, implies that the γ_s-plot is not symmetrical about this orientation. This is, in fact, what might be expected for a clean f.c.c. metal, as surfaces whose orientations lie along the $[01\bar{1}]$ zone will be composed of portions of (111) surface with linear (100) steps; along the $[1\bar{1}0]$ zone they consist of $(11\bar{1})$ steps and the step density increases more rapidly.

The occurrence of inverted twin boundary groove profiles on smooth crystal surfaces, indicates that the surface free energy varies over a range of orientations as well as possessing minimum values at (111) and (100) which account for the observed striations.

Conclusions

1. The dominant process causing material transport for the gold specimens used is volume diffusion. The activation energy for this process, as calculated from measurements on grain boundary grooving, is increased by the presence of impurity in the surface layers probably by blocking initial surface diffusion.

2. Evaporation rates are markedly dependent on surface orientation, the effect of evaporation being to produce surface roughening due to a non-uniform impurity distribution.

3. Sufficient impurity diffuses to the surface from the interior to accentuate the orientation dependence of the surface free energy

Vc. Experiments on Iron

Introduction

The surface diffusion experiments on nickel, described earlier, showed that the rate of surface migration is strongly influenced by the presence of adsorbed impurity. It was thought that this impurity might possibly have been carbon, derived from the residual atmosphere of the oil diffusion pump vacuum furnace. Since carbon is soluble in iron, it was hoped that a small percentage of carbon would have little effect on the surface properties.

The data of Birchenall and Mehl(75)(1950) and other workers (76)(1950) on volume diffusion by the radioactive tracer technique in iron, show a marked increase in diffusion coefficient below the transition temperature between the γ- and the α-phase. On decreasing the temperature below the transition temperature, the volume diffusion coefficient increases sharply by a factor of about 660(75), while the activation energy for bulk diffusion is approximately the same in both phases, $\approx$ 3.2eV per atom.

The present surface diffusion experiment on iron was carried out with the following aims:

(a) To measure surface self-diffusion coefficients, D_s, over a range of temperatures both in the b.c.c. α- and f.c.c. γ- phases.

(b) To investigate the presence of a discontinuity at the transition temperature of the values of D_s.

(c) To measure the activation energy, Q_s, for surface migration in both phases.

(d) To correlate the rate of surface migration with surface crystallographic orientation.

Experimental:

Experiments were carried out on pure iron sheet, 0.1 mm thick, AJ013, supplied by B.I.S.R.A. in the cold-rolled condition. Specimens, about 1 square cm, were mechanically polished down to alumina powder, or with Diaplast compound down to the 0.25 micron grade. Single scratches were then made on the polished surfaces with a razor blade and sets of parallel grooves ruled at spacings between 5 and 15 microns. No difference was detected in the surface behaviour of specimens annealed in the alumina or fused silica furnaces.

The rate of smoothing of single and multiple scratches and growth of grain boundary grooves was measured on specimens heated in the α-phase. At 880°C, for example, photographs of grain boundary grooves were taken after heating intervals of $8\frac{1}{2}$, $11\frac{1}{2}$, $20\frac{1}{2}$, 49 and 92 hr. Specimens used for diffusion measurements in the γ-phase were each subjected to one long annealing period only, as recrystallization occurs on cooling below the transition temperature, 910°C, and again on reheating above this temperature. For this reason no measurements on scratch smoothing were made for the δ-phase, but only grain boundary measurements, values of D_s being calculated using equation (3)p.16 .

Results

α-iron : Surface Diffusion Measurements

Striations appeared on the surfaces of a large number of grains although no visible impurity was detected except at the lowest temperature used, 750°C, where a number of small particles, probably oxide appeared on some grains (fig 41). Only unstriated grains were used for diffusion measurements. The average grain

size in all α-iron specimens was small being on the average about 100 microns in diameter.

Measurements of the rate of increase of grain boundary groove widths, W, for 30 boundaries between unstriated crystals, on a specimen heated at 880°C, showed that within experimental error W increased as $t^{1/4}$ up to widths of about 20 microns. An example of a grain boundary groove developing on an α-iron specimen at 880°C is shown in fig(43), together with the corresponding plot showing the variation of the groove width with time. The range in the measured slopes was 0.22 to 0.27 giving a mean value of 0.252. It was therefore assumed that for all temperatures used surface diffusion only need be considered in calculating values of D_s from measured groove widths up to 20 microns. Marked deviations from the $t^{1/4}$ law were found for boundaries between striated grains (fig(42)). This is not surprising as Mullins' theory (40) is based on a constant γ_s.

Specimens used for runs at lower temperatures, were first subjected to a 5 hr anneal at 880°C to produce stable grains, values of the diffusion coefficient subsequently being calculated using equation (16).

The rate of smoothing of single and multiple scratches was measured, in each case on about 30 different crystals at each temperature. The average wavelength used in these measurements was about 10μ, ranging from 8 to 13μ. In calculating diffusion coefficients from measured values of B ($= \frac{D_s \gamma_s d^4}{kT}$), the surface energy γ_s was taken $\approx$ 2000 ergs/cm^2 (77), and d the interatomic distance $\approx 2.48 \times 10^{-8}$ cm.

Table VIIa shows the mean values of D_s calculated from the

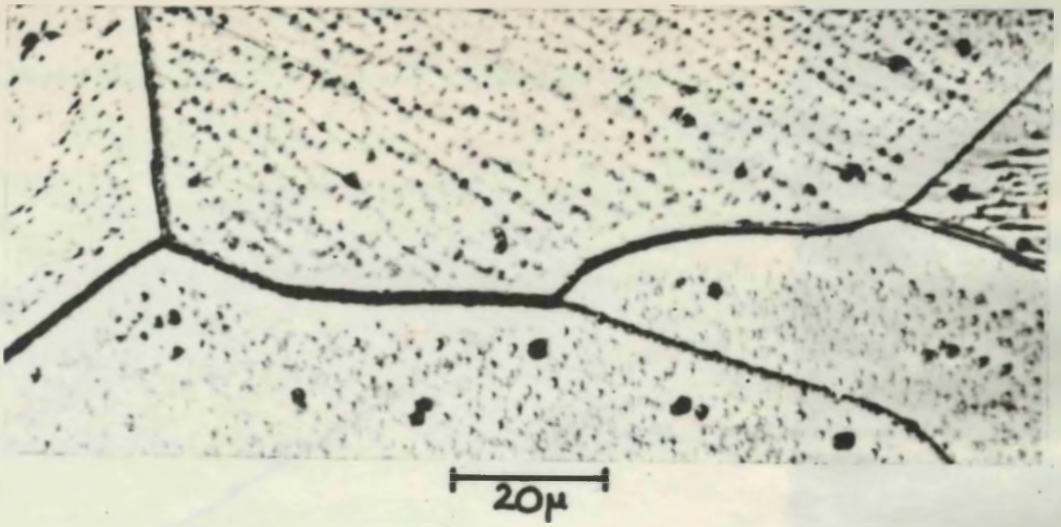

fig.41: Contamination on an α-iron surface after annealing for 10hr at 750°C in vacuum.

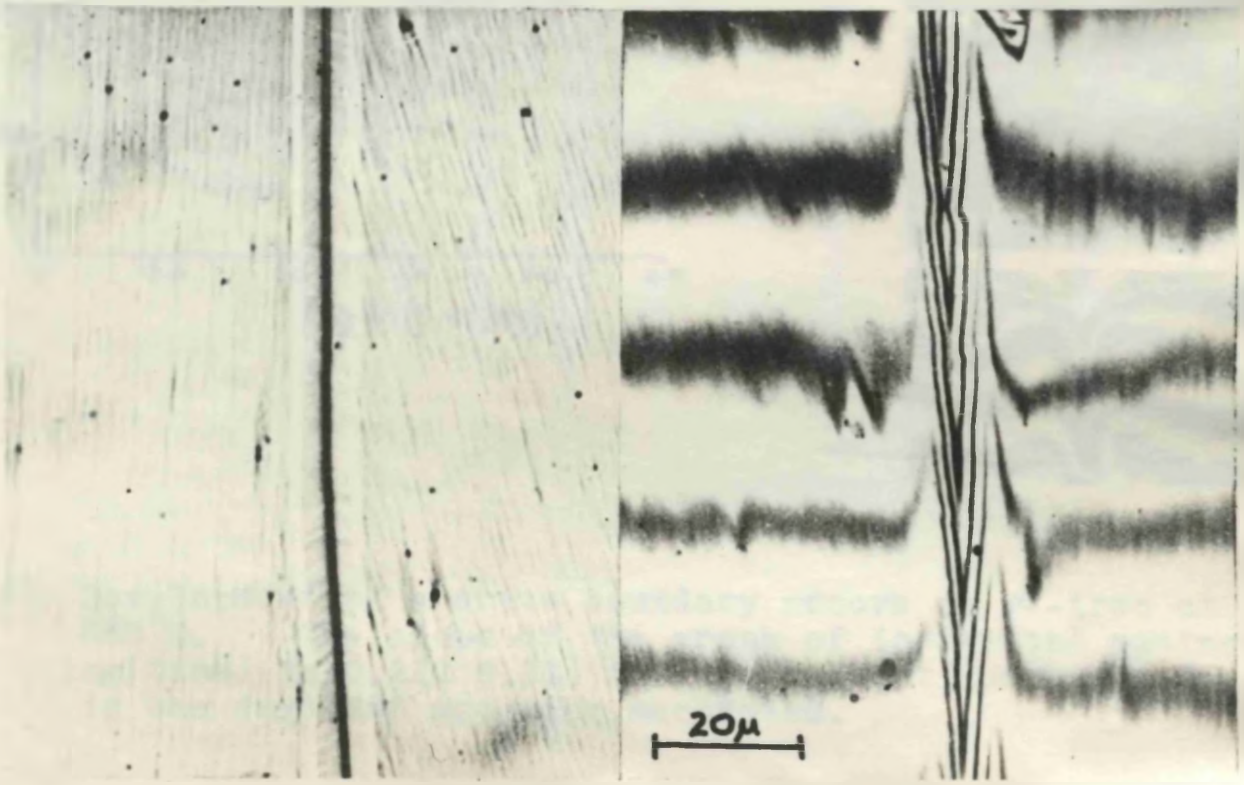

fig.42: Grain boundary between striated grains on α-iron. For such boundaries, the rate of increase in width does not follow a $t^{\frac{1}{4}}$ relationship.

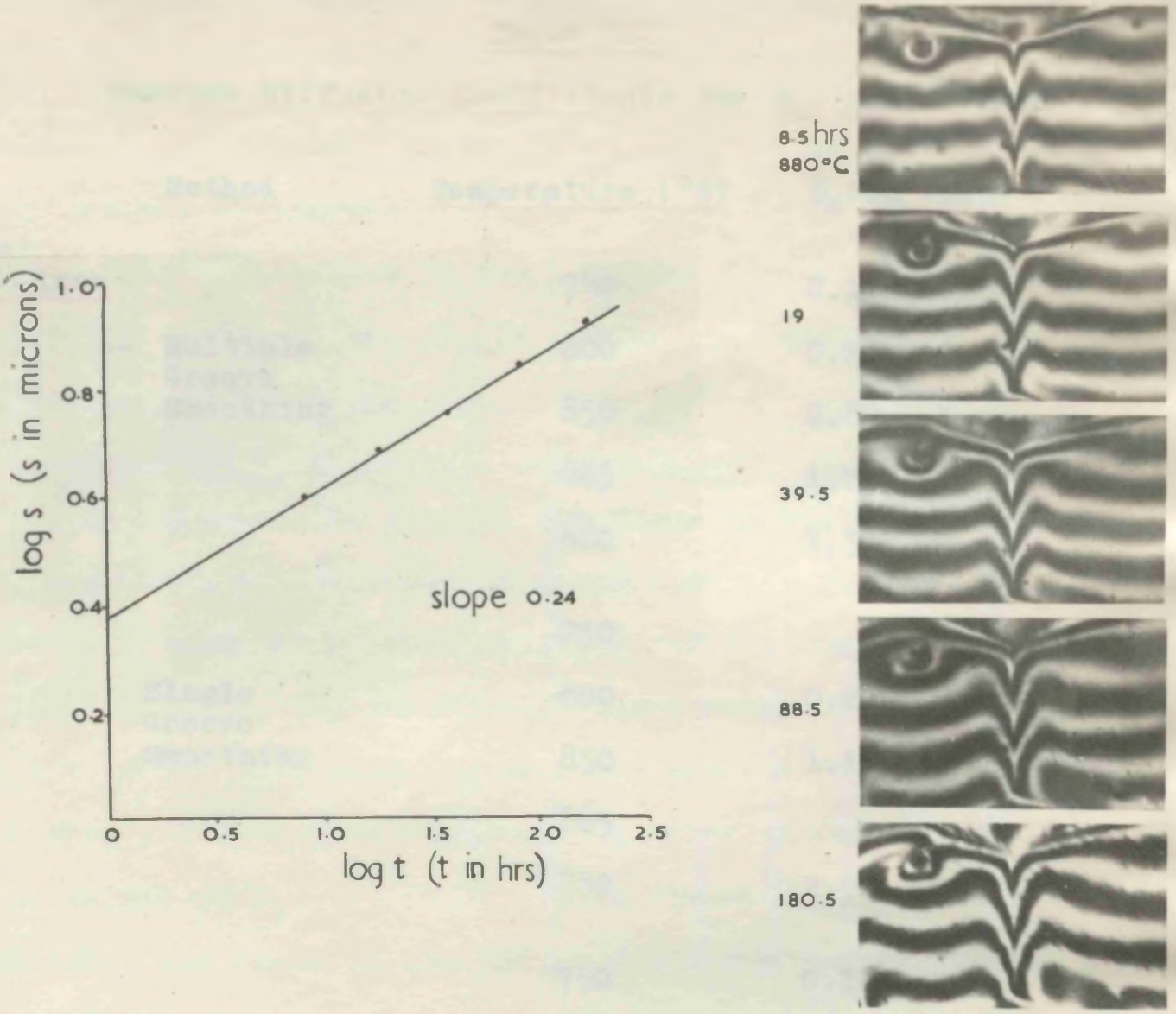

fig.43: Development of a grain boundary groove on α-iron at 880°C. The slope of the graph of log(width) against log(time) is 0.24 ± 0.01, indicating that surface diffusion is the dominant grooving mechanism.

Table VII

Surface Diffusion Coefficients for α- and γ-iron

	Method	Temperature (°C)	D_s (cm^2/sec)
(a) α-iron		750	0.11×10^{-6}
	Multiple Groove Smoothing	800	0.28 "
		850	0.89 "
		865	1.7 "
		880	2.3 "
		750	-
	Single Groove Smoothing	800	0.22 "
		850	1.1 "
		865	-
		880	2.9 "
		750	0.14 "
	Grain boundary measurements	800	0.43 "
		850	1.4 "
		865	-
		880	5.75 "
(b) γ-iron		925	1.45×10^{-6}
	Grain boundary measurements	975	1.9 "
		1060	7.7 "
		1100	22.4 "

different techniques. Representative distribution plots of the individual values of D_s are shown in fig(44). In fig(45a) the mean values of D_s are plotted as $\log_{10} D_s$ versus $1/T$, T being the temperature in degrees absolute. The straight line drawn through the points corresponds to the equation $D_s = D_o \exp(-Q_s/kT)$ with $D_o = 5.4 \times 10^5$ cm^2/sec and an activation energy, Q_s, for surface diffusion of 2.5eV per atom.

Dependence of D_s on surface orientation

As indicated in fig(44), the range in the measured values of D_s decreases with increasing temperature. Thus at 880°C, where the mean value of D_s from multiple scratch measurements is 2.3×10^{-6} cm^2/sec, the individual values range from 1.4×10^{-6} to 3.1×10^{-6}. This range is not very much greater than that expected from the estimated experimental error of $\pm$ 20% on the individual values of D_s. At 750°C, where the mean $D_s = 0.11 \times 10^{-6}$ cm^2/sec, the range in the values found was 0.04×10^{-6} to 0.21×10^{-6} cm^2/sec.

At each temperature, however, the rate of scratch smoothing on a number of grains was markedly slower than average, but such grains were invariably found to be striated, with facets along the scratch profiles. Here, as in the case of gold, the slow smoothing rate was attributed to the fact that the surface configuration produced by facetting was energetically stable.

Since annealing twins do not frequently occur in b.c.c. metals (see appendix B), the X-ray back reflection technique was used to determine the orientations of a number of the larger grains (100 to 250 microns diameter). For this a Hilger micro-focus X-ray tube was used, with a 100 micron diameter focal spot,

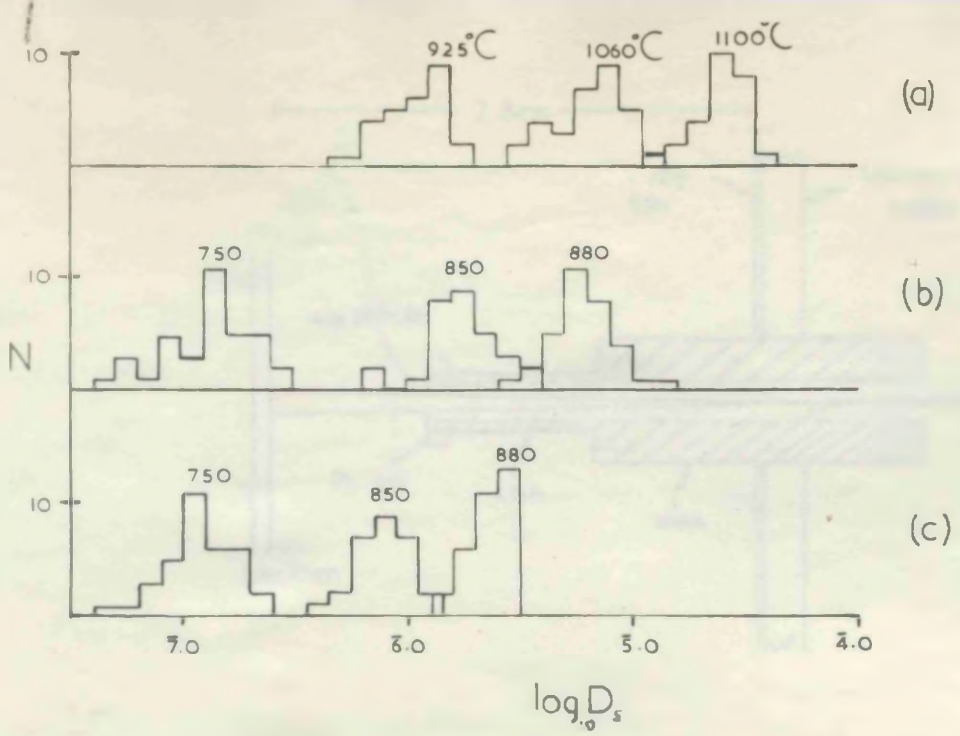

fig.44: Representative distribution plots of values of D_S (a) from grain boundary measurements in γ-iron, (b) grain boundary measurements in α-iron, (c) from multiple scratch measurements on α-iron.

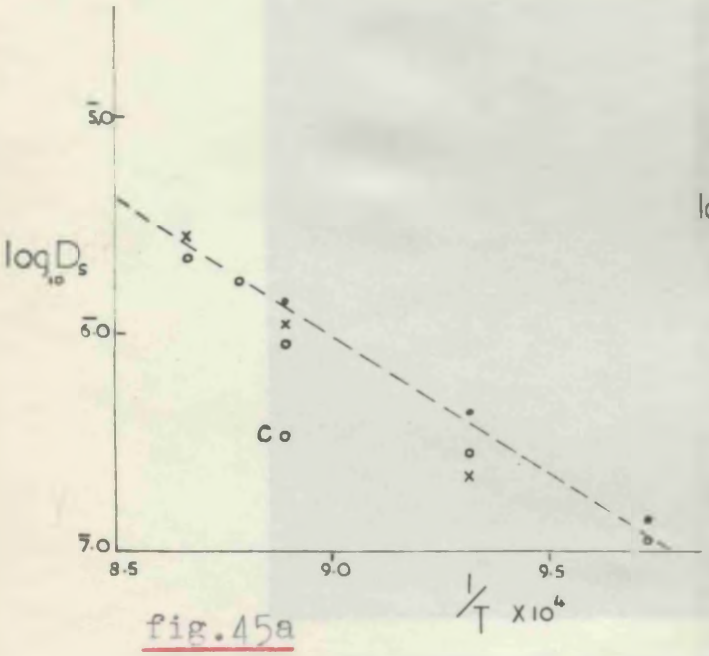

fig.45a

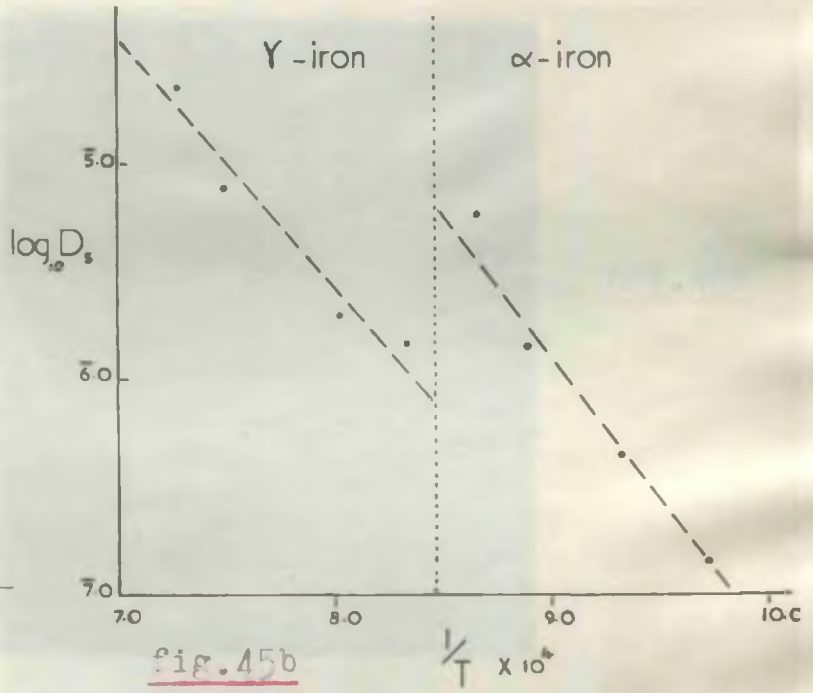

fig.45b

fig.45: Plots of $\log_{10} D_S$ against 1/T (a) for α-iron results, o multiple scratches, x single scratches, • grain boundary groove measurements (b) for grain boundary groove measurements in α- and γ-iron. This shows that at the transition temperature, D_S for α-iron is greater than that for γ-iron by a factor of about 8.

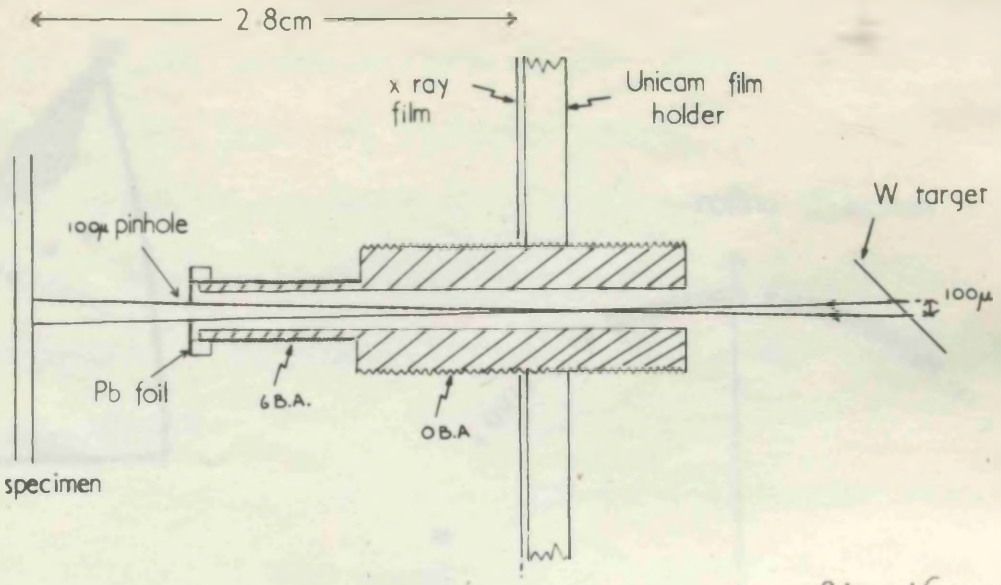

fig.46a

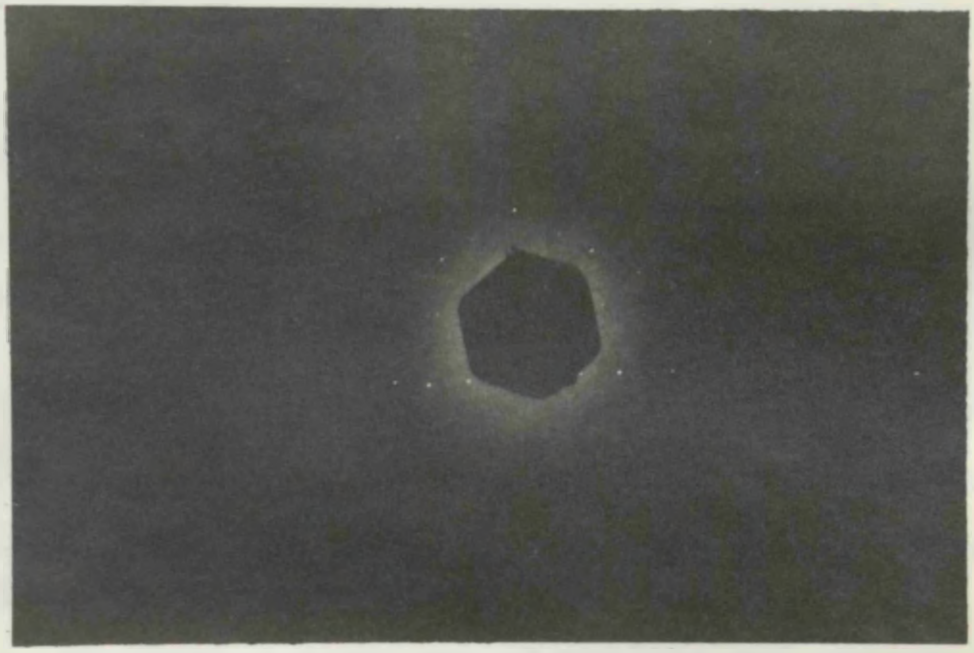

fig.46b

fig.46a: Diagram of experimental arrangement used in taking X-ray back reflection photographs of α-iron crystals. Using a 100 micron diameter pinhole in the lead foil, a region of about 150 μ diameter was irradiated. For smaller crystals, a 50 μ pinhole was used. A 16mm objective was substituted on the Unicam microscope to select individual crystals for measurement. A more refined technique has previously been described by Franks(78

fig.46b: Central portion of a back reflection pattern (actual film size)obtained from a crystal with its surface near a (211) plane. Larger angle spots could be identified on the actual film. The central shadow is due to the nut supporting the lead foil. For the interpretation of the back reflection patterns a Greninger chart, suitably reduced for a specimen to film distance of 2.8 cm, was used.

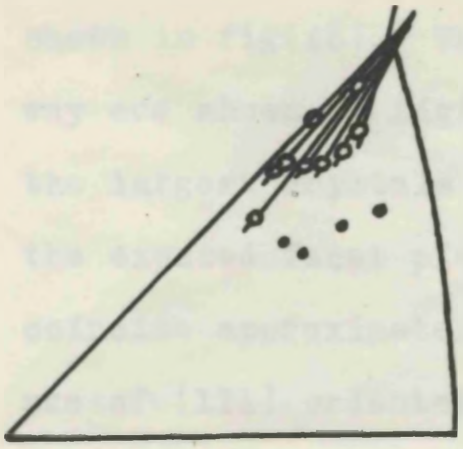

fig.47a

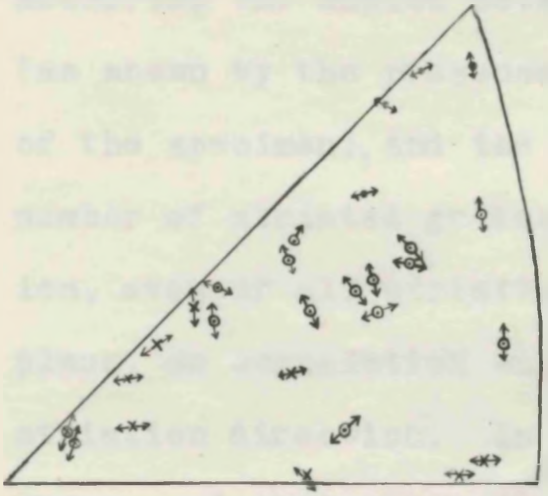

fig.47b

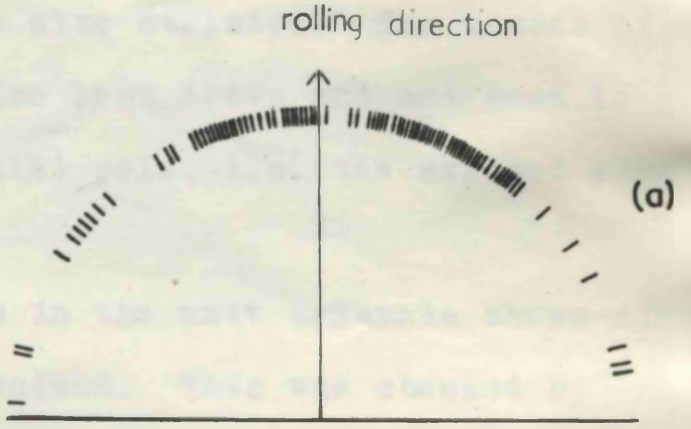

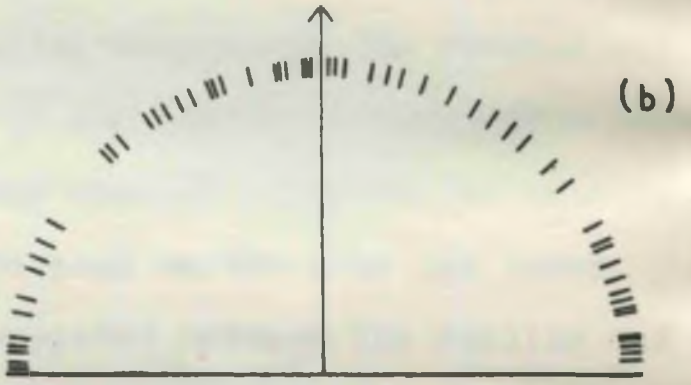

fig.48

fig.47a : Distribution in the unit triangle of striated (o) and unstriated (•) surfaces of ∝-iron. The traces of the exposed facet planes coincide approximately at the (111) pole.

fig.47b: Correlation of smoothing rate with orientation for ɣ-iron at 975°C. • fast, ⊙ medium, × slow, ⊗ very slow.

fig.48: Relative directions of rolling and striations on iron specimens (a) heated only in the ∝-phase, and (b) heated initially in the ɣ-phase followed by an anneal at 880°C.

in conjunction with a 'Unicam' camera. The arrangement used is shown in fig(46). The orientations of the crystals found in this way are shown in fig(47a). It will be noted that the majority of the largest crystals chosen were also striated. The traces of the exposed facet planes have also been drawn and are seen to coincide approximately at the (111) pole, i.e. the exposed planes are of (111) orientation.

This distribution of points in the unit triangle shows strong preferred orientation in the specimen. This was checked by measuring the angles between the rolling direction on the material (as shown by the presence of rolling grooves on the reverse surface of the specimen), and the traces of the exposed facets, on a large number of striated grains. In the absence of preferred orientation, even if all striations correspond to the same low index plane, no correlation would be expected between the rolling and striation direction. In fig(48a) these relative directions are shown, and their distribution serves to confirm the presence of preferred orientation.

To reduce the extent of preferred orientation, one ruled and polished specimen was annealed above the transition temperature, at 950°C, for 15 minutes, followed by a 40 hr anneal at 880°C . Examination showed a much wider range of smoothing rate on unstriated crystal surfaces. In addition, the direction of striations appeared to be almost random and unrelated to the rolling direction (fig 48b). The general surface had however large scale irregularities (fig 49) due to the volume change on passing through the transition temperature and the different rate of growth of individual crystals on transformation. To

eliminate this effect a specimen, previously annealed at about 1000°C for 50 hours, was mechanically polished, ruled, and annealed at 880°C. The resulting specimen showed a wide range of diffusion rates on different crystal surfaces (fig 50) and in addition the average grain size was considerably larger (300 to 400 microns in diameter). Specimens prepared in this way would be more suitable for X-ray measurements of orientation and for effecting a correlation of surface diffusion rates with orientation. It is hoped that this will be done in the near future.

γ-iron

Diffusion Measurements

In calculating diffusion constants from measured grain boundary groove widths, it was assumed that only surface diffusion need be considered. This appears reasonable since even at the highest temperature used (1100°C) the bulk diffusion coefficient (75) is less than that at 880°C by a factor of about 5. The type of surface irregularity produced on passing the phase change temperature (fig 49) was found on all γ-phase specimens, but the scale of such undulations was in general large compared to the groove dimensions, and should have negligible effect on the measurements. Also the change in shape on cooling below 910°C, (when the groove no longer marks the position of a grain boundary) should be negligible. Although some rounding off may occur at the groove root, no significant change in width would be expected during the short cooling times involved (~ 15 min in cooling from 1000°C to 600°C.).

Table VIIb shows the mean values of D_s calculated taking γ_s = 2000 ergs/cm^2 as for α-iron and d = 2.58 Å. The

fig.49

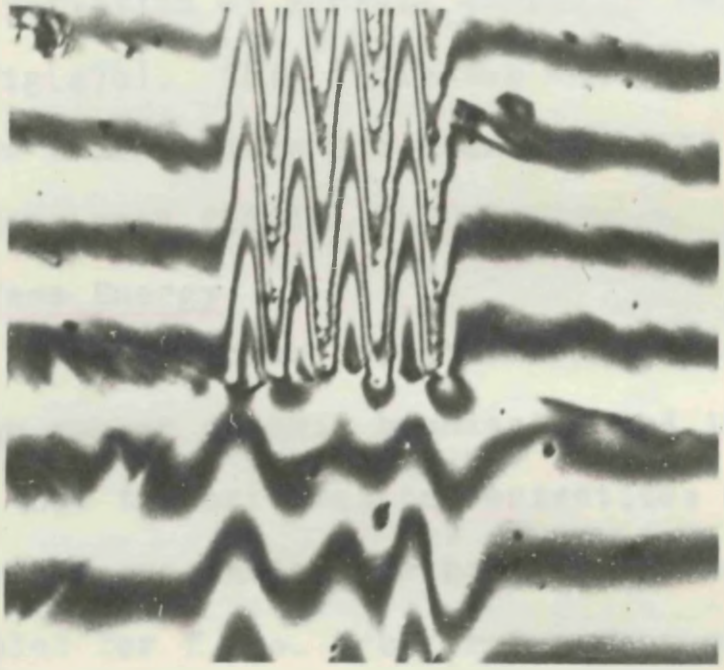

fig.50

fig.49 : Interferogram of the surface of an iron specimen after annealing for 15 min. at 950°C followed by 40hr. at 880°.

fig 50 : Example of marked orientation dependent smoothing on α -iron. This specimen was initially annealed at 1000°C, polished, ruled, and reheated at 880°C.

corresponding distributions of the individual values are shown in fig(44). In fig (45b) the values of D_s found from grain boundary measurements in α- and γ-iron have been plotted as $\log_{10} D_s$ versus $1/T$ At the transition temperature there appears to be an increase in the value of D_s by a factor of about 8. The value of D_0 for γ-iron given by the graph $\approx 10^5$ cm^2/sec, while the activation energy Q_s is, within the accuracy of the results, the same as for α-iron ($\approx$2.5eV).

Dependence of D_s on orientation

The relative rate of smoothing of single scratches, of width 10μ, on different crystals of the 975°C specimen was examined. A number of crystals were oriented by the twin trace technique. The variation of surface diffusion rate with orientation is shown in fig(47b). This indicates that diffusion is fast on surfaces whose orientations lie near the (111) pole, and slow for orientations near (100).

Surface Energy

The occurrence of striated surfaces was rare. However a large number of twin boundaries had inverted profiles, indicating that the orientation derivatives of the surface free energy γ_s are appreciable. We hope in the near future to compute the γ_s-plot for f.c.c. iron from measurements on twin boundaries as was done by Mykura (fig 14c) for Ni.

Discussion of Results

α-iron

The $t^{1/4}$ relationship regarding the variation of grain boundary groove width with time can be taken as evidence that the only transport mechanism contributing significantly to the grooving process is surface diffusion. In addition, the volume diffusion

contribution to the smoothing of multiple grooves of wavelength 10 microns at 880°C would lead to an apparent value of D_s of 0.3×10^{-6} cm^2/sec i.e. about 12% of the measured value. This was calculated using $D_v = 5 \times 10^{-11}$ cm^2/sec, extrapolated from the results of Birchenall and Mehl (75), by the method indicated on p.33 . This volume diffusion coefficient may, in fact, be considerably larger than the value applicable in cases where a nett transfer of material is involved; Meechan(35)(1960) has suggested that diffusion by a ring mechanism may occur in b.c.c. iron. Also taking the vapour pressure of iron at 880°C as 3×10^{-5} dynes/cm^2 (50), it can readily be shown that the evaporation-condensation process would lead to an apparent surface diffusion constant smaller than the experimental value by a factor of about 10^5.

The relatively small spread in the values of D_s for different crystal surfaces, together with the evidence for preferred orientation, suggests that the results apply for only a small range of orientations.

The activation energy Q_s (2.5eV) and frequency factor D_o (5.4×10^5 cm^2/sec), derived from the results, are very large. Writing $D_o = \frac{1}{4}a^2 f$, as before and putting $f = 3 \times 10^{12}$ sec^{-1} shows that the average atomic jump distance would require to be about 8 microns, which is quite unreasonably large. The large values of Q_s and D_o are thought to be due to the presence of impurity on the surface, probably oxygen from the residual furnace atmosphere, which increases the activation energy. This explanation is supported by the fact that a very low value of D_s was found at 850°C for a specimen annealed in a poor vacuum so that visible contamination was produced on a large number of crystal surfaces (point C fig(45)).

γ-iron

The large activation energy is again attributed to impurity adsorption. The marked dependence of smoothing rate on surface orientation supports the assumption that surface diffusion alone contributes significantly, as volume diffusion is expected to be isotropic for cubic materials (Herring(29)). That distinct humps occur at grain boundaries implies that the vapour transfer mechanism also contributes negligibly.

The variation of diffusion rate with orientation (fig 47b) suggests that the adsorption is greatest for orientations near (100) and least near the (111) pole. These conclusions are similar to those reached in the case of nickel. This is not surprising in view of the similarity of the f.c.c. lattices of nickel and γ-iron, and the fact that the same annealing conditions were used in both sets of experiments.

The discontinuity in the values of D_s from grain boundary measurements, fig(45b), is difficult to explain. The experimental points show no significant change in the activation energy suggesting that the surfaces for both phases are equally contaminated. Part of the discrepancy may be due to boundary migration in the γ-phase, which would lead to values of D_s smaller than the true values. This effect would not, however, be expected to introduce an error greater than about 10% (- at 925°C where an annealing time of 100 hrs was used, the time for boundary migration should be less than 10 hrs). The change in diffusion rate may be due to a difference in the structure of contaminated surfaces of the b.c.c. and f.c.c. crystals.

Vd. Experiments on Platinum

Introduction

The results of the experiments on the transition metals, nickel and iron, showed that adsorption, probably of oxygen, had a large effect on the surface behaviour. In the case of gold the effects observed were believed to be due to impurity initially present in the gold itself rather than to contamination from the atmosphere. Further surface diffusion experiments have been carried out on platinum. These investigations have not yet been completed, but sufficient results have been obtained to indicate the general surface behaviour.

Experimental

Experiments were carried out on pure platinum supplied by Johnson Matthey and Co. The main impurities detected in their spectrographic analysis were: Pd 6 p.p.m., Fe 4 p.p.m., Au 3 p.p.m., Cu 2 p.p.m., others less than 1 p.p.m. The material was supplied in the form of sheet 0.5 mm thick. The grain size on specimens, annealed without deforming the material further, was only of the order of 150μ diameter, while reducing the thickness by about 50% by flattening between 'mirror steel' plates, led to a grain size of about 500μ on recrystallization. Experiments were carried out at 890, 950, 1020, 1130 and 1250°C; diffusion results have so far only been found from the rate of smoothing of multiple scratches. At 1250°C the average wavelength used was about 11 microns while at 1250°C, to avoid excessively long annealing intervals, it was only about 6 microns. The heat treatment of all specimens was carried out in the same vacuum furnace in an alumina crucible with a lid of commercially pure platinum

foil. Specimens were mechanically polished with 'Diaplast' diamond compound before ruling.

Results

The smoothing of typical multiple groove profiles at 890°C and 1250°C are shown in figs (51, 52). In general surfaces were free from visible impurity; the exceptions to this statement will be described later. At the lowest temperatures, 890 and 950°C, no break-up of the surface into striations occurred. At 1020°C a few crystals showed faint striations after a total annealing time of 70 hrs while at the highest temperature, 1250°C, striations were present after an anneal of about 3 hrs and persisted after a further 76 hrs at this temperature. At 1250°C about 1/5 of the total surface broke up into striations.

The mean surface self-diffusion coefficients calculated from measurements on unstriated surfaces are shown in table VIII#. A value of 2000 ergs/cm^2 was assumed for the specific surface energy; no reference to a measurement of γ_s for solid platinum has been found in the literature. The temperature variation of D_s is plotted in fig(53); the corresponding frequency factor D_o = 9.8(±7) x 10^{-3} cm^2/sec, and the surface self-diffusion activation energy, Q_s = 1.2(±0.2)eV per atom.

Diffusion rates on smooth crystal surfaces were again found to be markedly dependent on crystal orientation. The photomicrographs in fig(54) illustrate this. Annealing twins were sufficiently frequent to allow a number of crystal surface orientations to be determined by the twin boundary trace method. This was carried out on the 1020°C specimen. The result is shown in the unit triangle of fig(55). The range of orientations covered by

Table VIII

Surface Diffusion Results on Platinum

Temp. (°C)	Mean D_s (cm^2/sec)	Range in values of D_s	Factor between largest & smallest	Average initial orientation range
890°	0.75×10^{-7}	$0.19 - 1.6 \times 10^{-7}$	~ 8.4	~ 33°
950	1.03 "	0.39 - 2.4 "	~ 6.2	~ 26°
1020	1.7 "	0.74 - 4.2 "	~ 5.7	~ 20°
1130	4.8 "	1.2 - 9.8 "	~ 8.1	~ 26°
1250	12.2 "	2.5 -27.0 "	~10.8	~ 19°

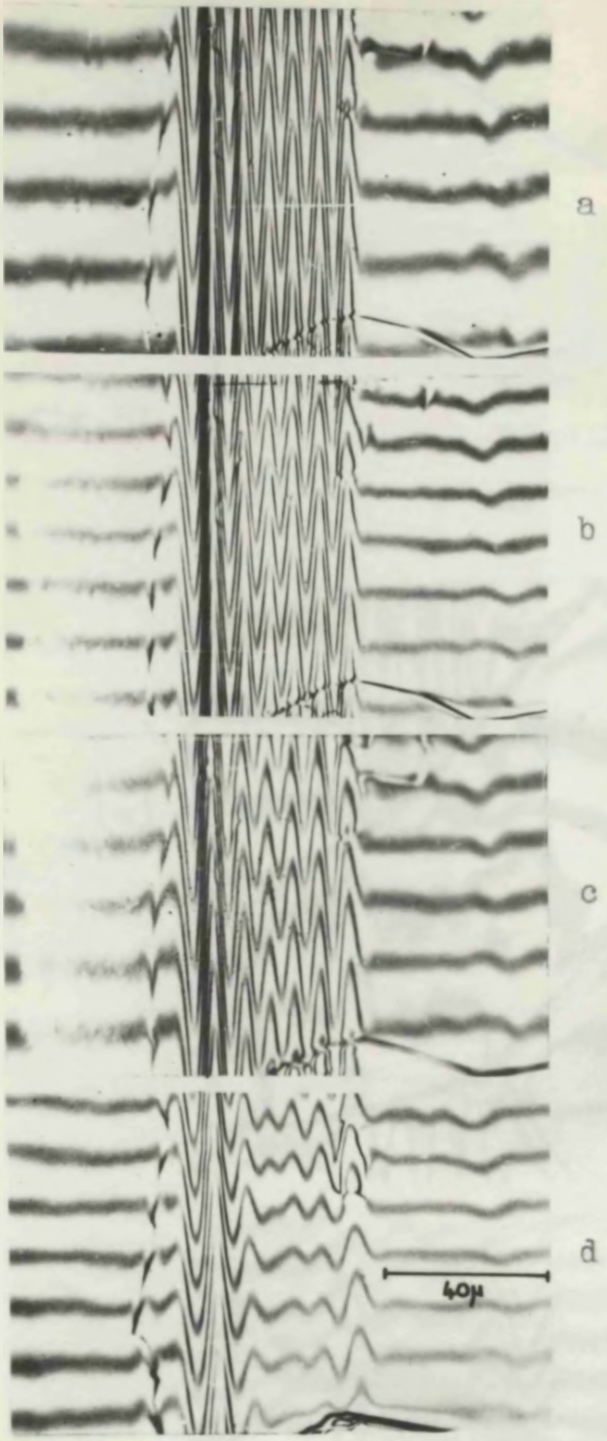

fig.51

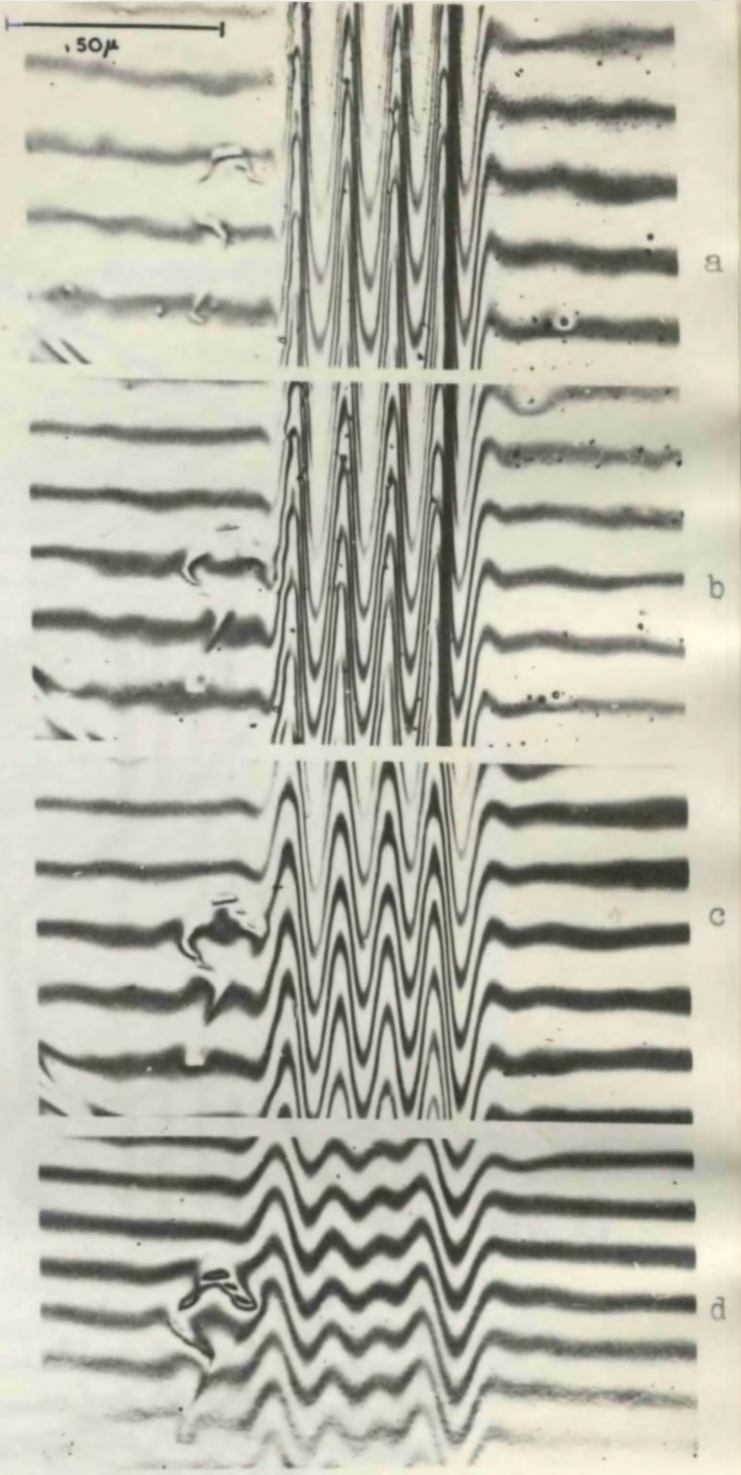

fig.52

fig.51: Smoothing of a set of multiple grooves of wavelength 6.6 microns at 890°C (a) after $\frac{1}{2}$ hr at 1180°C, (b) 3hr at 890°C, (c) 13 hr at 890°C, (d)53 hr at 890°C.

fig.52: Examples of the grooves used for 1250°C measurements. (a) after 1hr at 1250°C (higher harmonics are still present), (b) after 5 hr at 1250°C, (c)26 hr, (d) 76 hr at 1250°C. This illustrates the slow smoothing of the extreme grooves, due to the lateral shift of the extreme maxima.

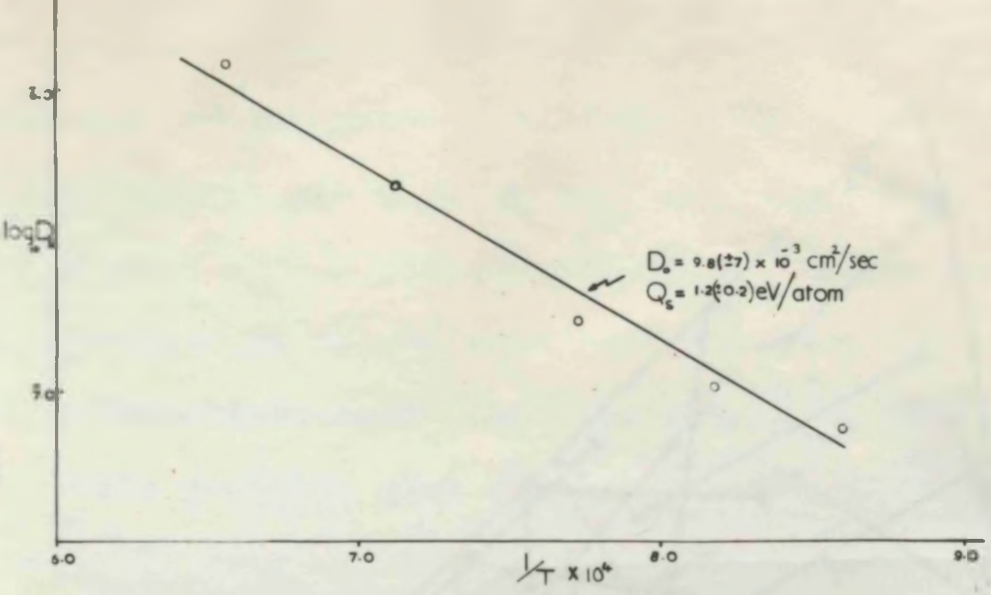

fig.53

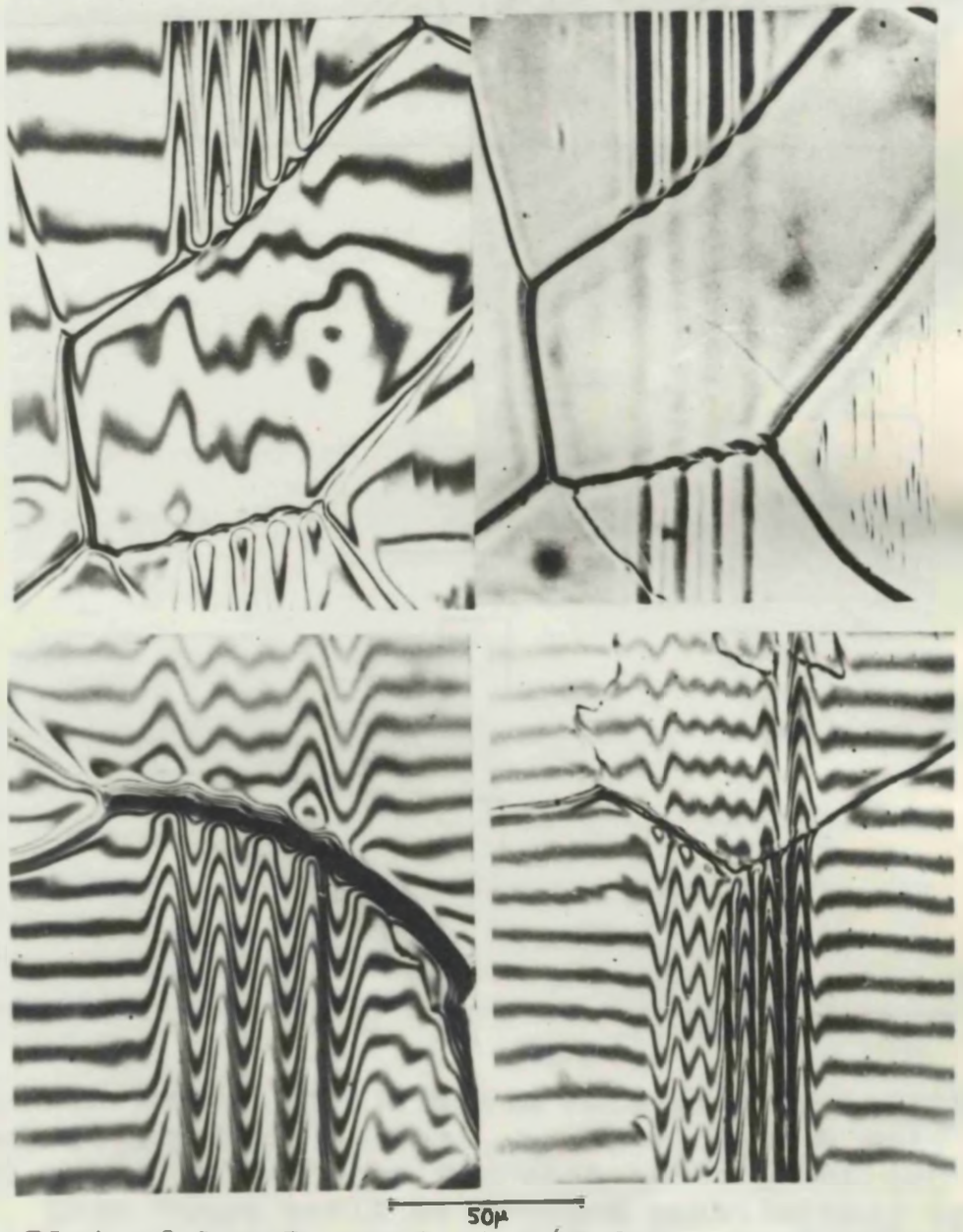

fig.54

fig.53: Plot of $\log_{10} D_S$ against 1/T for pure platinum. No corrections have been applied for the effect of volume diffusion
fig. 54: Orientation dependent smoothing on platinum, (a), (b) at 1250°C, (c) 950°C, (d) 890°C. In (d) the diffusion rates are different for all three crystals shown.

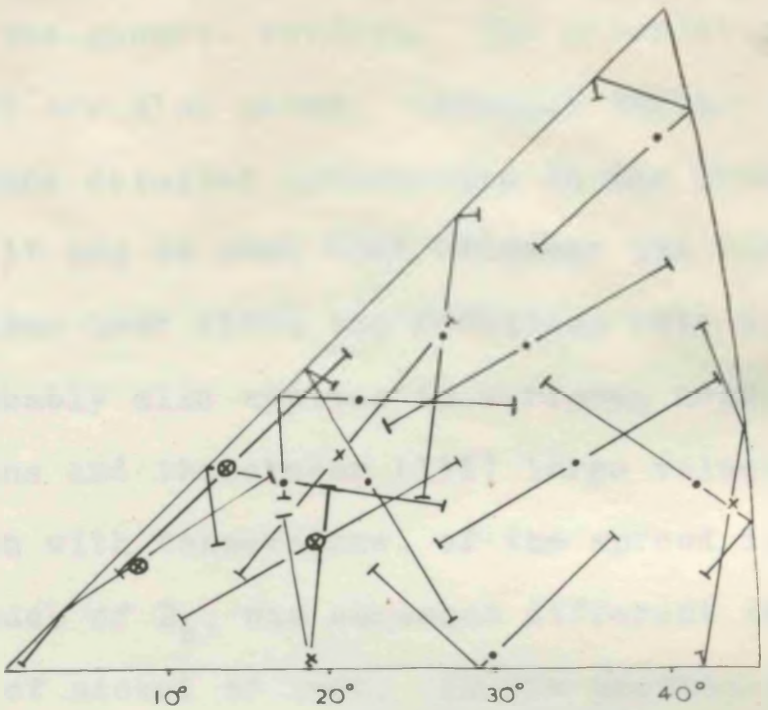

fig.55

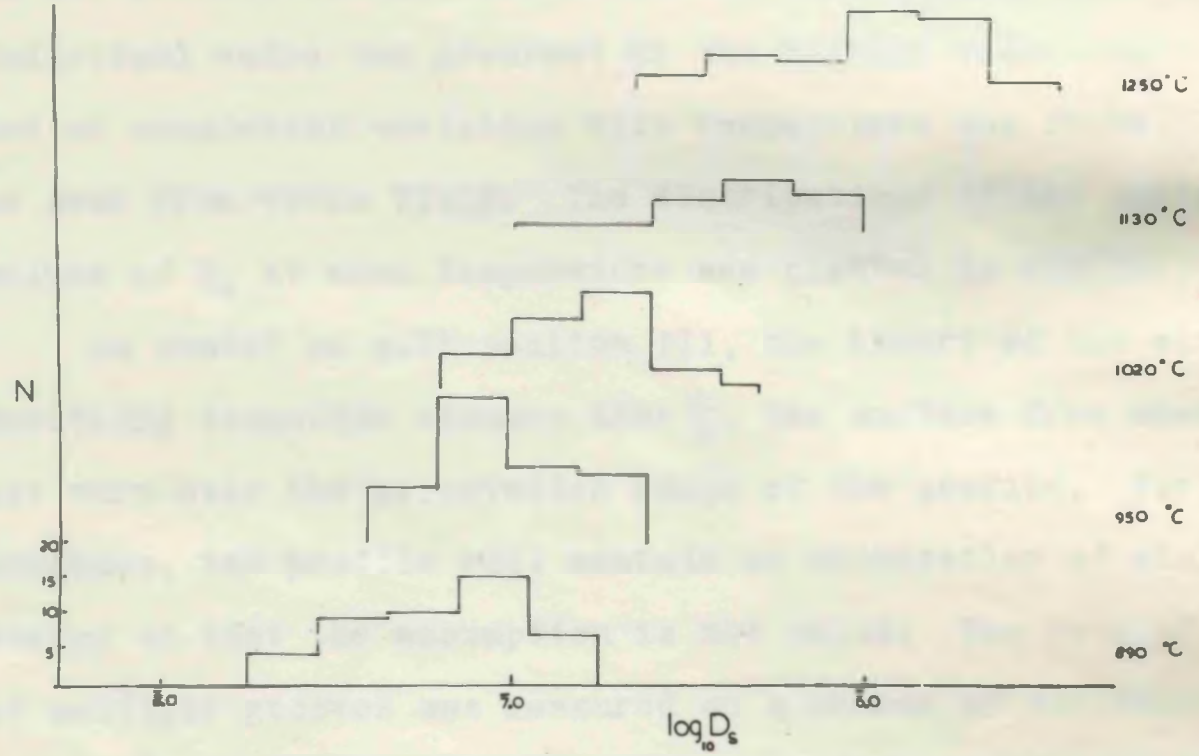

fig.56

fig.55: Variation of diffusion rate with orientation for platinum at 1020°C. • fast, x slow, ⊗ very slow. The initial orientation range for each measurement (20°) is also shown. This range could be reduced considerably by allowing smoothing to proceed until it was only about 5° say, but this would lead to some loss in accuracy.

fig.56: Distribution plots of values of D_s for Pt. The greatest range of values occurs at the highest temperature, 1250°C.

the initial sinusoidal profiles at this temperature was about 10° on either side of the general surface. The orientations covered in each measurement are also shown. Although further points are required to give more detailed information on the dependence of D_s on orientation, it can be seen that whenever the curved profile includes orientations near (100) the resulting rate of smoothing is slow. This probably also applies to surfaces near (110). For general orientations and those near (111) large values of D_s apply.

The variation with temperature, of the spread in the individual measured values of D_s, was somewhat different from that found in the case of nickel or iron. In the previous experiments the range of values of D_s decreased with increasing temperature. In the present results the factor between largest and smallest individual value was greatest at the highest temperature (≈ 10.8) and no consistent variation with temperature was found. This can be seen from table VIIIØ. The distributions of the individual values of D_s at each temperature are plotted in fig(56).

As stated on p.27 section III, the theory of the sine wave smoothing technique assumes that γ_s, the surface free energy, does not vary over the orientation range of the profile. For striated surfaces, the profile will contain an orientation of minimum energy so that the assumption is not valid. The rate of smoothing of multiple grooves was measured on a number of striated surfaces at 1250°C. In fig(57) the resulting values of B, calculated by assuming that the theory is valid, are plotted against the angle between the striation and groove directions. Fast smoothing occurs for striations at large angles to the grooves while for small angles the smoothing is very slow (fig(58)). The nett

decrease in surface energy is greater for striations at large angles than it would be for a general range of orientations, whereas for small angles it is smaller. For small angles, flattening might in fact cause an increase in surface energy.

Discussion

It has been assumed that surface diffusion only, contributes significantly to the observed topographic changes. From the vapour pressure of platinum at 1250°C of 5.2×10^{-6} dynes/cm^2 (50), calculations show that the vapour transfer mechanism would lead to an apparent D_s of about 1.3×10^{-14} cm^2/sec, which is completely negligible. Volume self-diffusion in pure platinum has been measured by the tracer technique by Kidson and Ross (79)(1957), in the temperature range 1325 to 1600°C. Using an extrapolated value of 5.2×10^{-11} cm^2/sec at 1250°C, it can be shown, by the method outlined on p.33, that the apparent D_s due to volume diffusion would be 2.93×10^{-7} cm^2/sec., i.e. about 25% of the experimental value. At 1130°C, volume diffusion would account for 10% of the experimental value, while at lower temperatures the contribution is negligible. These corrections would have little effect on the general conclusions to be drawn from the results. Over the range of wavelengths used at 1250°C (9.5 to 13.5μ), no dependence of the measured value of B on wavelength was detected (fig 59). These calculations indicate however, that it would be of interest to carry out a further experiment at 1300°C using sets of grooves of wavelength 5, 10, 15, 25μ say, and investigate the variation of the measured decay constant on wavelength. Such an experiment has been started.

The values for the constants Q_s, 1.2($\pm$0.2)eV, and D_o,

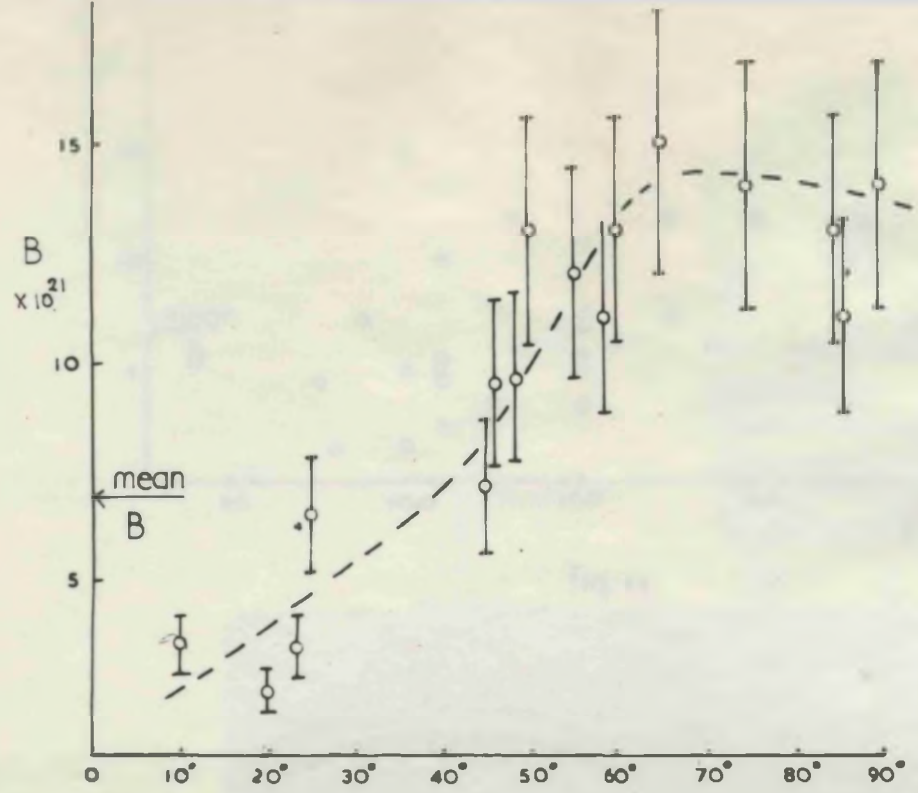

fig.57

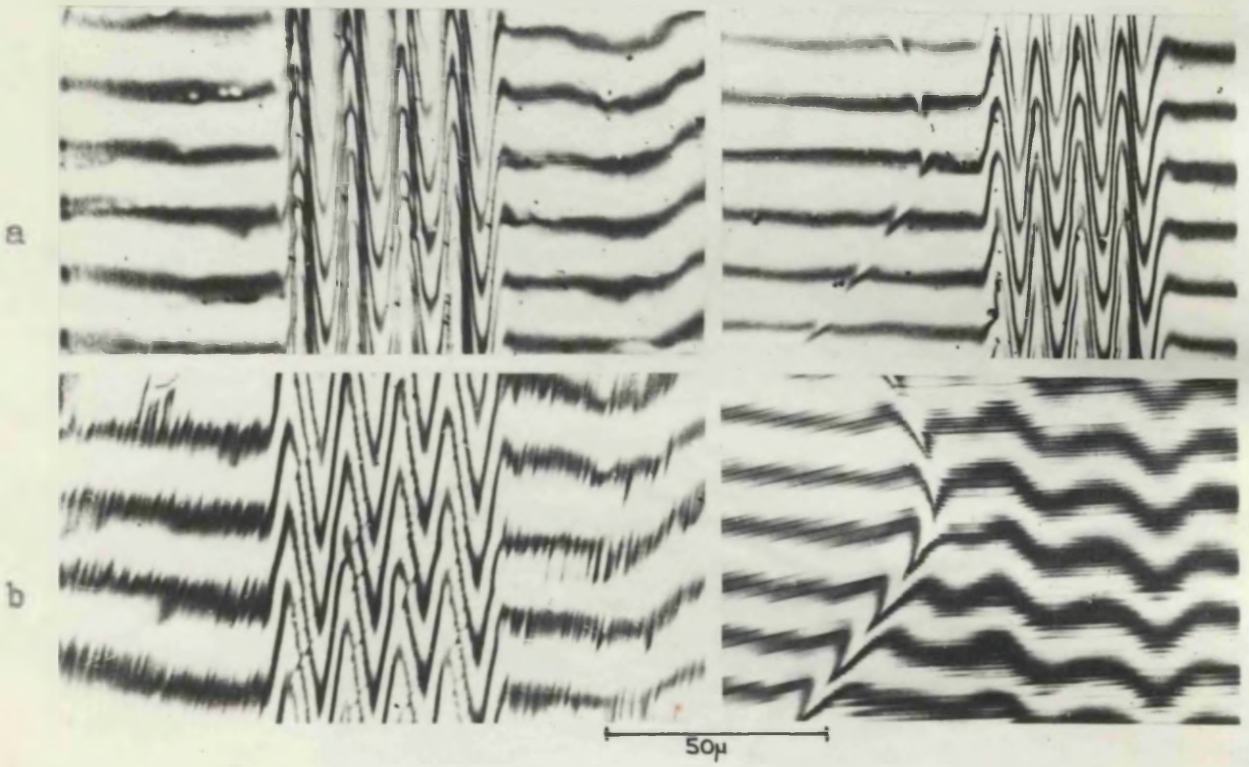

fig.58

fig.57: Variation of smoothing rate (expressed by the constant B) for striated surfaces, with the angle between striation and scratch direction.

fig.58: (a),(b) Example of slow smoothing when striations are nearly parallel to the scratches. (c),(d) Fast smoothing for striations near 90°. In (d) the original set of 4 grooves, $\lambda \sim 10\mu$, have smoothed off to produce a profile which is almost sinusoidal of wavelength near 30μ.

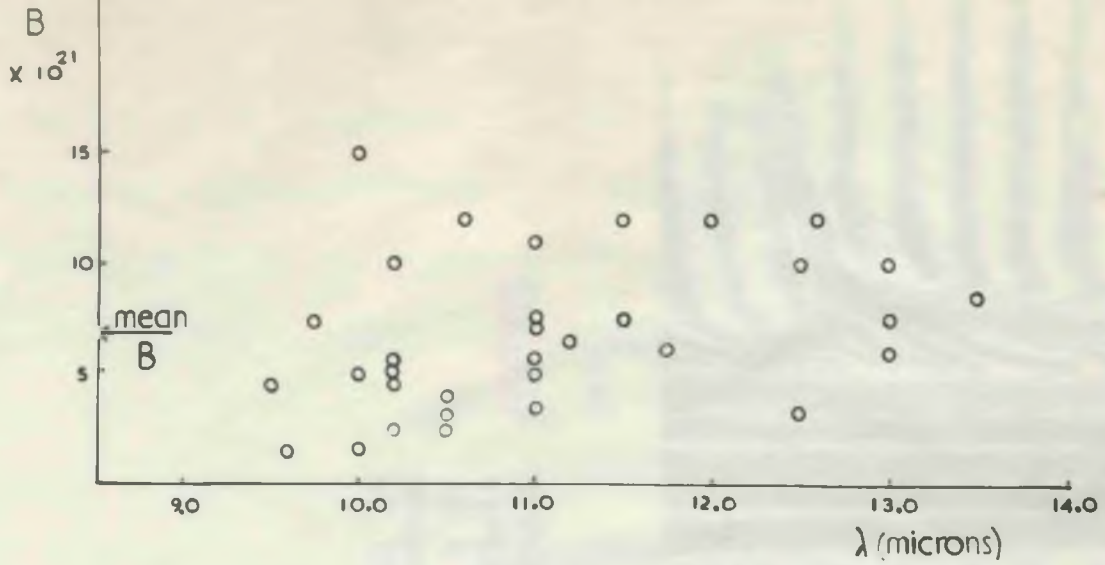

fig.59

fig. 59

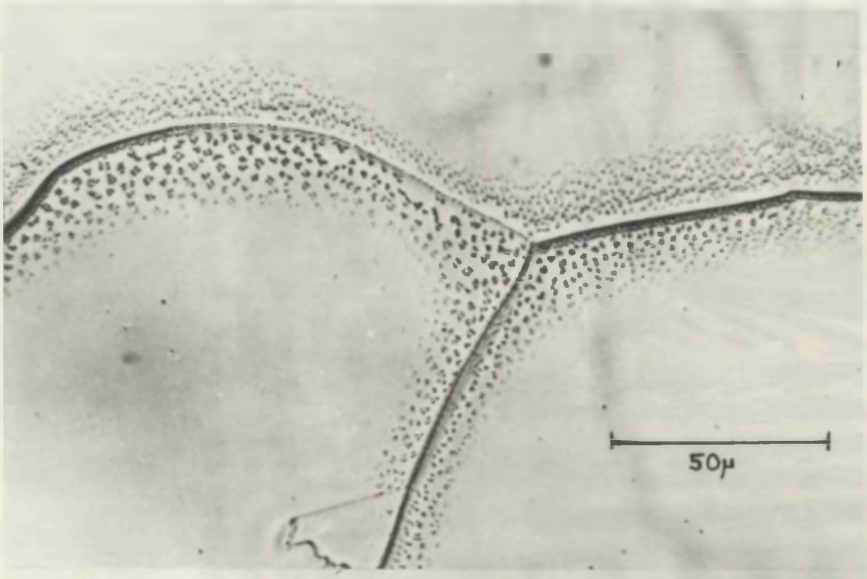

(a)

fig. 60

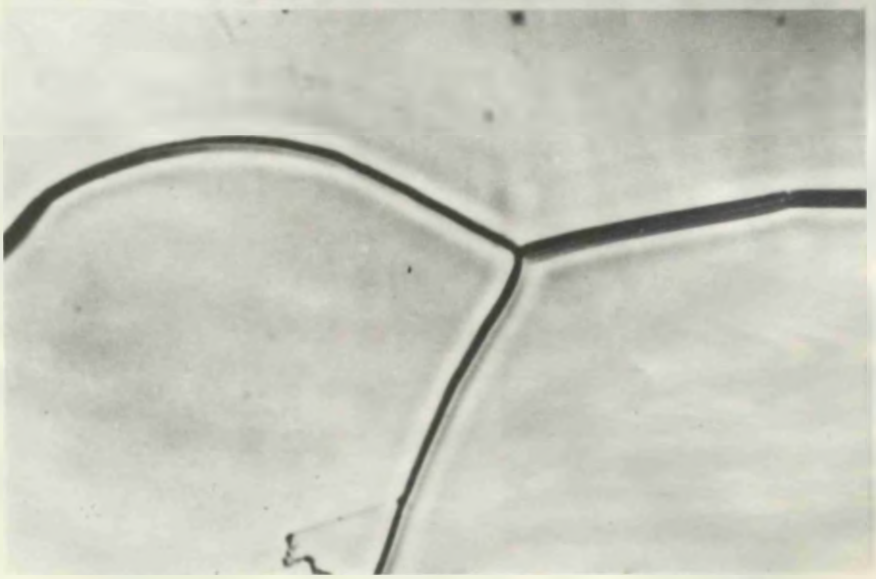

(b)

fig.59: Plot of the values of B found at 1250°C against the wavelength, λ, used. There is no general increase in B with increasing λ.

fig.60: (a) Impurity along grain boundaries in platinum, after $3\frac{1}{2}$ hr. at 1020°C. (b) same region after a further 24hr. at 1020°C.

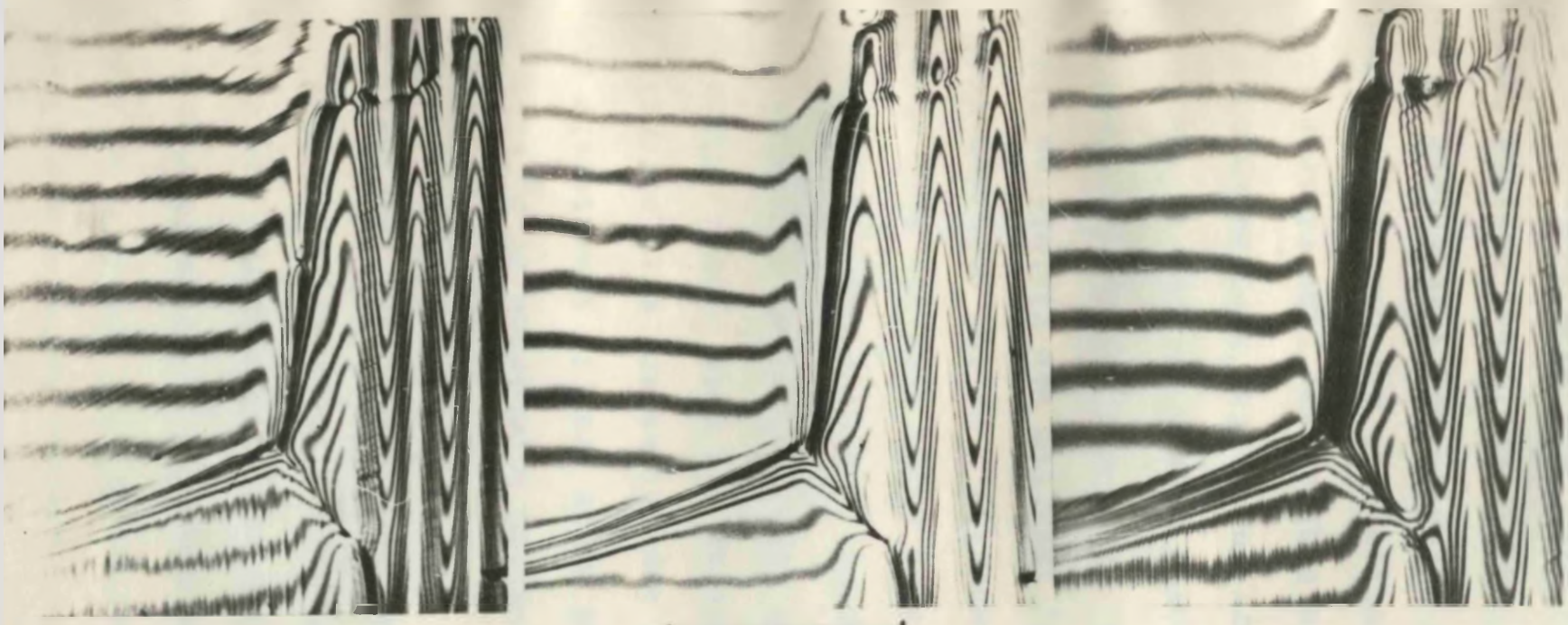

fig.61: Effect of annealing temperature on the appearance of striations on platinum. In (a) striations can be seen on a surface after annealing at 1250°C. After a further anneal (b) at 950°C they have smoothed off. Reheating at 1250°C has caused them to reappear (c).

$9.8\ (\pm 7) \times 10^{-3}$ cm^2/sec are of the expected order of magnitude. The value of D_o predicted by equation (4) is 8×10^{-4} cm^2/sec.; in view of the sensitivity of the measured D_o to small changes in Q_s the agreement is tolerable. The activation energy for volume self-diffusion in Pt found by Kidson and Ross(79) was 2.96eV. The value of Q_s obtained here is in agreement with the original postulate, $Q_s < \frac{1}{2}Q_v$.

The similarity of the orientation dependence of D_s with that found for nickel and face-centred cubic iron is immediately obvious. It therefore appears that impurities are most strongly bonded to surfaces whose orientations are near (100). Since platinum is also a transition element, the adsorption of impurities from the residual furnace atmosphere, probably occurs as on nickel and iron. However evidence has been found that the bulk metal itself is a source for surface impurity. On the specimen used for diffusion measurements at 1020°C, impurity was visible on the surface after heating for 3½ hrs. This was completely confined to regions along grain boundary grooves as can be seen in fig(60). It is believed that this impurity arrived on the surface by diffusion from the interior along the grain boundaries. The distribution is sufficient to justify this explanation but further support comes from the fact that the amount of impurity was independent of surface orientation and, therefore, was probably not derived from the atmosphere. Also twin boundaries were free from contamination; the coherent nature of twin boundaries suggests that they would not provide easy diffusion paths. The distance that the visible contamination extended from the boundary was dependent on orientation. This can be explained by different diffusion rates on

different crystal surfaces. On annealing the specimen for another $23\frac{1}{2}$ hrs at $1020^{\circ}C$ this impurity completely disappeared and did not reappear on further heat treatment, showing that the platinum surfaces were self cleaning (at least as regards visible impurity) under the vacuum conditions used.

The effect of temperature on the orientation dependence of D_s, and the appearance of striations only at high temperatures, may be explained as a result of bulk impurity. If it is assumed that the energy for removal of the impurity, by evaporation from the surface, is less than that for its diffusion to the surface, then it is possible that only at the highest temperatures is there any appreciable impurity concentration on the surface. The evidence on striations supports this suggestion. It was also found that striations, present after a high temperature anneal, disappeared on heating at a low temperature and re-appeared after further heating at the high temperature (fig(61)). The occurrence of inverted twin boundaries was less frequent at the lower temperatures indicating that $\frac{\partial \gamma_s}{\partial \theta}$ is in general smaller. That the spread in measured values of D_s does not decrease at high temperatures is also consistent with a greater concentration of surface impurity as the temperature is increased.

It is hoped that further investigations will be made on platinum from a different source.

The future programme of experiments on platinum includes (a) an investigation of the dependence on wavelength of the measured values of D_s at $\sim 1300^{\circ}C$; by using values of λ of about 5, 10, 15 and 25μ on the same specimen it should be possible to identify the dominant transport process.

(b) measurement of D_s at 800°C

(c) measurement of the rate of development of grain boundary profiles (i.e. w as a function of time) to provide a direct comparison of the multiple scratch and grain boundary groove methods for surface diffusion measurments.

(d) further studies of the dependence of D_s on orientation.

VI. General Discussion

The multiple scratch technique appears to be a successful method for the measurement of surface self-diffusion coefficients, and is particularly well suited to an investigation of the dependence of diffusion rate on surface orientation. Its main disadvantage with respect to a carefully performed tracer experiment would be that a range of orientations must necessarily be involved. However, with suitable refinements this range could be reduced to less than 5° on either side of the general surface.

The basic assumptions of the theory are that D_s and γ_s are constant over the profile and no large slopes are involved. When D_s varies with orientation, the measured rate of surface flattening will correspond to a mean value for the orientation range considered. In certain cases (fig 27) the variation of D_s can cause assymmetrical smoothing but this was rarely observed. The variation of γ_s with orientation makes the technique inapplicable for surfaces very close to planes of low index where minimum values of γ_s occur. In general such cases are easily recognized due to the formation of flats or striations. It will be noticed that in the experiments on platinum, orientation ranges of up to 33° were involved in some profiles i.e. $16\frac{1}{2}^{\circ}$ on either side of the general surface. As pointed out by Mullins (40)(1960), the small slope approximation used in the theory is valid up to angles of about 17°. The actual approximation involved is that the curvature, $K = \frac{\partial^2 Z}{\partial x^2}\left[1 + \left(\frac{\partial Z}{\partial x}\right)^2\right]^{-3/2} \approx \frac{\partial^2 Z}{\partial x^2}$. For angles of $16\frac{1}{2}^{\circ}$ ($\frac{\partial Z}{\partial x} = \tan 16\frac{1}{2}^{\circ}$) the error is about 10% and so within the experimental accuracy.

The values for the constants Q_s and D_o obtained for nickel and platinum, where contamination was least serious, are in

general agreement with the simple surface diffusion model discussed in section IIc. The collected values for the constants D_0 and Q_s are shown in table IX.

It has been found that impurity plays a major part in determining the surface behaviour of the metals investigated. For the face-centred cubic transition metals, Fe, Ni and Pt, the effects of adsorption are very similar and indicate that the properties of crystal surfaces near the (100) orientation are particularly liable to be affected by impurity. The volume of the material can also act as a source of surface impurity as was found with Au and Pt. These experiments thus illustrate that in order to obtain diffusion data for clean surfaces considerable care must be taken in eliminating contamination both from the metal itself and its environment. That such clean conditions are in fact attained could perhaps be checked by carrying out electron diffraction studies, such as performed by Germer and Hartman (72) during the diffusion anneals.

Further applications of the technique are possible such as the measurement of volume diffusion coefficients or of surface free energies. In the case of gold, for example, where the vapour pressure is small, volume diffusion could be measured by using large values of the wavelength. Surface energies could also be derived from the rate of surface smoothing if reliable values for surface diffusion coefficients were available from tracer measurements. Either of the quantities D_s or γ_s can be derived from the measured value of B ($= \frac{D_s \gamma_s d^4}{kT}$); in the present experiments D_s was treated as the unknown and previously determined values of γ_s substituted.

Table IX

Summary of Surface Diffusion Results

Metal	Method	Orientation
Ni (pure)	Single Scratches	near (111)
		near (100)
		all orientations
Ni (impure)	Single Scratches	all orientations
	Multiple Scratches	all orientations
α-Fe	Single & multiple scratches & grain boundary grooves	all orientations
γ-Fe	Grain boundary grooves	all orientations
Pt	Multiple Scratches	all orientations

Table IX (contd.)

D_o (cm^2/sec)	Expected D_o ($=\frac{1}{4} a^2 f$)	Q_s(eV)	Q_v(eV)
$1.9(\pm 1.5) \times 10^{-3}$		$0.62(\pm 0.08)$	2.75
$2.1(\pm 1.2)$	10^{-3}	$1.7 (\pm 0.2)$	"
$3.0(\pm 2) \times 10^{-3}$	to	$0.78(\pm 0.1)$	"
$6.8(\pm 4) \times 10^{-3}$	10^{-4}	$0.92(\pm 0.1)$	"
$2.1(\pm 1.2) \times 10^{-2}$		$1.2 (\pm 0.2)$	"
5.4×10^{5}		$2.5 (\pm 0.3)$	3.2
$\sim 10^{5}$		$2.5 (\pm 0.3)$	"
$9.8(\pm 7) \times 10^{-3}$		$1.2 (\pm 0.2)$	2.96

APPENDICES: Incidental Observations

A. Some observations on gold deposited from the vapour on a hot nickel substrate.

During the annealing of gold specimens in vacuo a large variety of gold deposits appeared on the nickel radiation shield S_2 (fig 10). For an evaporating Au surface temperature of 1040°C the Ni substrate was at about 950°C. The nature of the gold deposits was markedly dependent on the substrate condition.

When a pure Ni substrate, on which there was no visible contamination, was used, the form of the deposit was as shown in fig(62b). This shows a sort of mosaic pattern very similar in appearance to a system of grain boundary 'ghosts' i.e. grooves which mark the position of grain boundaries before grain growth occurred. However, all such grooves were completely smoothed off outside the region of deposition, (fig 62a), and in addition, the same type of pattern was found on a Ni substrate, previously annealed for 6 hrs at 1250°C in vacuum to produce smooth crystal surfaces. The discontinuity of the pattern at twin boundaries (fig 62c) suggests that it is related to the structure of the nickel surfaces.

The exact origin of the pattern is not known. It appears however that the gold atoms are prevented from diffusing into the nickel perhaps due to adsorbed oxygen on the surface. Gold layers may then nucleate at particular points on the surface and extend until they meet neighbouring layers with the junctions involving some degree of misfit, i.e. grain boundaries are formed. Such grooves can in fact be observed with the interference microscope.

Very different results were obtained with a contaminated Ni

substrate. The contamination had been produced during a run with the substrate at 800°C in a poor vacuum, so that many crystal surfaces had marked striations and visible impurity. After 17 hrs, (Au temperature 1040°C, Ni temperature ~ 950°C) a variety of discrete deposits were observed. The majority of these were small apparently round particles distributed randomly over the surface, except for clear regions in the vicinity of larger deposits. These clear regions were also smoother than other parts of the surface.

In addition other highly regular deposits occurred such as pyramids on (100) bases and (111) sides. Platelets were also frequent being of (111) orientation bounded by (100) or (111) planes. These deposits had very sharp corners the angles being 60 or 120°. One large equilateral triangular platelet was accidentally deformed, after being detached from the surface, and showed distinct slip along a plane parallel to one edge of the triangle illustrating that it was bounded by (111) planes (fig 63). Platelets attached at only one vertex, such as were first observed by Sears (80)(1956) for Hg, were also fairly common.

That the observed platelets etc. were actually of gold was confirmed by taking several X-ray rotation photographs of a 'stalk' of Durafix with a number of deposits embedded in it.

A large number of gold crystal whiskers were also found (Nabarro and Jackson (11)(1958)). Fig (64 abc) shows a large whisker, ~ 200μ in length, of width ~ 10μ and inclined at an angle of ~ 10° to the surface, growing from the end of a surface deposit. The interferograms of base and tip illustrate the smoothness of the whisker surface.

The theory of whisker growth is well known (Burton, Frank and Cabrera (10)(1951)), and depends on the presence of an axial screw dislocation. Eshelby(81)(1953) has predicted that the effect of the screw dislocation should be to cause an axial twist and derives the formula $\alpha = b/\pi r^2(1- \varepsilon^2/r^2)$ ..... (20) where α is the angle of twist per unit length, r is the radius (assuming the whisker to be cylindrical), b is the Burgers vector (b.v.) of the screw, and ε is the displacement of the dislocation from the axis.

An interferometric method has been used by Hamilton(82)(1960) to detect and measure an axial twist in SiC whiskers. The method consists in measuring the change, along the length of the whisker, in the angle between interference fringes and the whisker edge. This has been applied to a number of the gold whiskers observed here. To evaluate b from equation (20) from the measured value of α (assuming $\varepsilon = 0$), the cross-sectional area must be known. In general, only one face was visible for the whiskers on which measurements were made; those whose cross-section could be found by observing the tip were not suitable for interferometric measurements due to their large inclination to the substrate. Also in f.c.c. metals there are a number of possible growth directions leading to uniform cross-sections and low index faces (fig 65). It was assumed for the purpose of calculation that the cross section was an equilateral triangle, since this was the most common form of tip observed. The results obtained for the b.v.'s of different whiskers then were 33, 38, 17, 0, 16, 6 and 8 Å.

These values are probably reliable only to within a factor of about 5, but it will be noticed that they are greater than the

interplanar distance in the growth direction. Fairly extensive studies of whiskers to detect axial twists have been made by Webb et al (83)(1958) by an X-ray technique. Of the metals examined only palladium exhibited a definite twist. It may be concluded that the Au whiskers observed here do in general show an axial twist, though little can be said regarding the strength of the corresponding axial dislocation in view of the inaccuracies of measurement and the fact that small twists were probably below the limit of detection.

The whisker and platelet shapes observed are not equilibrium shapes on the basis of minimization of surface free energy, but occur as a result of an easy growth direction. Thus the large platelets for example, should, if annealed in a non-supersaturated atmosphere, be expected to round off at the corners and thicken to reduce surface area. Eventually according to the Wulff theorem on equilibrium shapes of crystals (see Herring(29)) an almost spherical form should be reached with facets corresponding to planes of low index. Fig(66a) shows a large platelet with rounded corners observed after reheating for 20 hrs at 950°C in the absence of gold.

In most cases, however, the further heating period caused cleaning of the Ni surface allowing the Au deposits to spread, so losing their regularity (fig 66b).

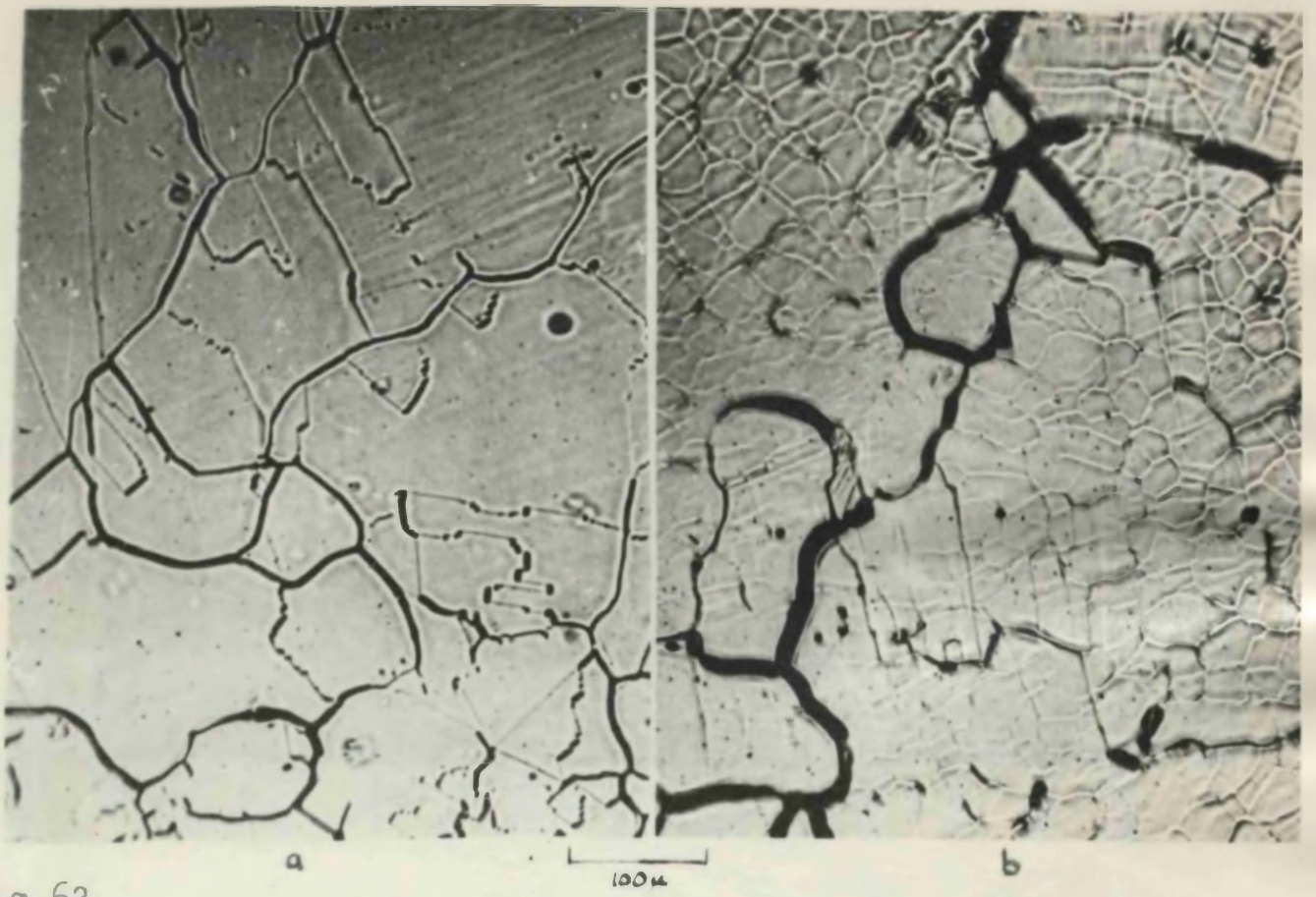

fig.62

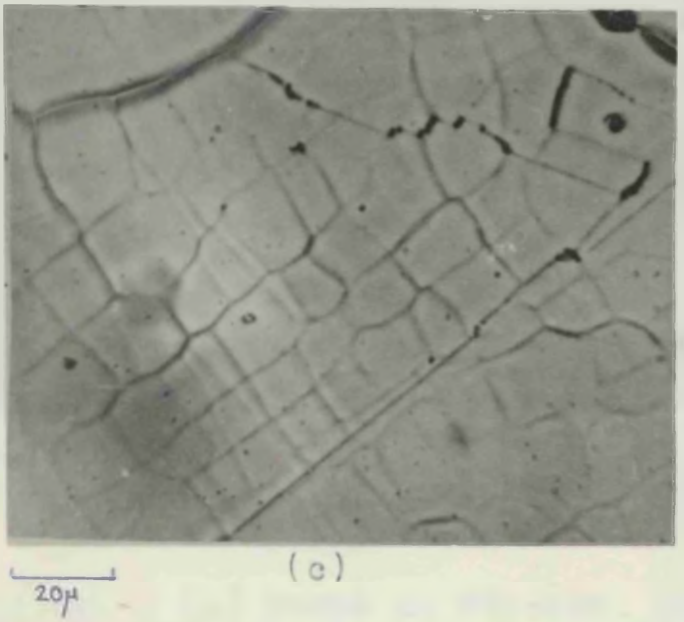

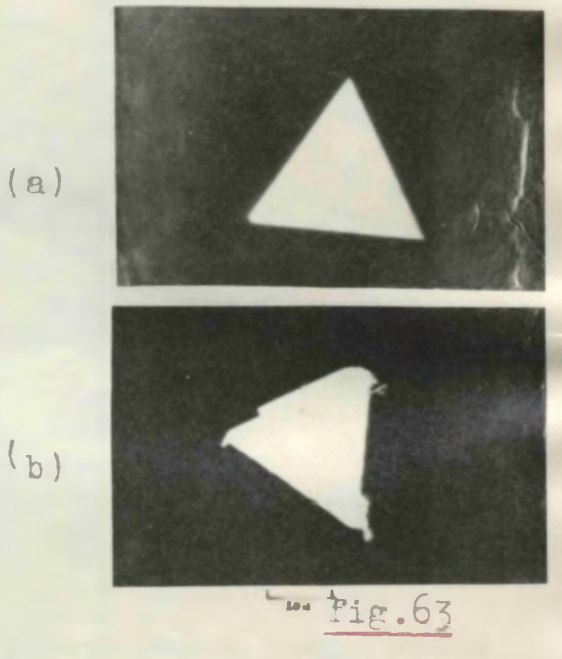

fig.63

fig.62: (a) Ni surface outside the region of deposition. Crystal surfaces are smooth. (b) Ni surface within the region of deposition showing mosaic pattern. (c) Discontinuity of mosaic pattern across twin boundaries.

fig.63: Equilateral gold triangular platelet on a glass slide. (b) After deformation. Slip has occurred parallel to the edges.

fig.64

(a) (b) (c)

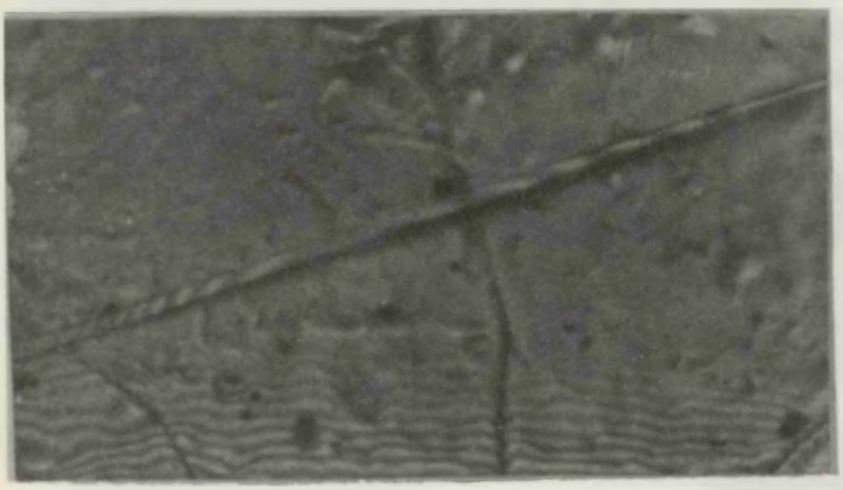

64d.

fig.65

fig.64: (a) Large Au whisker, about 200 microns long, growing from a gold deposit on a Ni surface. (b),(c) Interferograms of base and tip illustrating the surface smoothness.
(d) Interference fringes along a gold whisker exhibiting a twist.

fig.65: Some possible growth directions for whiskers of f.c.c. crystals, which would lead to low index faces.

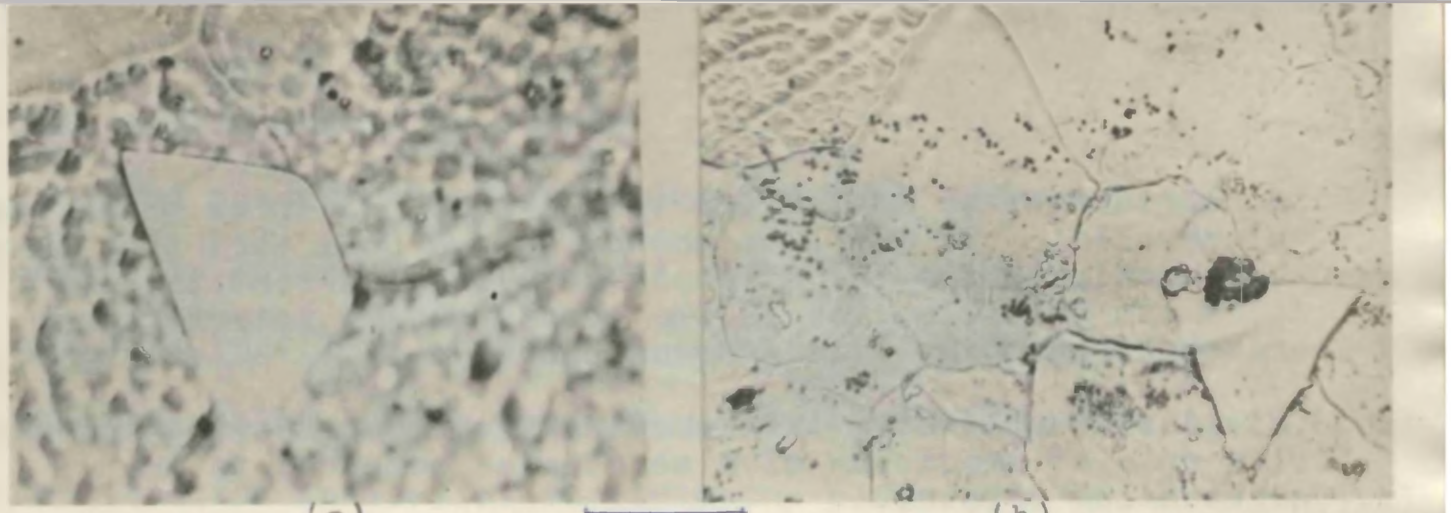

fig.66

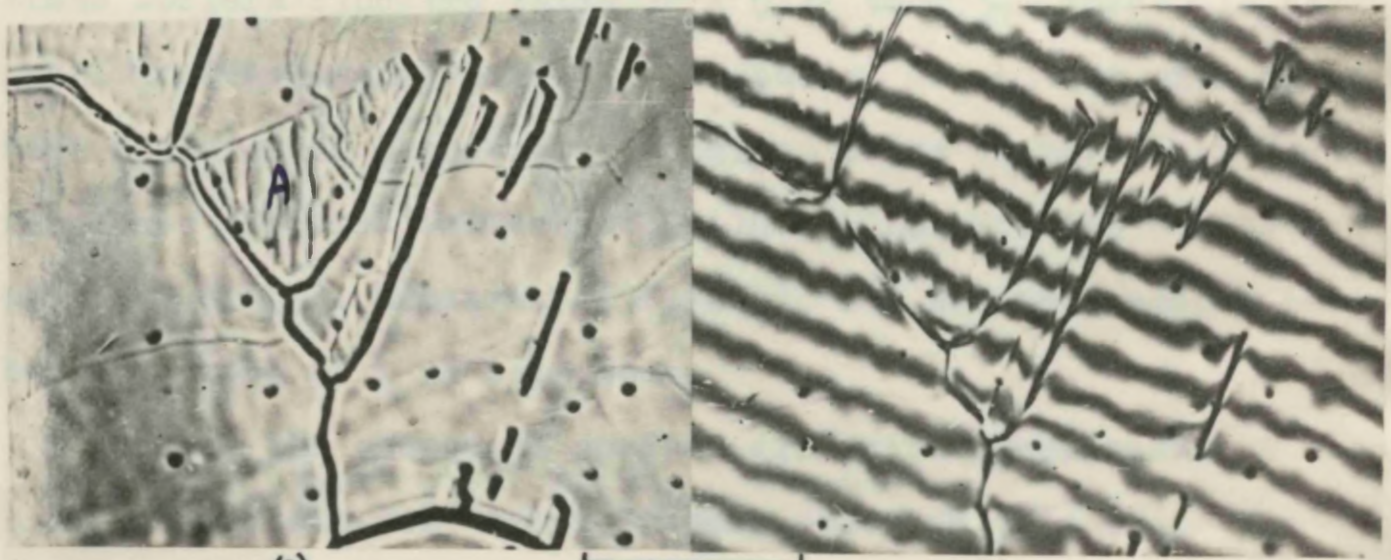

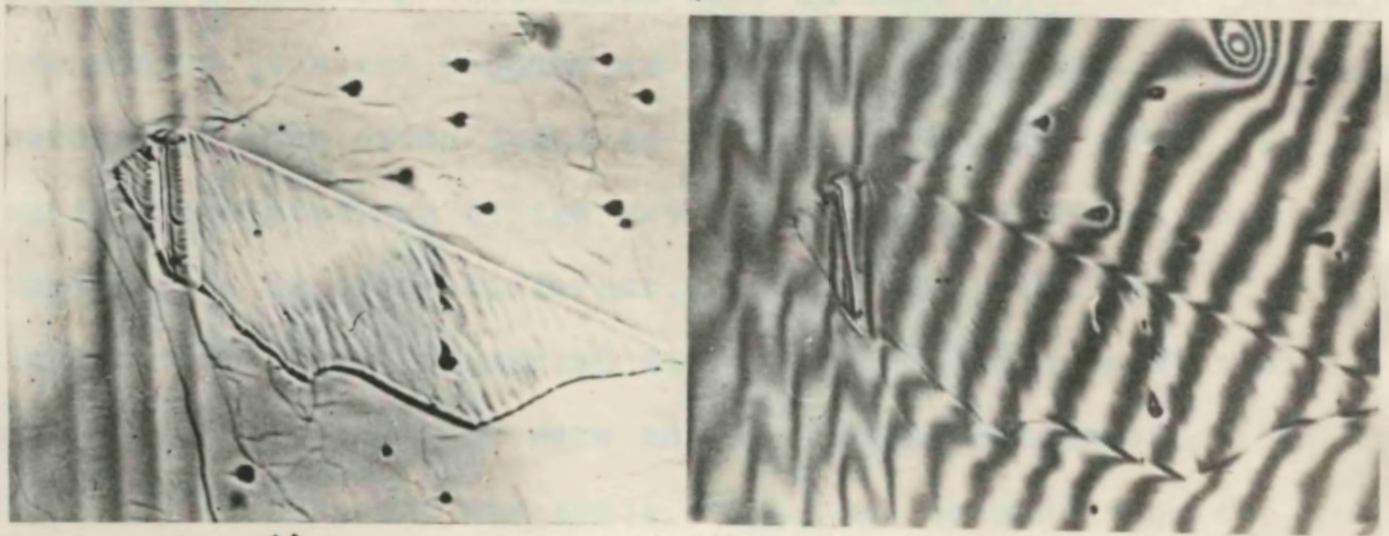

fig.67

fig.66: (a) rounding off of a Au platelet on reheating, in a non-supersaturated atmosphere, for 20 hr. at 950°C. (b) spreading of a gold deposit presumably due to cleaning of the substrate.

fig.67: Examples of twinning in α-iron. In (a) sets of parallel

Contd.Over./

boundaries can be seen. The twin A has boundaries which are not parallel; it has been shown (Cahn & Coll (84)) that when the twinning plane is {211} non-parallel coherent interfaces are possible. (b) is the corresponding interferogram and shows that inverted grooves occur.

(c),(d) Example of a twin showing inverted grooving and very slow rate of smoothing of a scratch as compared to the surrounding crystal.

B.

Twin-like Crystals in α-iron

The occurrence of annealing twins in body-centred cubic metals is generally considered to be infrequent. Recently Cahn and Coll (84)(1961) have made a study of twinning in a b.c.c. Fe - Al alloy. Both annealing and deformation twins were observed, and the indices of the twinning plane determined as the $\{211\}$ By measurement of the angles at twin-grain boundary intersections, these workers find the ratio $\frac{\gamma_T}{\gamma_b}$ = 0.23 to 0.30, where γ_T is the specific free energy of a twin boundary, and γ_b that of a normal high angle grain boundary. Annealing twins in pure iron have also been observed (McKeehan(85)(1928), Lehr(86)(1958), Hutton et al(87)(1959), Simonsen(88)(1960)), but no measurements have been reported of γ_T in this case.

During the course of surface diffusion experiments on iron a number of twin-like crystals were observed (fig 67). The evidence suggesting that these were in fact twins was: (i) Very frequently straight boundaries occurred. (ii) Sets of parallel boundaries were often found on the same crystal. (iii) The surface orientations of the crystal and its suspected twin often appeared to be quite different, (as judged by the rate of diffusion or smoothing, and marked differences as regards striations), and suggested that they were not low angle boundaries. (iv) The boundary free energy was small. This was deduced from the small displacement of normal grain boundaries at points of intersection with 'twin' boundaries. Also in many cases the surface profile, which developed at these boundaries was of the inverted type (Mykura (60)), previously only observed at twins in f.c.c. metals

A value of γ_T can be derived from measurement of the dihedral angles at a pair of parallel twin boundary grooves (60), if it is assumed that the boundaries are normal to the surface. For the example of fig 67(c, d) the ratio of twin to surface free energy $\frac{\gamma_T}{\gamma_s}$ is 0.11 ± 0.05. A large number of such measurements are of course necessary before a reliable value of γ_T can be obtained. However, since γ_b is generally about 0.3 to 0.4 of γ_s, the above result for pure iron is in fairly good agreement with that of Cahn and Coll on the Fe-Al alloy.

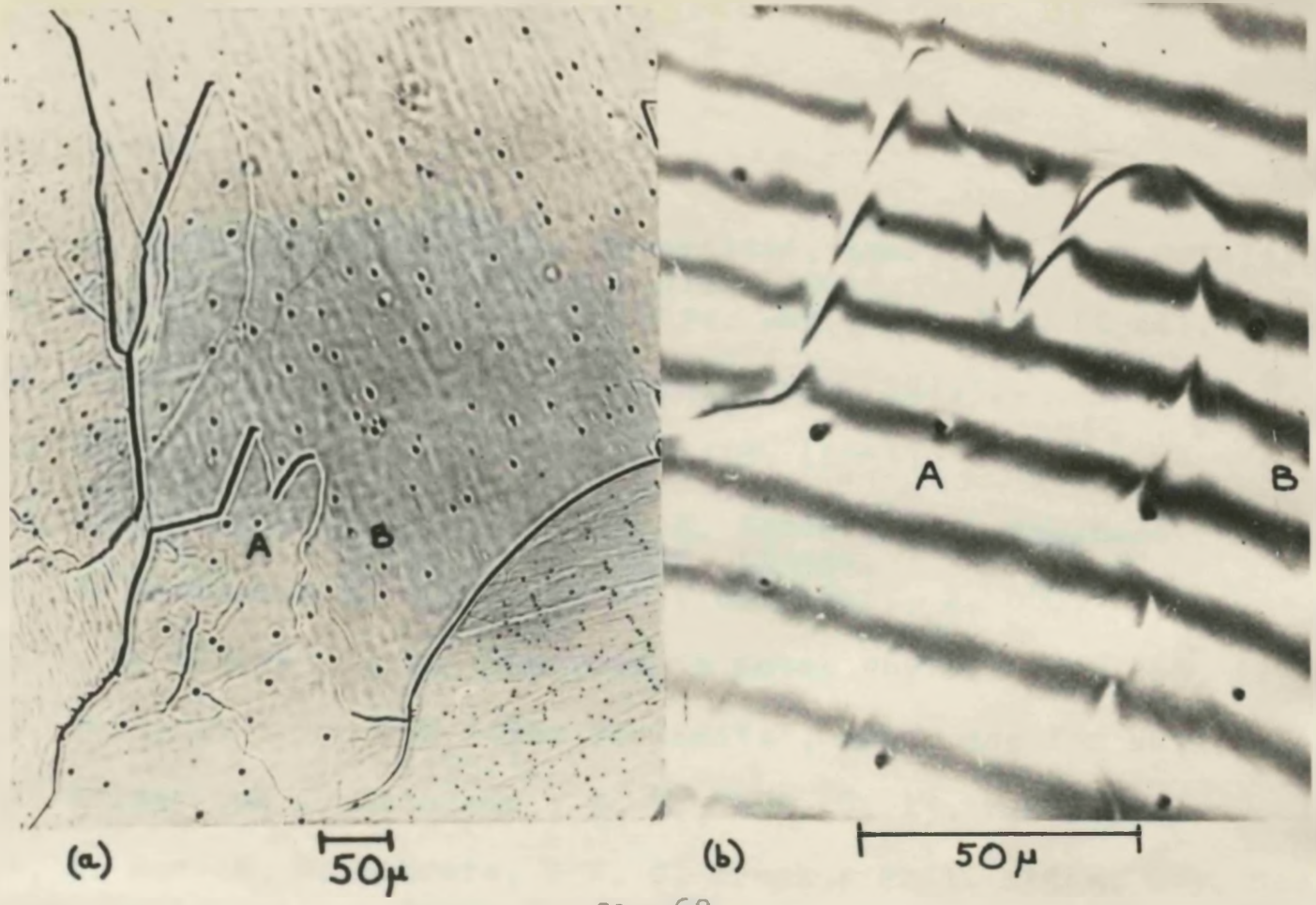

fig.68

Occurrence of an inverted profile along an apparently curved boundary. This boundary may in fact consist of coherent and incoherent portions.

References

(1) H. B. Huntington : in 'Atom Movements', Amer. Soc. for Metals, Cleveland, Ohio, (1951).
(2) H. B. Huntington & F. Seitz : Phys. Rev., 61, 315, (1942).
(3) H. B. Huntington : Phys. Rev., 76, 1728, (1949).
(4) A. D. Le Claire : Acta Met., 1, 438, (1953).
(5) A. Kuper, H. Letaw, L. Slifkin, E. Sonder, & C. Tomizuka : Phys. Rev., 96, 1224, (1954).
(6) C. J. Meechan & R. R. Eggleston : Acta Met., 2, 680, (1954).
(7) A. D. Le Claire : in 'Progress in Metal Physics', 4, 265, (1953)
(8) D. Turnbull : in 'Atom Movements', Amer. Soc for Metals, (1951).
(9) M. Volmer and J. Esterman : Z. f. Phys.,7, 13, (1921).
(10) W. K. Burton, N. Cabrera, & F. C. Frank : Phil. Trans. Roy. Soc., A243, 299, (1951).
(11) F. R. N. Nabarro & P. J. Jackson : in 'Growth and Perfection of Crystals', Doremus, N.Y., (1958).
(12) R. Gomer : J. Chem. Phys., Letter, 26, 1333, (1957). J. Chem. Phys., 28, 457, (1958).
(13) R. M. Barrer : 'Diffusion in and through Solids', C.U.P. (1941
(14) E. N. daC Andrade & J. G. Martindale : Trans.Faraday Soc., 31, 1137, (1935).
(15) E. T. S. Appleyard : Proc. Phys. Soc., 49, 118, (1937).
E. T. S. Appleyard & A. C. B. Lovell : Proc. Phys. Soc., A158, 718, (1937).
(16) C. J. Smithells :' Metals Reference Book', Butterworth, London, (1949), p.473.
(17) R.C. Bosworth : Proc. Roy. Soc., 150A, 58, (1935).
(18) I. Langmuir : Journl. Franklin Institute, 217, 543, (1934).
(19) S. Dushman & I. Langmuir :Phys. Rev., 20, 113, (1922).
(20) S. Makin, R. Rowe, & A. D. Le Claire :Proc. Roy. Soc.,70, 545, (1957).
(21) J. C. Fisher : J. Appl. Phys., 22, 74, (1951).
(22) R. A. Nickerson & E. R. Parker : Trans. Amer. Soc.Metals, 42, 37 (1950).
(23) R. E. Hoffman & D. Turnbull : J. Appl. Phys., 22, 634, (1951).

(24)W. A. Johnson : Trans. A.I.M.E., 143, 107, (1941).

(25)W. C. Winegard & B. Chalmers : Can. J. Phys., 30, 422, (1952).

(26)N. Hackerman & N. H. Simpson : Trans. Faraday Soc., 52, 628, (1956).

(27)W.W. Mullins & P.G. Shewmon : Acta Met., 7, 163, (1959).

(28)H. Fraunfelder : Helvet. Phys. Acta, 23, 371, (1950).

(29)C. Herring : in 'Physics of Powder Metallurgy', McGraw-Hill, Kingston, (1951).

(30)C. Herring : J. Appl. Phys., 21, 301, (1950).

(31)C. Herring : in 'Structure and Properties of Solid Surfaces' Gomer & Smith, (1953), p.35.

(32)G. C. Kuczynski : Trans. A.I.M.E., 185, 169, (1949).

(33)G. C. Kuczynski : J. Appl. Phys., 21, 632, (1950).

(34)N. Cabrera: : Trans. A.I.M.E., 188, 667, (1950).

(35)C. J. Meechan : Phys. Rev. letter, 4, 284, (1960).

W.D. Kingery & M. Berg : J. Appl. Phys., 26, 1205, (1955).

(36)E. W. Muller : Z. f. Physik, 126, 642, (1949).

(37)J. L. Boling & W. W. Dolan : J. Appl. Phys., 29, 556, (1958).

(38)J. P. Barbour, F. M. Charbonnier, W. W. Dolan, W. P. Dyke E. E. Martin, & J. K. Trolan :Phys. Rev., 117, 1452, (1960).

(39)B. Chalmers, R. King, & R. Shuttleworth : Proc. Roy. Soc., A193, 465, (1948).

(40)W. W. Mullins : J. Appl. Phys., 28, 333, (1957).

W. W. Mullins : Trans. A.I. M. E., 218, 354, (1960).

(41)H. Mykura : Ph. D. Thesis, London, (1954).

(42)N. A. Gjostein : (not yet published).

(43)C. H. Li & E. R. Parker : quoted from N. A. Gjostein (42).

(44)J. A. M. Van Liempt : quoted from Le Claire (7).

(45)A. J. W. Moore : Acta Met., 6, 293, (1958).

(46)R. Gomer : in 'Structure and Properties of Solid Surfaces', Gomer & Smith, (1953), p.76.

(47)W. W. Mullins : Acta Met. Letter, 7, 746, (1960).

(48)J. E. Lennard - Jones : Proc. Phys. Soc., 49, 140, (1937).

(49)O. Knacke & I. N. Stranski : in 'Progress in Metal Physics', 6, 181, (1956).

(50)O. Kubaschewski & E. LL. Evans : 'Metallurgical Thermochemistry' Butterworth, (1951).

(51)J. E. Reynolds, B. L. Averbach, & M. Cohen : Acta Met., 5, 29, (1957).

(52)R. E. Hoffman, F. W. Pikus, & R. A. Ward : Trans. A.I.M.E., 206, 483, (1956).

(53)R. Gomer : Disc. Faraday Soc., No.28, 23, (1959).

(54)L. G. Carpenter & W. N. Mair : Trans. Faraday Soc., 55, 1924, (1959).

D. Clark, T. Dickinson, & W.N. Mair : Trans. Faraday Soc., 55, 1937, (1959).

(55)H. Udin : in 'Metal Interfaces', Amer. Soc. for Metals, (1952), p.114.

(56)J. C. Fisher & C. G. Dunn : in 'Imperfections in Nearly Perfect Crystals', Wiley, N.Y.(1952)

(57)G. F. Smith : Phys. Rev., 94, 295, (1954).

(58)M. H. Nichols : Phys. Rev., 94, 307, (1954).

(59)J. L. Walter & C. G. Dunn : Acta Met., 8, 497, (1960).

(60)H. Mykura : Acta Met., 5, 346, (1957).

Acta Met., (to be published).

(61)W. W. Mullins : J. Appl. Phys., 30, 77, (1959).

(62)H. Mykura : Proc. Phys. Soc., 67, 281, (1954).

(63)E. Ingelstam : in 'Symposium on Interferometry', H.M.S.O., London, (1960).

(64)F. R. Tolmon & J. G. Wood : J. Sc. Instr., 33, 236, (1956).

J. W. Gates : J. Sc. Instr., 33, 507, (1956).

(65)C. S. Barrett : 'Structure of Metals', McGraw-Hill, N.Y., (1952).

(66)H. Mykura : Bull. Inst. Metals, 4, 102, (1958).

(67)E. R. Hayward & A. P. Greenough : J. Inst. Metals, 88, 217, (1960).

(68)S. Dushman : 'Vacuum Technique', Wiley, N.Y., (1949).

(69)C. Kittel : 'Introduction to Solid State Physics', Wiley, N.Y., (1957).

(70)W. R. Upthegrove & M. J. Sinnot : Trans. Amer. Soc. Metals, 50, 1031, (1958).

(71)A. F. Wells : 'Structural Inorganic Chemistry', Oxford,(1950).

(72)L. H. Germer & C. D. Hartman : J. Appl. Phys., 31, 2085,(1960)

(73)F. H. Buttner, H. Udin, & J. Wulff : Trans. A.I.M.E., 197, 313, (1953).

(74)J. E. Hilliard, B. L. Averbach, & M. Cohen : Acta Met., 8, 24, (1960).

(75)C. E. Birchenall & R. F. Mehl : Trans. A.I.M.E., 188, 144, (1950).

(76)F. S. Buffington, I. D. Bakalar, & M. Cohen : Trans. A.I.M.E., 188, 1375,(1950)

(77)A. P. Greenough (Swansea) : private communication.

(78)A. Franks : Brit. J. Appl. Phys., 9, 349, (1958).

H. M. Otte & R. W. Cahn : J. Sc. Instr., 36, 463, (1959).

(79)G. V. Kidson & R. Ross : Proceedings of the first (UNESCO) International Conference,Paris,1957. "Radioisotopes in Scientific Research", vol.1, p.185.

(80)G. W. Sears : J. Chem. Phys., 25, 637, (1956).

(81)J. D. Eshelby : J. Appl. Phys., 24, 176, (1953).

(82)D. R. Hamilton : J. Appl. Phys., 31, 112, (1960).

(83)W. W. Webb : in'Growth and Perfection of Crystals', Doremus, N.Y., (1958).

(84)R. W. Cahn & J. A. Coll : Acta Met., 9, 138, (1961).

(85)L. W. McKeehan : Trans. A.I.M.E., 78, 453, (1928).

(86)P. Lehr : quoted from ref.(84).

(87)D. S. Hutton, G. L. Coleman, & W. C. Leslie : Trans. A.I.M.E., 215, 680,(1959).

(88)E. Bull Simonsen : Acta Met., 8, 809, (1960).